

Aus dem Walter-Brendel-Zentrum für Experimentelle Medizin der

Ludwig-Maximilians-Universität München

Leiter: Prof. Dr. med. Ulrich Pohl

**MAST CELLS IN ARTERIOGENESIS:  
A PRE-CLINICAL STUDY EMPLOYING A MURINE HIND LIMB MODEL OF  
COLLATERAL ARTERY GROWTH**

Dissertation

zum Erwerb des Doktorgrades der Medizin

an der Medizinischen Fakultät der

Ludwig-Maximilians-Universität zu München

vorgelegt von

Omary Chillo

Aus Dar es Salaam

2014

Mit Genehmigung der Medizinischen Fakultät  
der Universität München

Berichterstatter: Priv. Doz. Dr. Elisabeth Deindl

Mitberichterstatter: Priv. Doz. Dr. Hans Theiss

Prof. Dr. Clemens von Schacky auf Schönfeld

Prof. Dr. Nikolaus Plesnila

Mitbetreuung durch den

Promovierten Mitarbeiter: Prof. Dr. med. Norbert Dieringer

Dekan: Herr Prof. Dr. med Dr. h.c. M.Reiser, FACR, FRCR

Tag der mündlichen Prüfung: 27<sup>th</sup> .November 2014

### **Affirmation in lieu of an oath**

I hereby declare and confirm that the work presented here is, to the best of my knowledge and belief, original and the result of my own investigations, except as acknowledged, and has not been submitted, either in part or whole, for a degree at any University. I gratefully acknowledge supervision and guidance I have received from Dr Elisabeth Deindl and Prof. Dr. Norbert Dieringer.

Omary Chillo

Date: 3 February 2014

### **ZUSAMMENFASSUNG**

Ziel der hier vorliegenden Arbeit war es, den funktionellen Beitrag von Mastzellen bei der Arteriogenese, dem Wachstum prä-existierender arteriöler Verbindungen zu natürlichen Bypässen, zu untersuchen. Hierzu wurde das Mausmodell der peripheren Arteriogenese verwendet, bei der durch Ligatur der Femoralarterie das Wachstum von Kollateralarterien induziert wird. Die Ergebnisse zeigten, dass Mastzellen nur im perivaskulären Raum von wachsenden Arteriolen aktiviert werden und degranulieren, während dies weder im distal davon gelegenen Unterschenkel, noch bei Scheinoperation beobachtet wurde.

Laser-Doppler-Perfusionsmessungen belegten, dass sowohl durch die Applikation von C48/80, von SCF, als auch von Diprotin A, welche zur Degranulation, zur Reifung, beziehungsweise zur Rekrutierung von Mastzellen führten, die Arteriogenese gesteigert werden kann. Bei kombinierter Applikation von C48/80 und Diprotin A wurden additive Effekte beobachtet. Die Applikation von Cromolyn hingegen, welches die Degranulation von Mastzellen blockiert, reduzierte den Prozess der Arteriogenese selbst wenn gleichzeitig Diprotin A verabreicht wurde. Diese Ergebnisse belegen erstmals, dass Mastzellen eine wesentliche Funktion bei der Arteriogenese übernehmen. Diese Funktion wurde genauer charakterisiert. Es zeigte sich dass Mastzellen sowohl (a) die vaskuläre Remodellierung über Aktivierung von Matrixmetalloproteinasen, (b) die Rekrutierung von Leukozyten über eine vermehrte Bioverfügbarkeit von MCP-1 und TNF- $\alpha$ , als auch (c) die Proliferation von vaskulären Zellen, vermutlich über die Freisetzung von Wachstumsfaktoren, fördern und somit wesentlich zum Prozess der Arteriogenese beitragen.

Der Verschluss einer Arterie hat unweigerlich zur Folge, dass das distal davon gelegene Gewebe aufgrund der Minderperfusion geschädigt wird, während dies durch effizientes Wachstum von natürlichen Bypässen verhindert oder zumindest verringert werden kann. Tatsächlich zeigen die hier erhobenen Daten, dass durch die

kombinierte Applikation von C48/80 und Diprotin A die Gewebefibrose im Unterschenkel der behandelten Tiere auf ein Minimum reduziert werden konnte, was mit einer signifikant reduzierten Kapillarsprossung und Infiltration von Leukozyten verbunden war.

Untersuchungen zum Auslöser der Degranulation von Mastzellen nach Gefäßverschluss zeigten, dass es sich hierbei um eine konzertierte Aktion handelt. Im Wesentlichen sind hierfür reaktive Sauerstoffspezies verantwortlich, welche von der Neutrophilen NADPH Oxidase 2 nach Plättchen-GPIIb $\alpha$  vermittelte Aktivierung und uPA abhängige Extravasation von Neutrophilen, gebildet werden.

Zusammenfassend zeigen die Ergebnisse dieser Arbeit erstmals, dass Mastzellen eine essentielle Rolle bei der Arteriogenese spielen und dass durch ihre aktive Rekrutierung und Degranulation der Prozess der Arteriogenese so effizient gesteigert werden kann, dass hierdurch Gewebeschäden, welche sich in Minderperfusion bedingen, fast vollständig verhindert werden können.

## **TABLE OF CONTENTS**

1.	INTRODUCTION.....	
	.....1	
1.0.	Importance of arteriogenesis and cardiovascular diseases.....	1
1.1.	Vascular adaptation in arteriogenesis.....	2
1.2.	Mechanism of arteriogenesis .....	4
1.3.	The role of leukocytes in arteriogenesis.....	6
1.3.1.	Monocytes and macrophages.....	6
1.3.2.	T-cell lymphocytes .....	7
1.3.3.	Mast cells .....	7
1.3.3.1.	The origin of mast cell.....	7
1.3.3.2.	Mast cell activation.....	8
1.3.3.3.	Mast cell derived mediators.....	9
1.3.3.4.	Mast cell in the vascular wall .....	10
1.3.3.5.	Mast cells, tissue remodelling and cardiovascular diseases.....	11
1.4.	Aim of the study .....	12
2.	MATERIALS AND	
	METHODS.....	13
2.1.	Materials.....	13
2.1.1.	Animals .....	13
2.1.2.	Femoral artery ligation.....	13
2.1.3.	Substance used for treatment.....	15
2.1.4.	Visualization of the hind limb .....	16
2.1.5.	Histology and immunohistochemistry.....	16
2.1.6.	Antibodies used in fluorescence-activated cell sorting (FACS).....	19
2.1.7.	Commercial kits for MMP, TNF-alpha, MCP-1 and serum protein array.....	20
2.1.8.	RNA extraction.....	21
2.1.9.	cDNA synthesis and qRT-PCR .....	21
2.2.	Methods.....	23
2.2.1.	Surgical procedures for arteriogenesis.....	23
2.2.2.	Experimental design. ....	24

2.2.3. Measurements of hind limb blood flow.....	25
2.2.4. Visualization of the hindlimb arterial system.....	27
2.2.5. Tissue perfusion, fixation and isolation .....	28
2.2.6. Histology and immunohistochemistry.....	30
2.2.6.1. Histology.....	31
2.2.6.1.1. Haematoxylin and eosin staining.....	31
2.2.6.1.2. Giemsa staining.....	32
2.2.6.2. Immunohistological staining.....	32
2.2.6.2.1. Ki67 staining.....	33
2.2.6.2.2. CD45 staining.....	33
2.2.6.2.3. CD31 staining.....	34
2.2.7. Fluorescence-activated cell sorting (FACS) .....	35
2.2.8. Collateral vessel diameter.....	37
2.2.9. Quantification of leukocytes.....	37
2.2.10. Quantification of Ki67 or CD31 positive cells.....	38
2.2.11. Serum Proteins Antibody Array .....	38
2.2.12. MMP's activity assay.....	39
2.2.13. TNF- $\alpha$ analysis.....	40
2.2.14. MCP-1 ELISA .....	41
2.2.15. SDF-1 $\alpha$ ELISA .....	42
2.2.16. RNA extraction and real-time polymerase chain reaction (RT-PCR) .....	43
2.2.17. Statistical analysis.....	47

### 3. RESULTS

.....	48
-------	----

3.1.	Collateral arteries change their shape after femoral artery occlusion .....	48
3.2.	Mast cells respond to femoral artery ligation with degranulation in the vicinity of growing collateral vessels .....	49
3.3.	Prevention of perivascular mast cell degranulation impairs arteriogenesis .....	50
3.4.	Effect of stem cell factor and diprotin A on hindlimb reperfusion recovery following femoral artery ligation.....	53
3.5.	Mast cell degranulation with the help of C48/80 accelerates hindlimb perfusion recovery.....	55
3.6.	Mast cell degranulation promotes vascular remodeling through increased MMP enzymatic activity in collaterals .....	59
3.7.	Protein array analysis revealed elevated serum levels of PDGF-BB, angiopoietin-1 and MMP-3 and 9 .....	60
3.8.	The extent of mast cell degranulation covaries with the progress of vascular cell proliferation .....	62
3.9.	Degranulation of mast cells increases the expression of MCP-1 in collateral.....	64
3.10.	Inhibition of mast cell degranulation reduces the release of TNF- $\alpha$ and lower its plasma levels.....	66
3.11.	Mast cell degranulation recruits leukocytes .....	67
3.12.	Treatment of mice with C48/80 + diprotin A results in an increase in collateral vessel diameter .....	75
3.13.	Improved perfusion reduces distal tissue ischemic damage.....	77
3.14.	Mechanism of mast cell degranulation during untreated arteriogenesis .....	79
4.	DISCUSSION.. .....	84
5.	SUMMARY.....	102
6.	REFERENCES .....	104



7.	INDEXES	116
i.	Acknowledgement.....	1
	16	
ii.	List of abbreviations	117
iii.	Curriculum vitae.....	118

# **1. INTRODUCTION**

## **1.0. Importance of arteriogenesis in cardiovascular diseases**

Cardiovascular diseases are the leading cause of death worldwide. The spread of western life style will increase the cardiovascular disease prevalence in developing countries and most significantly at younger population. An estimated 17.3 million people died from cardiovascular diseases in 2008, representing 30% of all global deaths. Of these deaths, an estimated 7.3 million were due to coronary heart disease and 6.2 million were due to stroke, all of these were the result of coronary or cerebral artery occlusion respectively (WHO, September 2011). Peripheral artery disease affects a large segment of the adult population, with an age-adjusted prevalence between 4% and 15%, affecting more than 5 million adults in the United States (Kasapis and Gurm, 2009). Atherosclerosis (narrowing of arterial lumen due to accumulation of fatty substances and plaque formation) remains to be the main cause of chronic peripheral arterial occlusive diseases. Embolism, thrombosis and trauma are acute causes of arterial occlusion. The risk of formation and progression of atherosclerosis, and hence of arterial occlusion is much higher in patients with multilevel arterial involvement, such as diabetes mellitus, chronic renal insufficiency, and heavy smoking (Cox et al., 1993).

Therapeutic options to treat occlusive arterial diseases include surgical revascularization techniques such as percutaneous transluminal angioplasty and bypass surgery. These techniques have been developed over the last decades and can now be performed with low morbidity and mortality in patients with chronic artery diseases. Despite of these surgical options to treat arterial stenosis, 25–30% of the patients with coronary artery disease cannot be revascularised by percutaneous coronary intervention or coronary artery bypass grafting. Therefore, therapeutic

promotion of the growth of pre-existing collateral arteries (i.e. arteriogenesis) is a valuable treatment strategy in those patients (Seiler, 2003, Hunt, 2006). Arteriogenesis provides alternate routes for blood flow bypassing occluded arteries with the result of preventing or reducing ischemic injuries in downstream tissues (Schaper et al., 1976).

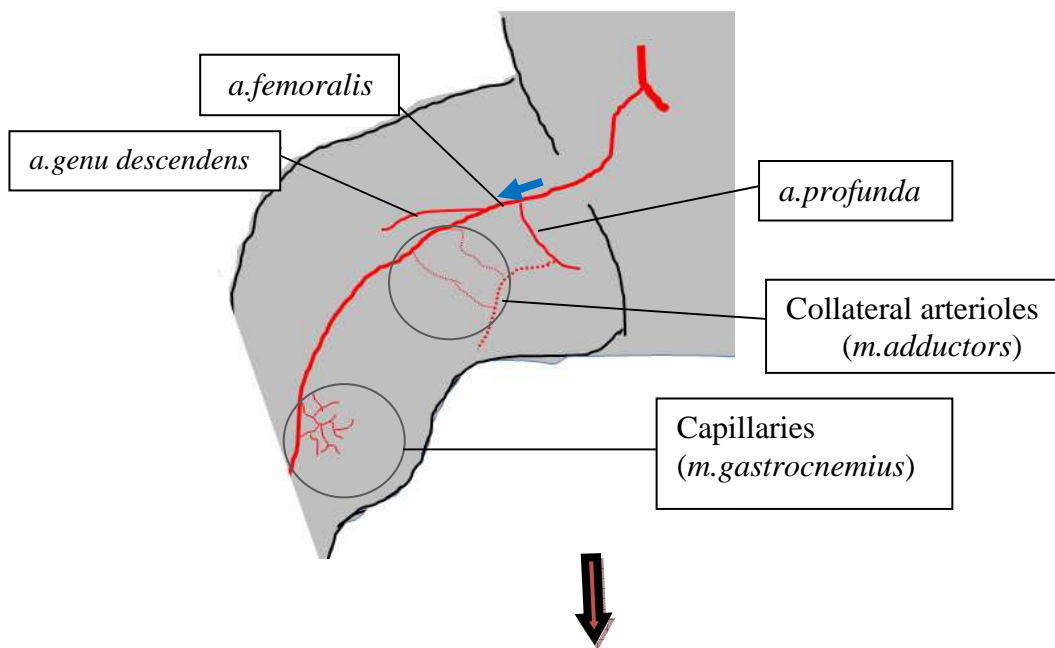
### **1.1. Vascular adaptations in arteriogenesis**

Chronic changes in blood flow e.g. due to arterial occlusion results in vascular adaptation. This adaptation includes both arteriogenesis and angiogenesis (see figure 1). Collateral arteries are present in almost all organs. During arteriogenesis, these collaterals become larger in diameter and can reach up to 25 times of their original size (Scholz et al., 2001). Enlarged collateral arteries can efficiently supply blood flow with the result that tissue necrosis is prevented or limited (Scholz et al., 2002). Therefore, arteriogenesis can also prevent angiogenesis by restoring blood flow to the ischemic tissue (Deindl et al., 2001). Angiogenesis is the sprouting of capillaries from pre-existing vessels (Carmeliet, 2000) in response to hypoxia in the downstream tissue. In contrast to angiogenesis, ischemia is not a direct driving force in arteriogenesis (Deindl et al., 2001).

Arteriogenesis involves enlargement of small pre-existing arteriole into a conductance artery that substitute the diseased large occluded artery. The process includes proliferation of endothelial and smooth muscle cells and reorganization of extracellular matrix followed by vessel maturation and stabilization (Schaper et al., 1971). Collateral arteries are present essentially in every tissue/organ of the body but the number and size of these anastomosis varies greatly between tissues as well as between species (Helisch and Schaper, 2003, Helisch et al., 2006). A well known

model for the study of arteriogenesis and angiogenesis is the experimental occlusion of the femoral artery in the mouse hind limb. In response to femoral artery occlusion collateral arteries enlarge (arteriogenesis) due to shear stress in the upper leg and capillaries sprout (angiogenesis) due to ischemia in the lower leg (figure 1).

A. Before occlusion



B. After occlusion

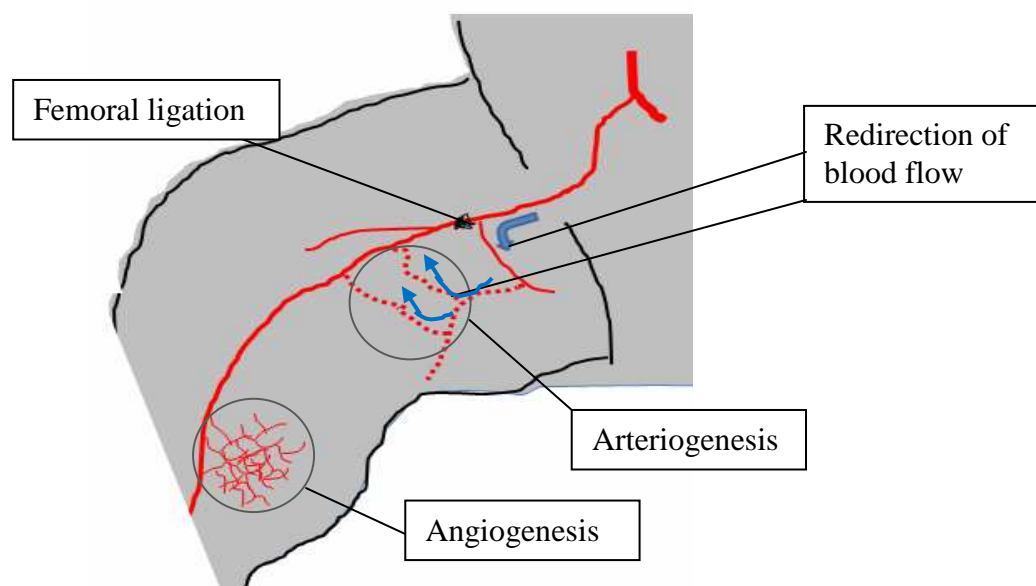


*Figure 1. Murine hind limb model of collateral artery growth.*

A: Sketch diagram shows the hind limb vascular blood flow through the femoral artery to downstream tissues. Minimum amount of blood is passing through the *a.profundus* to the deep interconnecting arterioles in the adductor muscles.

B: Femoral artery occlusion leads to redirection of blood flow through interconnecting arterioles back to the distal part of femoral artery. This phenomenon is associated with the development of collateral arteries (arteriogenesis) and the formation of new capillaries in the gastrocnemius muscle (angiogenesis).

## **1.2. Mechanisms of Arteriogenesis**

Arteriogenesis is triggered after arterial occlusion by fluid shear stress in the vessel wall of collateral arteries (Resnick et al., 2003). Following increased blood flow in collateral arteries, their endothelial cells become activated, which is seen first as cell swelling, caused by loss of osmotic control (Schaper et al., 1976, Chalothorn and Faber, 2010). This mechanical force will activate transcriptional factors such as *egr-1*, which then up-regulates monocyte chemoattractant molecules (MCP-1) and intracellular adhesion molecules (ICAM) -1 in the collateral endothelium (Ito et al., 1997, Hoefer et al., 2004, Pagel et al., 2012). MCP-1 recruits circulating monocytes, which adhere to the endothelium and finally extravasate to the perivascular space (Heil et al., 2002). Perivascular inflammatory cells, consisting mainly of monocytes, in the growing collaterals secrete growth factors and proteases necessary for endothelial and smooth muscle cell proliferation as well as vascular remodelling (Arras et al., 1998) (figure 2). Collateral arteries enlarge and remodel outwardly, which results in an increase in the luminal diameter (Scholz et al., 2000). As the luminal diameter increases, the fluid shear stress decreases and the process of

arteriogenesis terminates. If collateral arteries have developed adequately, distal perfusion will be restored.

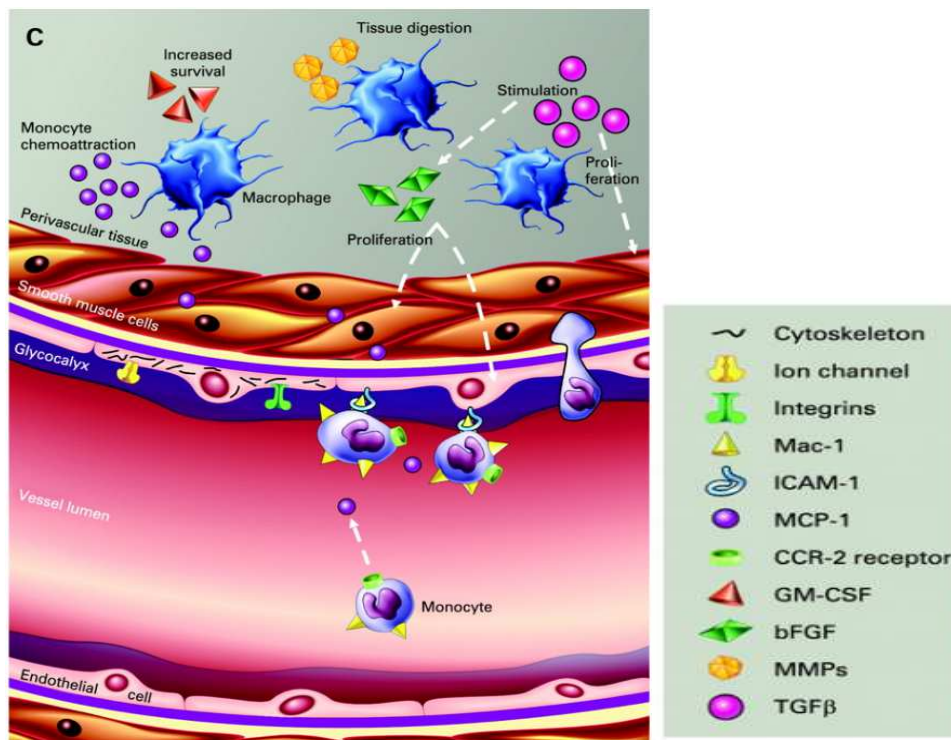


*Figure 2: Mechanism of arteriogenesis*

The endothelium senses increased fluid shear stress via its surface stress receptors such as integrins. This increased shear stress activates the endothelium, which there upon expresses adhesion molecules i.e. ICAM-1, to which circulating monocytes bind via their Mac-1 receptor. Monocytes extravasate into perivascular tissue, differentiate to macrophages and finally secrete growth factors (such as FGF-2) and cytokines (e.g. MCP-1) that attract further monocytes and stimulate proliferation of smooth muscle cells and endothelial cells.

(Schirmer et al., 2009)

Fluid shear stress triggers after arterial occlusion a cascade of signals, which mediate arteriogenesis. A number of cell types such as monocytes/ macrophages, T-cell lymphocytes, mast cells and stem cells have been suggested to play a role in this process (Schaper et al., 1976, Heil et al., 2004, van Weel et al., 2007). However, the

sequence of events leading from initial shear stress to remodelling of arterial collaterals and to an increase in reperfusion is so far only poorly understood.

### **1.3. The role of leukocytes in arteriogenesis**

#### **1.3.1 Monocytes and macrophages**

*Monocytes and macrophages* were the first bone marrow derived cells shown to play a role in arteriogenesis (Schaper et al., 1976). Monocytes facilitate arteriogenesis and their suppression delays arteriogenesis significantly (Schaper and Scholz, 2003). The upregulation of chemokine MCP-1 on the endothelium during arteriogenesis attracts monocytes via integrin receptor Mac-1. The attracted monocytes finally adhere to the endothelium and extravasate to the perivascular space (Schaper et al., 1976). In the vicinity of collateral arteries monocytes mature to become macrophages. (Arras et al., 1998, Scholz et al., 2000, Stabile et al., 2006). Macrophages release proteases like matrix metalloproteinases (MMP)-2 and MMP-9, which digest matrix and internal elastic lamina, relevant for outward remodelling of the collateral vessel (Tyagi et al., 1996, Haas et al., 2007, Kovanen, 2007). Macrophages also serve as important sources for cytokines like tumor necrosis factor (TNF)- $\alpha$ , which has been shown to enhance arteriogenesis (Hoefer et al., 2002). Furthermore macrophages release growth factors including fibroblast growth factor (FGF-2), and transforming growth factor (TGF)- $\beta$  which induce endothelial and smooth muscle cell proliferation (Arras et al., 1998, Heil et al., 2002, Deindl et al., 2003). In addition, enhancing chemoattraction of monocytes to the region of collateral artery growth leads to enhanced arteriogenesis and significant improvement of limb perfusion, whereas lack of circulating monocytes impair arteriogenesis and limb perfusion (Heil et al., 2002).

### **1.3.2. T-cell lymphocytes**

T-lymphocytes have been shown to promote arteriogenesis (Stabile et al., 2003). In this study, a reduced number of macrophage and an impaired perfusion recovery by 25% were shown in CD4<sup>-/-</sup> mice after femoral artery ligation. Additionally, CD4<sup>+</sup> T cells depleted mice exhibited a significantly impaired blood flow restoration (van Weel et al., 2007). In another study CD8<sup>-/-</sup> mice exhibited an attenuated blood flow recovery in comparison to controls, and exogenous transfusion of CD8<sup>+</sup> T cells in these mice improved blood flow recovery (Stabile et al., 2006). However, another study that investigated the role of leukocyte subpopulations (T-lymphocytes and granulocytes) resulted in controversial findings, since chemoattractants specific for T-lymphocytes and granulocytes were insufficient to stimulate arteriogenesis. Only the monocyte chemoattractant factor, which recruits monocytes was shown to promote arteriogenesis (Hoefer et al., 2005).

### **1.3.3. Mast cell**

#### *1.3.3.1. The origin of mast cells*

Mature mast cells originate from multipotent haematopoietic stem cells that commit to the mast cell lineage (CD34<sup>+</sup>, c-kit<sup>+</sup>, FcεRI<sup>-</sup>) in the bone marrow (Kirshenbaum et al., 1991). Progenitor mast cells leave the bone marrow and circulate in the blood as CD34<sup>+</sup> precursor cells (Kitamura and Ito, 2005). In the presence of specific chemotactic signals, such as stroma cell derived factor (SDF)-1α, mast cell precursors migrate across the vascular endothelium into peripheral tissues involving their chemokine receptor CXCR4 (Lin et al., 2001). Depending on the site of tissue infiltration and under the influence of stem cell factor (SCF, a c-kit ligand) mast cell



precursors proliferate and differentiate either into connective tissue-type or mucosal-type mast cells (Costa et al., 1996, Oskeritzian et al., 2005) (figure 3).

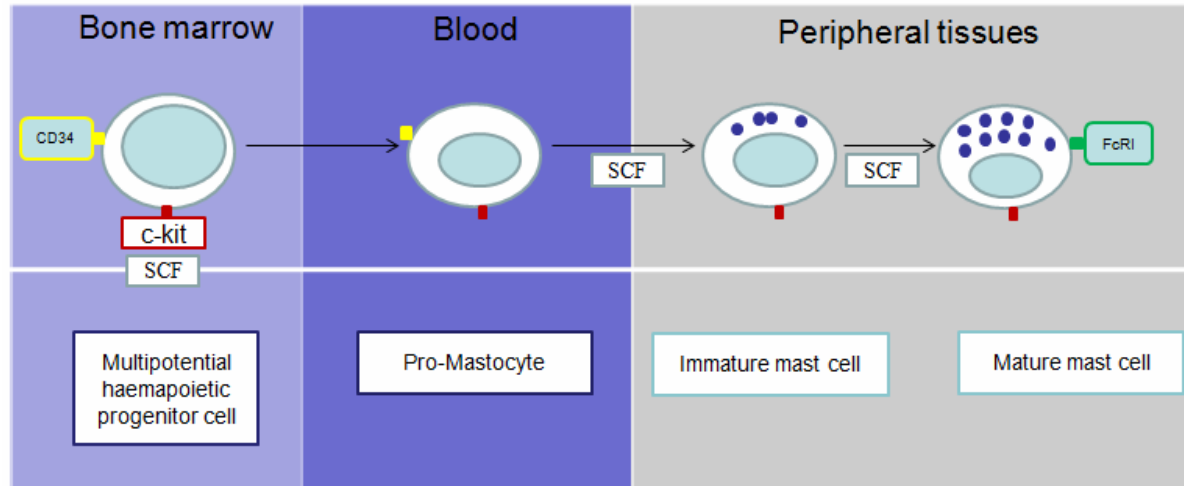


*Figure. 3. Mast cell differentiation and maturation*

Diagram illustrating important stages of mast cell differentiation and maturation under the influence of SCF. Mast cells differentiate from the hematopoietic progenitors in the bone marrow to pro-mastocytes, which enter the blood vessel and finally mature in the peripheral tissue, especially in the vicinity of blood vessels.

#### 1.3.3.2. Mast cell activation

The two known pathways of mast cell activation are IgE dependent and IgE independent pathways. IgE dependent is the widely known pathway of mast cell activation through its high affinity receptor FcεRI (Blank et al., 1989). Cross-linkage of IgE by direct interaction of IgE with allergens initiates mast cell activation. The pathways that are IgE independent do not involve the mast cell receptor FcεRI. They are activated by polybasic molecules, such as compound 48/80 and by polymyxin B (Lagunoff et al., 1983), by neuropeptides such as substance P, nerve growth factor, neurotensin and vasoactive intestinal polypeptide (Mazurek et al., 1986, Li et al.,

2012) and also by reactive oxygen species (Brooks et al., 1999, Santos et al., 2000). Mast cells have the ability to release several mediators, which initiate both immunological and non-immunological responses. However, it is so far unknown, whether mast cells are activated during arteriogenesis.

#### *1.3.3.3. Mast cell derived mediators*

Mast cells contain a wide variety of preformed mediators that are secreted upon mast cell activation. These preformed mediators include histamine, proteases (i.e. tryptase and chymase), growth factors (i.e. platelet-derived growth factor (PDGF), fibroblast growth factor (FGF)-2 and transforming growth factor (TGF)- $\beta$ ) and cytokines (i.e. tumor necrosis factor (TNF)- $\alpha$ , monocyte chemoattractant molecule (MCP)-1, and granulocyte monocyte–colony stimulating factor (GM-CSF)). Most of these mediators have been shown to promote arteriogenesis when applied exogenously (Schwartz et al., 1987, Falus and Meretey, 1992, Qu et al., 1995, Ito et al., 1997, Buschmann et al., 2001, Hoefer et al., 2002, Cao et al., 2003, Grundmann et al., 2005, de Paula et al., 2009). In addition to the preformed mediators, activated mast cells also produce lipid mediators of which prostaglandins and leukotrienes are the major ones (Boyce, 2007) (figure 4). However, the contribution of these mast cell mediators in arteriogenesis is still unknown.

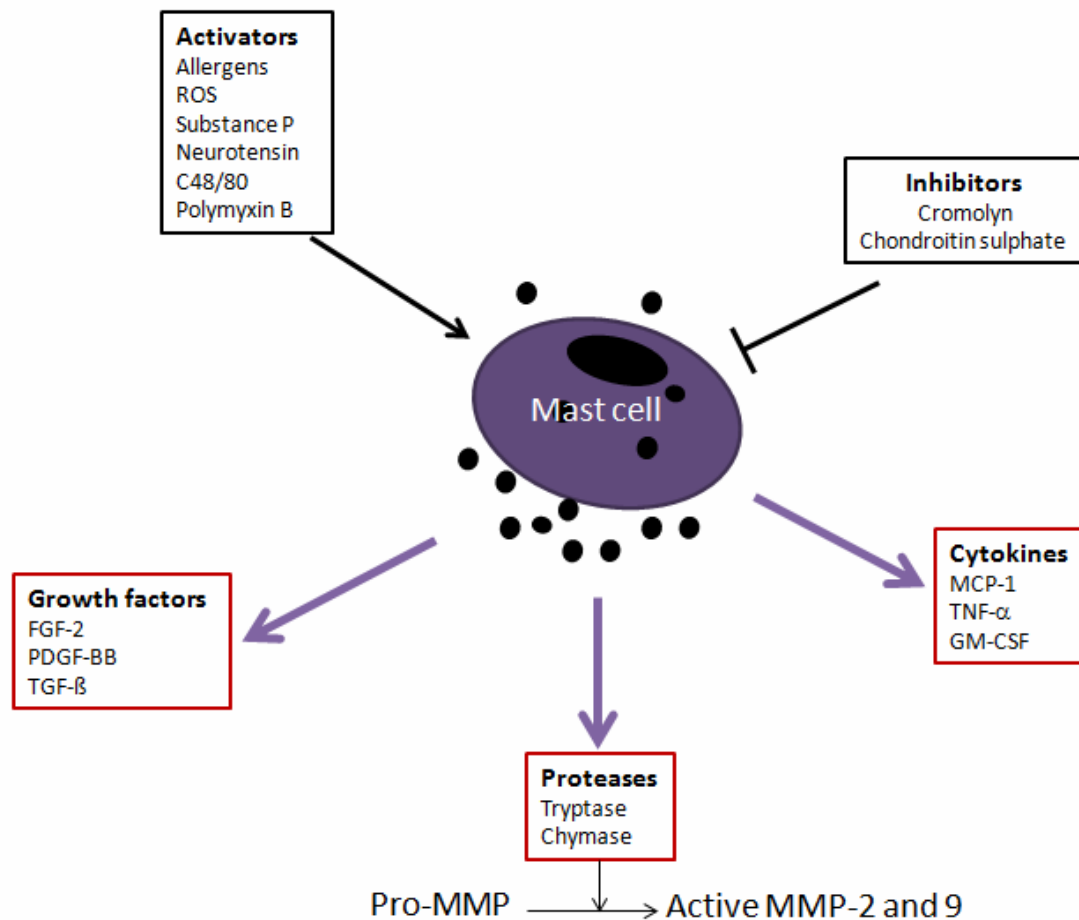


Figure 4: A sketch diagram summarising different activators and inhibitors of mast cells and mediators released by mast cells.

ROS for reactive oxygen species; C48/80 for compound 48/80; FGF-2 for fibroblast growth factor-2; PDGF-BB, for platelet-derived growth factor-BB; TGF-β for transforming growth factor-β; MMP for matrix metalloproteinase; TNF-α for tumor necrosis factor α; MCP-1 for monocyte chemoattractant protein-1 and (GM-CSF for granulocyte monocyte-colony stimulating factor.

#### 1.3.3.4. Mast cells in the vascular wall

Mast cells are localized in the close vicinity of the vascular wall. This location of mast cells in the perivascular space is promoted by the endothelial cell release of SCF (Mierke et al., 2000). Mast cells were first detected by (Wolf et al., 1998) in the

adventitia of growing collaterals, however, so far no study has investigated the role of mast cells in arteriogenesis.

#### *1.3.3.5. Mast cells, tissue remodelling and cardiovascular diseases*

Mast cell proteases such as tryptase and chymase directly degrade the connective tissue matrix of the vascular wall (Saito, 2005). In addition, the release of tryptase from mast cells activates the latent matrix-degrading metalloproteases to active MMP-2 and 9 (Gruber et al., 1989). Tryptase, chymase and MMPs altogether digest tissue matrix, collagen and internal elastic lamina of blood vessels, which is essential for tissue remodelling and repair. Furthermore, MMP-2 and 9 have been described to be involved in arteriogenesis (Cai et al., 2000).

A correlation between mast cells and MMP has been reported in a study which showed a significant increase in the number of mast cells and in MMP activity and concomitant fibrillar collagen degradation after the experimental induction of an aortocaval (arterial venous) fistula in rats. Such an increase was prevented by a treatment with cromolyn, a mast cell stabilizing drug (Marone et al., 1995, Patella et al., 1997, Brower et al., 2002). In addition, increased numbers of cardiac mast cells have been reported in patients with end-stage cardiomyopathy (Marone et al., 1995) and in animal models of hypertension (Panizo et al., 1995), mitral regurgitation (Dell'italia et al., 1997), and myocardial infarction (Engels et al., 1995). However, the contribution of mast cells in vascular remodelling during arteriogenesis has yet to be investigated. Since mast cells are capable of synthesizing and releasing several important mediators of tissue remodelling as well as growth factors, the general aim of the study was to investigate the functional role of mast cells in arteriogenesis.

#### **1.4. Aim of the study**

Arteriogenesis, the growth of pre-existing arteriolar anastomosis into natural bypasses substituting for an occluded artery, is well known to be dependent on monocytes supplying growth factors and cytokines to the growing vessel. Monocytes, however, have to be recruited to the perivascular space. Wolf et al. have found that mast cells are localized in the perivascular space growing collateral arteries (Wolf et al., 1998). From the literature it is known that mast cells contain a variety of factors that promote arteriogenesis when applied exogenously (e.g. FGF-2, TNF- $\alpha$  and MCP-1) (Ito et al., 1997, Hoefer et al., 2002, de Paula et al., 2009). Therefore, the aim of this study was to investigate whether mast cells play a role in arteriogenesis and if yes,

- a. What is the functional role of mast cell in arteriogenesis?
- b. What triggers mast cell degranulation during arteriogenesis?

## **2. MATERIALS AND METHODS**

Animal care and experimental procedures were performed in strict accordance with the National Institute of Health animal registration guidelines and were approved by the local animal care committee (Regierung von Oberbayern; Germany; protocol number Gz.55.2-1-54-2532-73-12). Animals and animal-derived materials were treated in accordance with the guide for the care and use of laboratory animals (National Institutes of Health, Publication No.85-23, revised 1996)

### **2.1. Materials**

#### **2.1.1. Animals**

Wildtype (SV129) mice were obtained from the Walter Brendel Institute, and C57Bl6 were purchased from Charles River Laboratories, Sulzfeld, Germany.

Urokinase plasminogen activator (uPA)<sup>-/-</sup> and NADPH oxidase 2 (Nox2; gp91<sup>phox</sup>; B6.129S6-Cybbtm1Din/J)<sup>-/-</sup> mice were a generously gift from from Christoph A Reichel from Walter Brendel Centre for Experimental Medicine, Munich Germany and from Norbert Weissmann of Justus-Liebig-University Giessen, Giessen Germany respectively. Both uPA<sup>-/-</sup> and Nox2<sup>-/-</sup> mice were breed originally from Charles River Laboratories, Sulzfeld, Germany. (Reichel et al., 2011, Schulz et al., 2014)

#### **2.1.2. Femoral artery ligation**

##### *Surgical instruments*

1. Suture, Vicryl 6,0 and Perma Hand Seide 4,0, ETHICON (Norderstedt, Germany)
2. Non sterile REEL silk 002, PEARSALL LIMITED (Taunton, UK)
3. FORCEPS SCIENCE TOOLS (Heidelberg, Germany)

4. FINE FORCEPS SCIENCE TOOLS (Heidelberg, Germany)
5. FINE SCISSORS SCIENCE TOOLS (Heidelberg, Germany)
6. Scalpel No. 20, FEATHER (Osaka, Japan)
7. Compress, NOBA VERBANDMITTEL (Wetter/Ruhr, Germany)
8. Cotton-tipped applicators (Puritan, Hardwood Products)
9. Temperature control unit with heating pad, FHC (Bowdoinham, USA)
10. Microscope stemi DV4 Spot, ZEISS (Jena, Germany)
11. Light source KI 1500, SCHOTT (Mainz, Germany)
12. Venofix 25G, B.BRAUN (Melsungen, Germany)
13. Injection cannula 27G and 30G, B.BRAUN (Melsungen, Germany)
14. Syringe 5 ml, B.BRAUN (Melsungen, Germany)
15. Syringe 1 ml, Microlance 23G, BECTON DICKINSON (Franklin Lakes, USA)
16. Falcon Tubes, 15 ml and 50 ml, BECTON DICKINSON (Franklin Lakes, USA)
17. Cryotube Vials, NUNC (Roskilde, Denmark)
18. Aluminium foil

#### *Materials and chemicals*

1. Sodium chloride solution 0,9%, B.BRAUN (Melsungen, Germany)
2. Cutasept F, BODE CHEMIE (Hamburg, Germany)
3. Bepanthen eye and nose cream, BAYER (Leverkusen, Germany)
4. Latex, CHICAGO LATEX (Chicago, USA)
5. Dry ice

*Anaesthesia:*

1. Medetomidin 1 mg/ml, Dorbene Vet®, FORT DODGE/PHIZER (New York, USA)
2. Midazolam 15mg/3ml, RATIOPHARM (Ulm, Germany)
3. Fentanyl® 0,5 mg, JANSSEN-CILAG (Neuss, Germany)

*Neutralisation:*

1. Altipamezol 1 mg/ml, Revertor®, CP-PHARMA (Burgdorf, Germany)
2. Naloxon 0,4 mg/ml, INRESA (Freiburg, Germany)
3. Flumazenil 0,1 mg/ml, INRESA (Freiburg, Germany)

*Laser Doppler imaging technique*

1. Laser Doppler, moorLDI2-IR, MOOR INSTRUMENTS (Wilmington, USA)
2. Isoflurane vaporiser, ABBOTT (Chicago, USA)
3. Heating chamber (self constructed)
4. Two-sided tape Nupi, tesa SE (Hamburg, Germany)

**2.1.3. Substances used for treatment**

1. 0.9% saline ( $\text{NaCl}_{(\text{aq})}$ ): B.Braun Meisungen AG Cat No. 34209
2. Compound (C) 48/80: Sigma Aldrich Cat No. C2313
3. Diprotin A (Ile-Pro-Ile): Sigma Aldrich Cat No. I9759
4. Sodium cromoglycate (cromolyn): Sigma Aldrich Cat No. C0399
5. Stem cell factor (SCF): ImmunoTools Cat No. 11343325
6. PR-68570: Tocris bioscience Cat No. 1635
7. N-acetylcystein (NAC): Sigma Aldrich Cat No. A7250



8. Ly6G; neutrophil antibody (1A8): BioXcell Cat No. BE0075-1
9. Apocynin: Santa Cruz Biotechnology, sc-203321

#### **2.1.4. Visualization of the hind limb**

1. Polysciences, Inc. Batson's No. 17 Plastic Replica and Corrosion Kit. Cat.No. 07349)
2. Maceration solution (Fa. Polysciences, Inc Cat.No. 07359)

#### **2.1.5. Histology and Immunohistochemistry**

##### *Instrumentation*

1. Embedding cassettes, 70071-series, ELECTRON MICROSCOPY SCIENCES (Hatfield, USA)
2. Tissue processors for histology, Shandon Hypercenter XP, THERMO ELECTRON
3. CORPORATION (Pittsburgh, USA) and Tissue-Tek<sup>®</sup> VIP<sup>™</sup>, SAKURA (Tokyo, Japan)
4. Embedding station, AP280-1, MICROM/ THERMO FISHER SCIENTIFIC (Rockford, USA)
5. Sliding microtome, JUNG (Heidelberg, Germany)
6. Microscope slides (Menzel), superfrost Plus, THERMO FISHER SCIENTIFIC (Rockford, USA)
7. Tissue Stainer COT 20, MEDITE (Burgdorf, Germany)
8. Leica DMD108 microscope with an integrated camera, LEICA (Wetzlar, Germany)
9. ImageJ software, version 1.45. (Wayne Rasband, NIH, USA)

### *Chemicals*

1. Phosphate buffered formalin 4% (PFA), in-house pharmacy
2. Ethanol 70%, 96% and 100%, in-house pharmacy
3. Xylol55, MERCK (Darmstadt, Germany)
4. Xylene, MERCK (Darmstadt, Germany)
5. H2O2 7,5%, MERCK (Darmstadt, Germany)
6. TRS 6, DAKO (Glostrup, Denmark)
7. Target Retrieval Solution, DAKO (Glostrup, Denmark)
8. Avidin-biotinylated enzyme complex rat IgG, VECTOR (Burlingame, USA)
9. Hematoxylin Gill's sedimentary coefficient formula, VECTOR (Burlingame, USA)
10. Kaiser sedimentary coefficient glycerol gelatin, VECTOR (Burlingame, USA)
11. ImmPress Reagent Kit anti-goat IgG, VECTOR (Burlingame, USA)
12. Streptavidin AP, VECTOR (Burlingame, USA)
13. Chromogen red, AEC (Fa. Invitrogen, Cat. No. 00-1122)
14. Dako Ark™ Peroxidase Kit, DAKO (Glostrup, Denmark)
15. Vectastatin ABC-Kit Elite Rat IgG (Fa. Vector, Cat. No. PK6104)

### *Haematoxylin and Eosin staining*

1. Haematoxylin (Fa. Merck Cat.No. 1.09249.2500)
2. Eosin solution (Fa. Chroma Cat.No. 2C 140)

### *Giemsa staining*

1. May-Grünwald solution (Merck cat No. 1.01424)
2. Giemsa solution (Fa. Applichem, Cat.No. A0885)

### *Primary and secondary antibodies*

1. CD45, rat anti-mouse, Fa. BD PHARMINGEN, Cat. No. 550539

2. Ki67, rat anti-mouse, Fa. Dako, Cat No. M7249
3. CD31 rat anti-mouse, Fa. Santa Cruz Biotechnology, Cat.No. sc-1506
4. Secondary antibody, biotinylated anti-rat IgG (Fa. Vector, Cat.No. BA 4001).

*Buffers and solution preparation*

1. Adenosine phosphate buffered saline, containing 0,1% adenosine, SIGMA-ALDRICH (St. Louis, USA) and 0,05% bovine serum albumin, SIGMA-ALDRICH (St. Louis, USA)
2. 1L of 10x Tris Buffered Saline (TBS):  
-24.2 g Trizma base ( $C_4H_{11}NO_3$ ) and 80 g sodium chloride (NaCl) to 1 L of distilled water. pH adjusted to 7.6 using concentrated HCl.
3. 1L of 10x Phospahte Buffered Saline (PBS):  
-80g of NaCl, 2g of KCl, 14.4g of  $Na_2HPO_4$  and  $KH_2PO_4$  were added in 1L of distilled water and finally adjusted to a pH of 7.4.
4. 1L of antigen retrieval, 10mM citrate buffer  
-2.94g of sodium citrate trisodium salt dehydrate ( $C_6H_5Na_3O_7 \cdot 2H_2O$ ) were added to 1L of distilled water and the pH adjusted to 7.4.
5. 3% Hydrogen Peroxide.  
-10 ml of 30%  $H_2O_2$  were added to 90 ml of distilled water.
6. 5% BSA  
-5mg of bovine serum albumin were added to 100ml of distilled water.
7. 2.5 ml of ABC-kit solution. (Vectastatin ABC-Kit Elite Rat IgG (Fa. Vector, Cat. No. PK6104)  
-1 drop of solution A was added to 2.5ml of PBS followed by vortex, then one drop of substance B was added and again the solution were vortexed.

8. 5ml of chromogen AEC-kit. (Fa. Invitrogen, Cat. No. 001122)

-2 drops of buffer, 3 drops of AEC and 3 drops of H<sub>2</sub>O<sub>2</sub> were added to 5 ml of distilled water and vortexed.

9. Cell-Lysis-Buffer

-25mM Tris (Ph 7.5)

-1% Triton X-100

-0,5mM Ethylenediaminetetraacetic acid (EDTA)

-150mM Sodium chloride NaCl

-10mM Sodium Fluoride (NaF)

-1% Phenylmethanesulfonyl fluoride (PMSF)

#### **2.1.6. Antibodies and isotopes controls used in fluorescence-activated cell sorting (FACS)**

S/N	Antibodies	colour	Amount	Company	Expression
1	CD45 clone	APC-Cy7	1µl	BD. Cat.No. 557659	leukocytes
2	CD11b clone	FITS	1µl	eBioscience. Cat.No. 11-0112	Monocytes, granulocytes, macrophages and activated lymphocytes
3	Gr-1 clone	PE	0,2µl	BD. Cat.No. 553128	Neutrophils
4	CD115 clone	APC	0,3µl	eBioscience. Cat.No. 17-1152	Monocytes and macrophages
5	CD8a clone	PE-Cy5	1µl	eBioscience. Cat.No. 25-0081	CD8 T-cells, thymocytes
6	CD4 clone	AlexaFluor700	1µl	eBioscience. Cat.No. 56-0041	CD4 T- cells
7	F4/80 clone	eFluor450	2.5µl	eBioscience. Cat.No. 48-4801	Macrophages

### Isotypes controls

S/N	Isotypes	colour	Amount/probe	Company
1	IgG2bk	APC-Cy7	1µl	BD. Cat.No. 552773
2	IgG1k	FITS	1µl	eBioscience. Cat.No. 11-4301
3	IgG2bk	PE	0,2µl	BD. Cat.No. 553989
4	IgG2ak	APC	2,5µl	eBioscience. Cat.No. 17-4321
5	IgG2ak	PE-Cy5	1,25µl	eBioscience. Cat.No. 45-4321
6	IgG2bk	AlexaFluor700	0.625µl	eBioscience. Cat.No. 56-4031
7	IgG2ak	eFluor450	2.5µl	eBioscience. Cat.No. 48-4321

- BD FACS-Lysing solution: BD biosciences Cat No. 349202
- Collagenase II: Biochrom Cat No. C2-22
- FACS machine: Beckman coulter, Gallios flow cytometer 2/8
- Analysis software: Kaluza version 1.2

### 2.1.7. Commercial kits for MMP, TNF-alpha, MCP-1, SDF-1alpha and serum protein array

The procedures of the commercial kits are unique and were performed according to the individual manufacturer's instructions

- SensoLyte 520 Generic MMP Assay Kit \*Fluorometric\* (Fa. AnaSpec, Cat No. 71158).
- Mouse TNF alpha ELISA Ready-SET-Go!® Catalog Number: 88-7324
- Mouse MCP-1 ELISA Ready-SET- Go!® Catalog Number: 88-7391
- Mouse CXCL12/SDF-1alpha Immunoassay; Cat. No. MCX120 (serum)
- Mouse SDF-1alpha ELISA Kit; Cat. No. ELM-SDF1alpha-001 (collaterals)
- Mouse serum protein array; Proteome Profiler TM Mouse angiogenesis antibody array. (Fa R&D Systems, Cat No. ARY015).

### **2.1.8. RNA extraction**

#### Material:

- TRIzol (Ambion, Life technologies, 155596026, store at RT)
- Chloroform (Sigma-aldrich 372978, store at 4°C)
- Phenol solution, saturated with 0,1M citrate buffer pH4,3 (Sigma-aldrich P4682, store at 4°C)
- Isopropanol (Sigma-Aldrich, I9516) and 70% and 80% Ethanol (Sigma-Aldrich, I485143932) diluted with pure H<sub>2</sub>O (Aqua injectabilia) (4°C, -20°C)
- RQ1 DNase I Promega (M6101)
- 10mM Tris HCl pH 7,5
- RNeasy MinElute cleanup kit (74204, Qiagen)

#### Machines

- Homogenisator Speed Mill PLUS from Analytik Jena
- Eppendorf centrifuge: (Cat No. 5424, Hamburg, Germany).
- Eppendorf BioPhotometer (Eppendorf, 6915636)

### **2.1.6. cDNA synthesis and qRT-PCR**

#### Material:

- 1st strand cDNA synthesis kit (Roche, 11483188001)
- RNA samples
- Power Sybr Green master mix (Life technologies, 4368577)

#### Machines

- Thermal Cycler 2720 Applied Biosystems
- StepOnePlus (Life technologies, 5835124)
- Analysis software: StepOne software version 2.2.2

*a. Primers*

Primer	Sequence (5'--> 3')
18s forward	5`-GGACAGGATTGACAGATTGATAG-3`
18s reverse	5`-CTCGTTCGTTATCGGAATTAAC-3`
MCP1 forward	5`-CTCAAGAGAGAGGGTCTGTGCTG-3`
MCP1 reverse	5`-GTAGTGGATGCATTAGCTTCAG-3`

## 2.2. Methods

### 2.2.1. Surgical procedures to induce arteriogenesis

General anaesthesia was induced in mice by a sub-cutaneous injection of a combination of midazolam (5 mg/kg), medetomidine (0.5 mg/kg) and fentanyl (0.05 mg/kg). The depth of anaesthesia was controlled and accepted if the response to a toe pinch was absent. Mice were monitored with a rectal probe and body temperature was maintained at 37°C with a homoeothermic heating pad connected to a rectal temperature probe (FCH-BOWNDONHAM, ME04008 USA). Both inguinal regions were sprayed with skin disinfectant and the hairs were shaved with a sterile surgical blade. Afterwards mice were fixed on a working table using sole tapes with the foot sole facing upward in order to expose the inguinal areas.

The skin in the inguinal area was opened on either side by a surgical incision. The underlying fat tissues were placed aside with minimal tissue damage and without injuries of the vessels. Under a light microscope, the femoral artery, veins and nerves were exposed. The femoral artery was then separated and a loop was made around the femoral artery with a suture (7/0 braded). On the right limb the suture was tightened with three nods distal to the *a. profunda femoris* branch and proximal to the *a. genu descendens*. On the left sham operated side, the suture was placed under the vessel without a nod and remained there. Finally, the skin was sutured using 6/0Vicryl on either side after the wound had been irrigated with sterile normal saline. Mice were then injected sub-cutaneously with an antidote using a mixture of Naloxon, Flumazenil and Antipamezol, and left freely to recover.



### 2.2.2. Experimental design

Arteriogenesis was induced in 6 – 8 weeks old mice by surgical occlusion of the right femoral artery distal to the *a. profunda femoris* and proximal to the *a. genu descendens* (figure 1). On the left, the sham operated side, the suture was placed loosely under the femoral artery but no nod was tied. Mice were randomly assigned to control and experimental groups, as follows: in the control group, mice were treated with 50µl of a 0.9% saline ( $\text{NaCl}_{(\text{aq})}$ ) injected either subcutaneously in the inguinal region of both hind limbs or intraperitoneally corresponding to the route of treatment in the experimental group. Experimental mice were subjected to different treatments in which the researcher was non-blinded: a first group received daily intraperitoneal (i.p.) injections of a mast cell stabilizer (cromolyn, 20mg/kg per day, (Liao et al., 2010)) starting 3 days prior to ligation until day 20 after ligation. A second group received i.p. injections of diprotin A (70 µg/kg/day), a substance known to enhance SDF-1 $\alpha$  levels due to inhibition of enzymatic activity of dipeptidylpeptidase (DPP) IV (Zaruba et al., 2009, Zhang et al., 2010), twice a day starting 3 days prior to ligation until day 20 after ligation. A third group received subcutaneous injections in the right and left inguinal region of compound (C) 48/80 (1mg/kg/inguinal region, (Tang et al., 2009)), a mast cell degranulator, immediately after ligation, at days 1, 2 and 3 and again at days 7, 8 and 9 after ligation. A fourth group received i.p. injections of stem cell factor (SCF; 50µg/kg/day, (Keller et al., 2006)), which promotes mast cell differentiation and proliferation, once a day starting 3 days before ligation until day 20 after ligation. A fifth group received diprotin A + cromolyn and a sixth group received a combination of C 48/80 + diprotin A. A seventh group received a combination of diprotin A + C 48/80 + SCF (figure 5 and 6). Other substances were also applied, including an inhibitor of substance P release (RP-67,580; 2mg/kg i.p. twice a day

starting 3 days before ligation (Kennedy et al., 1997)), an inhibitor of the NADPH oxidases (apocynin; 0.25mg/ml = 50mg/kg/day in drinking water; starting 3 days before ligation (Sovari et al., 2008, Liu et al., 2013). N-acetylcystein an anti-oxidant through increasing cellular glutathione levels (Zafarullah et al., 2003, Reliene et al., 2004) was also added to the drinking water (6 mg/ml =1g/kg/day; starting 3 days before ligation). Urokinase plasminogen activator (uPa; 0.2mg/kg; intramuscular injection, (Reichel et al., 2011)) was applied once after femoral ligation. The neutrophil depletion antibody 1A8 (100 µg/kg) was injected i.p 2 days before ligation, immediately after ligation and again at days 2, 4 and 6 after ligation (Drechsler et al., 2010).

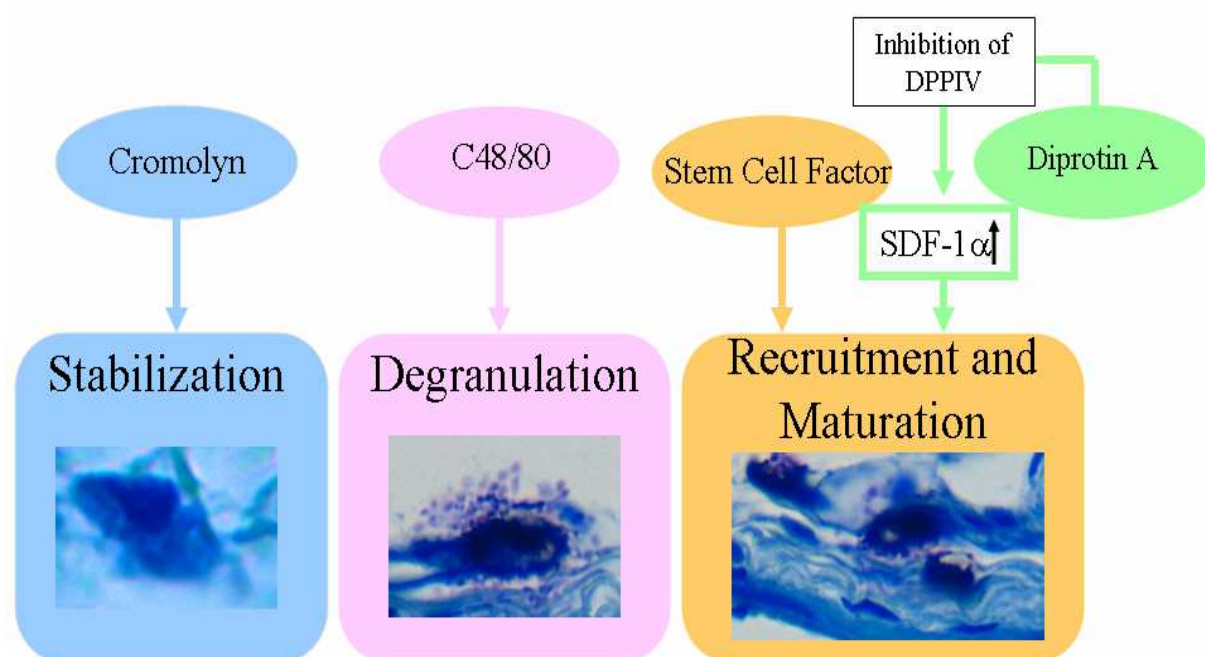
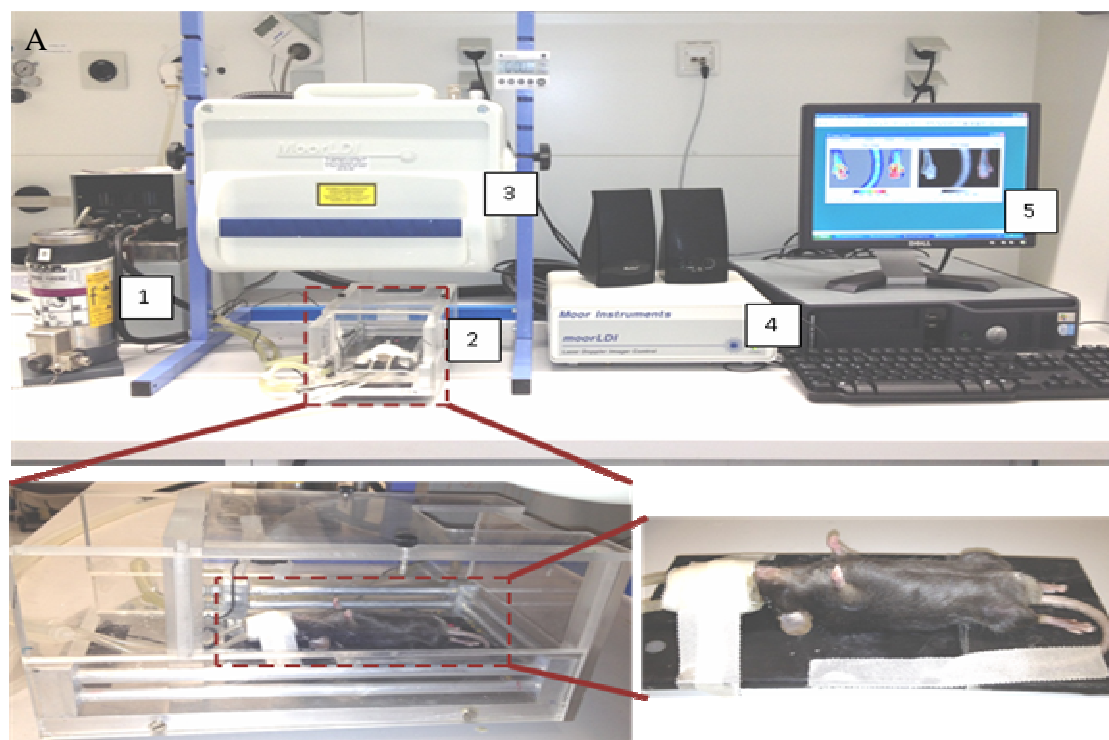


Figure 5. Showing images of mast cell(s) in response to the application of different substances. Dipeptidylpeptidase (DPP)-IV, stromal cell derived factor (SDF)-1α, Compound (C) 48/80.

### 2.2.3. Measurements of hind limb blood flow

Blood flow in the distal hind limbs of mice was recorded in vivo with a Moor Laser

Doppler Perfusion Imager (MLDI 5063, Moor Instruments Ltd., Devon, UK). For these measurements, mice were first anaesthetized with 1.5% of isoflurane supplemented with 2.0 l/min of oxygen and then placed in supine position in a temperature-regulated chamber (37°C) for 10 minutes before the onset of measurements. A laser Doppler imager was used to quantify the blood flow in the plantar surface within defined regions of interest (ROIs). The ratios of occluded over non-occluded (sham) values were recorded for comparison between control and experimental groups. Measurements were performed before, immediately after ligation and at days 3, 7, 14 and 21 after ligation (figure 6). In one of the experiment, the measurement was performed at 6, 12, 24 and 48 hours after femoral ligation. After the last laser Doppler measurements, animals were anaesthetized with isoflurane and killed by cervical dislocation.



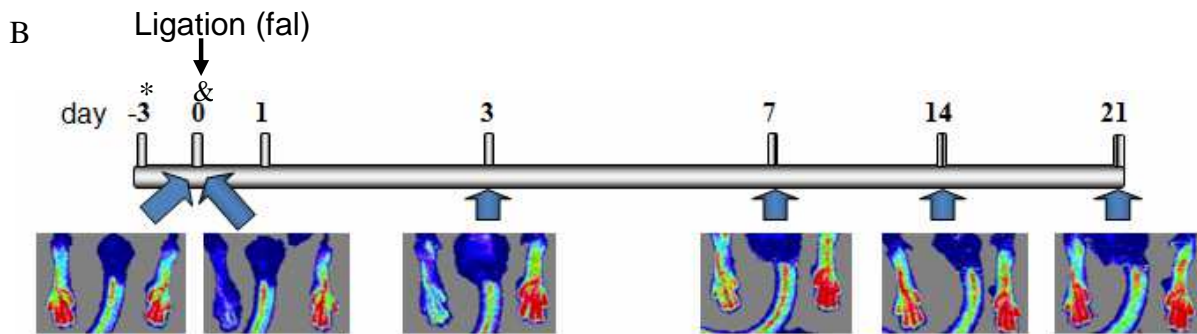


Figure 6. LDI perfusion measurements in the distal hind limb and application of substances:

- (A) Experimental setting of hind limb perfusion measurements showing: 1. Isoflurane gas jar which supplies isoflurane, 2. Regulated heating chamber (37°C), 3. Laser scanner, 4. Processor, 5. Programmed computer recording the scanned hind limb blood flow images for measurements.
- (B) Laser Doppler scan images of hind limbs of mice showing progressive blood flow perfusion recovery on the occluded side (left) at different time points before occlusion, after femoral artery ligation (fal) and at days 3, 7, 14 and 21 in comparison to sham operated side (right – constantly perfused with blood).
- And application of
- & Compound 48/80 (1mg/kg subcutaneous in the left and right inguinal region starting immediately after ligation until day 3, then day 7 to day 9) -> degranulation of mast cells.
  - \* SCF (50µg/kg/day i.p.daily starting 3 days before ligation) -> maturation of mast cells.
  - \* Diprotin A (70µg/kg/day i.p. daily starting 3 days before ligation) -> SDF-1α ↑-> recruitment of mast cells.
  - \* Cromolyn (20mg/kg/day i.p. daily starting 3 days before ligation) -> blocking of mast cell degranulation.

#### 2.2.4. Visualization of the hind limb arterial system

For a visualization of the hind limb arteries, we produced plastic replica of the hind limb arterial system. Seven days after femoral artery ligation mice were

anaesthetised and the hind limbs were perfused with cast solution (Polysciences, Inc. Batson's No. 17 Plastic Replica and Corrosion Kit. Cat.No. 07349) via an aortic cannula. The cast solution was prepared by dividing the monomer base solution A into two parts (10ml each). Afterwards the pigment was added to base solution A in the amount of 10% and stirred vigorously prior to adding the catalyst and promoter. To the first part we added 4 ml of catalyst and stirred the mixture. To the second part we added 3 drops of promoter C to base solution A and mixed slowly with a magnetic stirrer. Finally the two solutions were added together and stirred. The final solution was then injected with a cannula and a 20 ml polyethylene syringe. The specimens were then kept in cold ice for 3 hours before we placed them at 50°C in a maceration solution (Fa. Polysciences, Inc Cat.No. 07359) for about 3 hours to corrode. Afterwards, the muscle tissue was slowly removed and the images were captured using Leica microscope M 205 FA.

#### **2.2.5. Tissue perfusion, fixation and isolation**

For molecular genetic studies and histological analysis, we isolated collateral arteries as well as adductor and gastrocnemius muscles of the hind limbs of control and experimental mice. Mice were anaesthetized, placed in supine position under the microscope with the limbs spread and fixed. For molecular biological studies, the abdominal cavity was opened to expose the abdominal aorta below the renal branches and to separate it from fat tissue. Then the aorta was cannulated (figure 7 A) and the inferior vena cava was cut. Catheters were made from a winged infusion set cutting off the tip of the needle and blunting the end of the needle. A white latex contrast medium (compound of natural and synthetic latex; Chicago latex, Crystal lake, IL 60039) was then injected through the catheter (figure 7 B). Collateral arteries from experimental and control animals were excised, snap-frozen, and stored at

–80°C for further investigations.

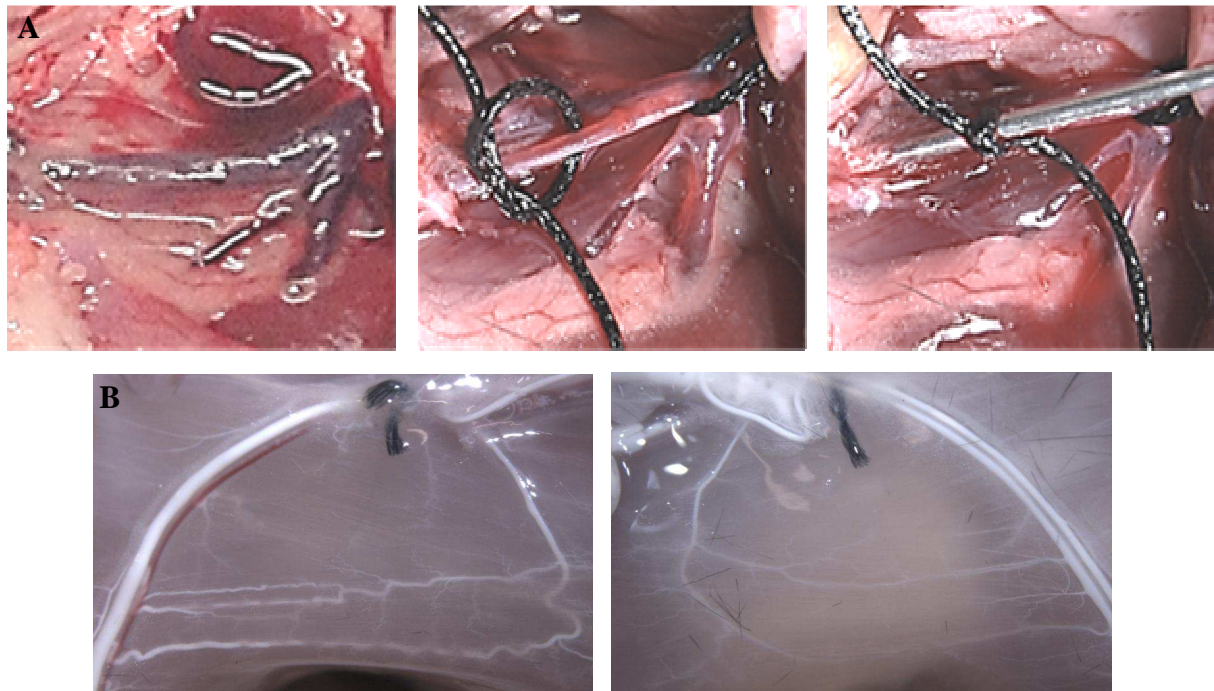


*Figure 7. Isolation of hindlimb collaterals*

(A). Images showing several cannulation steps in the abdominal aorta. (B). Images showing superficial collateral arteries 7 days after ligation (left) and sham operated limb (right). The contrast medium latex (white) was injected for visualization of collaterals during isolation.

For isolation of adductor and gastrocnemius muscles for histological analyses, the cannula was inserted through a small cut in the abdominal aorta and the hind limb vessels were perfused for 3 minutes with a dilatation buffer containing 0.1 % adenosine (Sigma) and 0.5 % bovine serum albumin (BSA; Sigma) in phosphate-buffered saline (PBS; with pH 7.4). Adductor muscles of both hind limbs (ligated and non-ligated) were cut in a triangular comprising the area supplied by collaterals of the femoral artery. The basis of the triangle was cut proximally to the A. profunda femoris. The other side was cut laterally from the A. femoralis towards the knee, and the third side connecting the knee with the medial side of the A. profunda femoris

(figure 8 A and B). The gastrocnemius muscle was isolated by cutting the two heads located close to the knee joint and by detaching the muscle from its distal attachment via the Achilles tendon (figure 8 C).

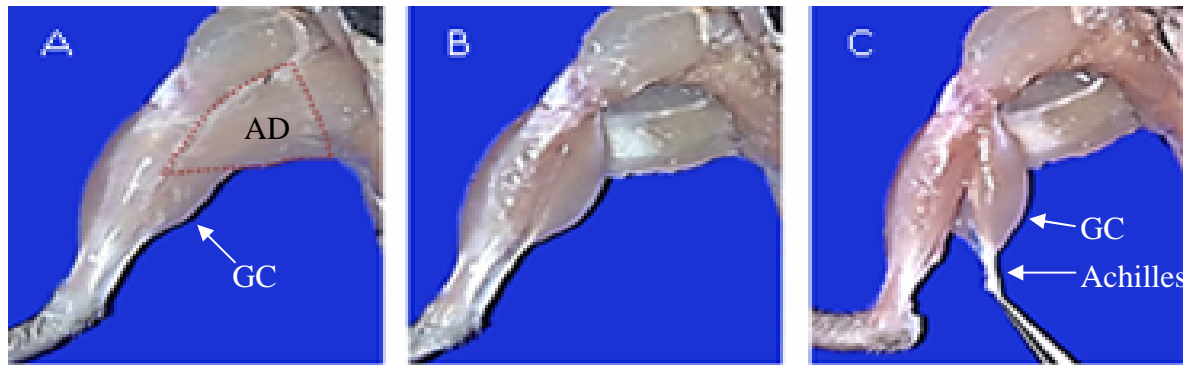


*Figure 8: Isolation of hind limb adductor and gastrocnemius muscles.*

A: Triangular cut during the isolation of adductors (AD) as seen by red dots.

B: After isolation of adductor muscle from the mouse hind limb.

C: Isolation of gastrocnemius (GC) muscle.

#### **2.2.6. Histology and immunohistochemistry**

For a detailed microscopic examination of adductor and gastrocnemius muscles, we prepared histological sections for an assessment of perivascular mast cells, for collateral diameter measurements and for an analysis of the tissue damage in the distal hind limb. In addition, for an identification of perivascular leukocytes, vascular cell proliferation and capillaries we performed immunohistochemical experiments.

Isolated adductor muscles were fixed in 4% paraformaldehyde solution for 30 minutes. Then the muscles were washed with running tap water and immersed in 70% alcohol for 24 hours. The adductor and gastrocnemius muscles were processed in an automatic tissue processor (Thermo Fischer Scientific; Shandon citadel 1000, Dreieich, Germany) for 12 hours. Tissues were cut transversally in 2 mm thick probes

and placed in labeled embedding cassettes containing liquid paraffin. The paraffin in the cassettes was left to solidify on a cooling plate (-4°C) for 30 minutes. For histological and immunohistological analysis, tissues were sectioned in 5µm thick slides using a CM 3000 cryomicrotome (Leica, Germany) and placed on microscope slides. The slides containing the sections were left to dry at room temperature for 24 hours before further processing.

#### **2.2.6.1. Histology**

The slides containing the sections were placed in a rack then followed by a series of washes to remove the paraffin (deparaffinization):

1. Xylene 2: for 5 minutes
2. Xylene 1:1 with 100% ethanol: 5 minutes
3. 100% ethanol: 15 minutes
4. 96% ethanol: 15 minutes
5. 70 % ethanol: 15 minutes
6. Then washed in running cold tap water to rinse and to avoid drying of the sections.

##### **2.2.6.1.1. Haematoxylin and eosin staining**

For morphological identification and measurement of collateral diameters as well as distal hind limb tissue damage, we stained the tissues with haematoxylin and eosin.

After deparaffination, 5µm sections were immersed in haematoxylin (Fa. Merck Cat.No. 1.09249.2500) for 1 minute and then rinsed with tap water until the running water was clear. Subsequently the sections were transferred in an eosin solution (Fa. Chroma Cat.No. 2C 140) for 1-2 minutes and then rinsed with tap water until the running water was clear. Afterwards slides were dehydrated in ascending alcohol solutions (70% for 3 min, 96% for 3 min, 100% for 5 minutes), and then cleared with



xylene (2 X for 10 minutes). Finally the slides were mounted on cover slip onto a labeled glass slide using Eukit (Fa. O. Kindler GmbH & Co) for histological examination.

#### **2.2.6.1.2. Giemsa staining**

In order to identify and quantify degranulated and non-degranulated mast cells in the region around collateral arteries, both adductor and gastrocnemius muscles were stained with Giemsa. Following deparaffination, 5µm sections were immersed in May-Grünwald solution (ratio of 1:8 with distilled water; Merck cat No. 1.01424) for 10 minutes and then washed with running tap water. The slides were then stained with Giemsa (Fa. Applichem, Cat.No. A0885) for 6 minutes, washed with running tap water and counterstained with 1.5% acetic acid. Afterwards, the stained tissues were subsequently transferred in ethanol (75% then 95% and then 100%; 1-2 minutes each). The slides were then transferred to xylene for about 5 minutes followed by mounting with cover slips using eukit. Degranulating mast cells were identified by the presence of stained granules outside of its cell membrane.

#### **2.2.6.2. Immunohistological staining**

With the help of immunohistology I stained tissue sections of adductor for an identification of perivascular leukocytes and for the detection of vascular cell proliferation. In the gastrocnemius muscles I investigate the number of capillaries per muscle fibre and for the detection of leukocyte infiltration in the gastrocnemius muscle.

For a heat induced epitope retrieval, a pressure cooker containing a target retrieval buffer (citrate buffer pH 6.0; Fa.Dako,Cat.No. S1699) at a molar concentration of 10 mM was placed on a hot plate to boil. The slides were then immersed in a boiling citrate buffer for 10 minutes until the cooker reached full pressure. Then the rack was

removed and the slides were cooled at room temperature for 20 min followed by washing twice in 10 x tris buffered saline (TBS) at pH 7.6.

#### **2.2.6.2.1. Ki67 staining**

Ki67 was used to identify proliferating endothelial and smooth muscle cells of collaterals in the hind limbs. Following antigen retrieval, sections were incubated in 3% hydrogen peroxide ( $H_2O_2$ , Roth, cat # 7070.1) for 15 minutes and then washed twice in 10 x TBS. Each section was then blocked with 100 $\mu$ l of 5% bovine serum albumin (BSA) for 1 hour. The blocking solution was removed and the sections were incubated with 200 $\mu$ l of a primary antibody Ki-67 (Fa. Dako, Cat.No. M7249) in a 1:100 dilution over night at 4°C. The next day, sections were removed from 4°C to room temperature and 1 hour later they were washed with 10 x TBS for 5 minutes in a shaking plate at a rate of 100/min. The sections were then incubated with secondary antibody biotinylated anti-rat IgG (Fa. Vector, Cat.No. BA 4001) in a 1:100 dilution for 1 hour and then washed again 2 x 5 minutes using 10 x TBS. Sections were incubated with ABC-kit solution for 1 hour (Vectastatin ABC-Kit Elite Rat IgG (Fa. Vector, Cat. No. PK6104), then washed twice with 10 x TBS. The sections were then covered with chromogen red AEC (Fa. Invitrogen, Cat.No. 00-1122) for 10 minutes, then washed two times with 10 x TBS followed by counterstaining with hematoxylin for 10 seconds and mounted with Kaiser glyceringelatin (Fa. Merck, Cat.No. 1.09242.0100). Images were taken with a two photon microscope (Leica DMD108, Leica Microsystems CMS GmbH, Wetzlar Germany).

#### **2.2.6.2.2. CD45 staining**

For the identification and quantification of perivascular leukocytes in the hind limb collaterals and infiltrated leukocytes in the gastrocnemius muscle, tissue sections of

adductors and gastrocnemius muscles were stained with CD45. Following antigen retrieval, sections were incubated in 3% hydrogen peroxide (H<sub>2</sub>O<sub>2</sub>, Roth, cat # 7070.1) for 15 minutes and then washed twice in 10 x TBS. Each section was then blocked with 100µl of 5% bovine serum albumin (BSA) for 1 hour. The blocking solution was removed and the sections were incubated with 200µl of a primary antibody CD45 (Fa. Dako, Cat.No. M7249) in a 1:100 dilution over night at 4°C. Next day, sections were removed from 4°C to room temperature and 1 hour later they were washed with 10 x TBS for 5 minutes on a shaking plate at a rate of 100/min. The sections were then incubated with secondary antibody biotinylated anti-rat IgG (Fa. Vector, Cat.No. BA 4001) in a 1:100 dilution for 1 hour and then again washed 2 x 5 minutes using 10 x TBS. Sections were incubated with ABC-kit solution for 1 hour (Vectastatin ABC-Kit Elite Rat IgG (Fa. Vector,Cat. No. PK6104), then washed twice with 10 x TBS. The sections were then covered with chromogen red AEC (Fa. Invitrogen, Cat.No. 00-1122) for 10 minutes, then washed two times with 10 x TBS followed by counterstaining with hematoxylin for 10 seconds and mounted with Kaiser glyceringelatin (Fa. Merck, Cat.No. 1.09242.0100). Images were taken with a two photon microscope (Leica DMD108, Leica Microsystems CMS GmbH, Wetzlar Germany).

#### **2.2.6.2.3. CD31 staining**

CD31 was used to identify the sprouting of capillaries endothelial cells in the gastrocnemius muscle of both control and experimental animals three days after femoral artery ligation. Following antigen retrieval, sections were incubated in 3% hydrogen peroxide (H<sub>2</sub>O<sub>2</sub>, Roth, cat # 7070.1) for 15 minutes and then washed twice in 10 x TBS. Each section was then blocked with 100µl of 5% bovine serum albumin

(BSA) for 1 hour. The blocking solution was removed and the sections were incubated with 200µl of a primary antibody CD31 (rat anti-mouse monoclonal CD-31, Fa. Santa Cruz Biotechnology, Cat.No. sc-1506) in a 1:100 dilution over night at 4°C. The next day, sections were removed from 4°C to room temperature and 1 hour later they were washed with 10 x TBS for 5 minutes in a shaking plate at a rate of 100/min. The sections were then incubated with secondary antibody biotinylated anti-rat IgG (Fa. Vector, Cat.No. BA 4001) in a 1:100 dilution for 1 hour and then washed again 2 x 5 minutes using 10 x TBS. Sections were incubated with ABC-kit solution for 1 hour (Vectastatin ABC-Kit Elite Rat IgG (Fa. Vector, Cat. No. PK6104), then washed twice with 10 x TBS. The sections were then covered with chromogen red AEC (Fa. Invitrogen, Cat.No. 00-1122) for 10 minutes, then washed two times with 10 x TBS followed by counterstaining with hematoxylin for 10 seconds and mounted with Kaiser glyceringelatin (Fa. Merck, Cat.No. 1.09242.0100). Images were taken with a two photon microscope (Leica DMD108, Leica Microsystems CMS GmbH, Wetzlar Germany).

#### **2.2.7. Fluorescence-activated cell sorting (FACS)**

For the identification and quantification of leukocyte sub-populations in the adductor muscles and in the blood, we used the technique of fluorescence-activated cell sorting (FACS) with different leukocyte antibody markers. Hind limb adductor muscles were isolated from saline (control) and C48/80 + diprotin A treated mice. The muscles were mechanically sliced into small 2 – 3 mm pieces and digested using collagenase II 1mg/ml in 1% PBS/BSA for 90 minutes at 37°C followed by gentle shaking every 30 minutes. The suspension was then filtered with 4 ml of 1% PBS/BSA through a 70 µm cell strainer (BD Falcon™), spun 10 min at 1200 g at

room temperature and the pellets were finally resuspended in 200 µl of 1% PBS/BSA. The samples were incubated with directly conjugated monoclonal antibodies against CD45 APC-Cy7, CD11b FITS, Gr-1 PE, CD115 APC, and F4/80 eFluor450 in dark for 10 minutes at room temperature. Afterwards the samples were lysed using 2ml of lysing buffer solution (BD-FACS: Cat.No. 349202) in a dilution of 1:10 PBS for 10 minutes followed by spinning at a rate of 1200 g. The final pellets were resuspended in 200 µl of 1% PBS/BSA in FACS tubes for cytometry.

Whole blood was collected from the left ventricle using a 1ml syringe containing 0.5µl of heparin. 100µl of each blood sample were incubated with directly conjugated antibodies against CD45 APC-Cy7, CD11b FITS, Gr-1 PE, CD115 APC, CD4 AlexaFluor700, and CD8a PE-Cy7 in dark for 10 minutes at room temperature. Afterwards erythrocytes were lysed using 2ml of lysing buffer solution (BD-FACS: Cat.No. 349202) in a dilution of 1:10 PBS for 10 minutes. The solutions were then spun for 10 min at a rate of 1200 g at room temperature. Finally, the pellets were resuspended in 200 µl of 1% PBS/BSA.

We adjusted our flow cytometer settings for adductor muscle and blood probes and established a data range for the general autofluorescence from a cell labelled with a conjugated antibody. The isotype control conjugated to the same fluorochrome as the primary antibody were both run with the same concentration in a FACS machine. Isotype controls allowed a distinction between background (non-specific binding) and specific binding of the primary antibody. For analysis, the samples were placed in a FACS machine (Beckman coulter, Gallios flow cytometer 2/8) and were run automatically to obtain different cell populations with respect to the antibody. The individual cell populations displays a fluorescence parameter on a light scatter cytogram were gated. Therefore the computer was instructed to show and count only

the cells that fall in a gated region. The corresponding regions were marked with fluorescence antibodies against CD45, CD11b, CD4, CD8, Gr-1, CD115, F4/80. For CD11b, CD4 and CD8 positive cells the gating were done after selecting total CD45 population. Gating for CD115, Gr-1 and F4/80 cell populations was selected after gating CD45 positive cells followed by CD11b. Finally, using Kaluza Software Version 1.2, we calculate the percentage of each cell type and plot in a graph.

#### **2.2.8. Collateral vessel diameter**

In order to determine the extent of the increase in the vessel diameters, we measured the diameters of collateral arteries of the adductor muscles in histological sections. Formalin-fixed tissue sections from mice 3 or 7 days after femoral artery ligation were processed for routine histopathology. 5- $\mu$ m-thick paraffin-embedded sections were stained with haematoxylin and eosin for evaluating collateral vessel morphology and determining the vessel diameters. A computerized image program (image J 1.45s Wayne Rasband. NIH, USA) was used to calculate the inner and outer circumference of four collaterals from each tissue sections under the microscope with a screen display. From the mathematical equation  $c_i = \pi d$  (where,  $c_i$  = inner circumference,  $\pi$  =3.14 and  $d$ =diameter), we obtained the vessel diameter. All values were tabulated and saved in Microsoft office excel sheet for analysis.

#### **2.2.9. Quantification of leukocytes**

For a quantification of perivascular leukocytes, tissue sections from adductor muscles were stained with CD45 antibody and viewed under a light microscope (Leica DMD108) at a magnification of  $\times 400$ . A digital image was taken from the sections. Leukocytes were quantified manually from the microscope with a wide screen display

image on individual collaterals. Positive cells (leukocytes) stained against CD45 antibody were counted in a region around 4 collateral arteries in the tissue sections of controls and of mice treated with cromolyn, a combination of Diprotin A + C48/80, cromolyn + Diprotin A. An average number of positive leukocytes was counted per collateral. Furthermore, muscle sections from the middle part of the gastrocnemius of saline (control) and C48/80 + Diprotin A treated mice were also stained against CD45 antibody and the positive leukocytes were counted per area (mm<sup>2</sup>).

#### **2.2.10. Quantification of Ki67 or CD31 positive cells**

For a quantification of proliferating endothelial and smooth muscle cells, tissue sections from adductor muscles stained with Ki67 antibody were viewed under the light microscope (Leica DMD108) at a magnification of  $\times 400$ , and a digital image was taken from the sections. Ki67 positive cells were counted in the four collaterals from each tissue section in saline (control), cromolyn, combination of cromolyn + diprotin A, and C48/80 + diprotin A treated mice. An average number of positive Ki67 vascular cells were expressed per collateral. CD31 staining was also performed in the gastrocnemius muscle to determine the number of capillaries per fibre in mice treated with saline or with C48/80+DipA.

#### **2.2.11. Serum Proteins Antibody Array**

In order to detect specific proteins that are associated with collateral artery growth we analysed the serum protein profile. A Proteome Profiler TM Mouse Angiogenesis Antibody Array (R&D Systems) was used according to the manufacturer's protocol. The nitrocellulose membranes were first incubated in blocking buffer for 1 hr. A cocktail of biotin-labelled antibodies against different individual angiogenesis-related

proteins was incubated with 140  $\mu$ l of serum from mice that were treated with saline (control with ligation), saline (control without ligation), or with C48/80 + diprotin A (with ligation). The sample and antibody mixture were then incubated with the membranes overnight at 4°C on a rocking platform. After three times washing to remove unbound material, the membranes were incubated with horseradish peroxidase (HRP) conjugated streptavidin for 30 minutes at room temperature. Then the membranes were washed three times before they were transferred to the signal detector using an ECL system (Amersham Pharmacia Biotech Aylesbury, UK). The array was run in duplicates. The image J software was used to analyse the proteins mean pixel density.

#### **2.2.12. Matrix metalloproteinase (MMP) activity assay**

In order to identify the MMP enzymatic activity, we performed kinetic measurements of MMP enzymes in the collateral arteries of control and experimental animals. In these mice collaterals were homogenised in assay buffer containing 250 $\mu$ l of 0.1% (v/v) Triton -X100 at 4°C for 30 minutes. The tissues were then centrifuged (10,000 x g, at 4°C, for 15 minutes) and the supernatant was collected and stored at -70°C. Pro-MMP containing tissue samples (109  $\mu$ l) were then activated with 1.1 $\mu$ l of 1mM of APMA, which afterwards was incubated for 2 hours in a water bath at 37°C. 50 $\mu$ l of the samples and of controls were placed in 96-well plate per well incubated with 50 $\mu$ l of MMP-substrate solution. For control, the fluorescence reference standard was diluted to 5 $\mu$ M in assay buffer followed by different dilution concentration (2.5 – 0.3125 $\mu$ M). The tissue samples and control in the plate were allowed to shake gently for 30 seconds. For kinetic measurements, the fluorescence signal was measured immediately at Ex/Em=490nm/520nm and the data were recorded continuously for



60 minutes once a minute. For end-point measurements, the reaction was incubated at room temperature for 60 minutes and fluorescence intensity was measured at Ex/Em=490 nm/520 nm (Fa. TECAN, Infinite 200, S/N 711003634). A standard curve was obtained by plotting the absorbance values against the concentration of the standards. Data were normalised to the reference standard curve.

### **2.2.13. TNF- $\alpha$ analysis**

To quantify the amount of TNF- $\alpha$  in the plasma, we performed TNF- $\alpha$  ELISA in plasma of control mice without ligation, in control mice with ligation and in cromolyn treated mice. The coating solution was diluted to a final concentration of 1  $\mu$ g/ml. 100  $\mu$ L of the diluted antibody were added to a flat bottomed, high protein binding 96-well plate per well, then sealed and incubated at +4°C over night. The coating solution was aspirated and the plate washed three times using wash buffer (1x PBS, 0.05% Tween-20). 200  $\mu$ L per well of blocking buffer (1 x Assay Diluents) were added and incubated for 1 hour at room temperature. The plate was then emptied. To prepare standard concentrations, using 1 x Assay Diluent 2 fold serial dilutions of 1.7 ng/ml of TNF- $\alpha$  of the top standard was added to make the standard curve for a total of 8 points. 100  $\mu$ L of the plasma samples were added to the appropriate wells, the plates were then sealed and incubated at room temperature for 2 hours. The plates were then washed four times using washing buffer. 100  $\mu$ L of detection antibody (biotin-conjugated antibody) diluted in 1 x Assay Diluent was added in the plate per well, sealed and incubated for 1 hour at room temperature. The detection antibody was then aspirated and washed four times. Afterward 100  $\mu$ L of Avidin-Horse radish peroxidase (HRP) were added per well and incubated at room temperature for 30 minutes. The plates were then soaked with wash buffer for 1 to 2 minutes, repeated

for 5 times. A substrate solution (Tetramethylbenzidine) was added to each well and incubated for 15 minutes at room temperature followed by 50  $\mu$ L of stop solution (1M  $\text{H}_3\text{PO}_4$ ). The absorbance at 450 nm using a microtiterplate spectrophotometer was measured. A standard curve was obtained by plotting the absorbance values against the concentration of the standards. The concentration of TNF- $\alpha$  in the sample was determined by using the standard curve.

#### **2.2.14. MCP-1 ELISA**

To quantify the amount of MCP-1 in the collaterals, we performed MCP-1 ELISA from the plasma and from isolated collaterals of C48/80 + diprotin A treated mice and the controls. Collaterals were pestled and sonicated under liquid nitrogen. PBS was added afterwards to solubilise the collaterals.

The coating solution was diluted to a final concentration of 1  $\mu$ g/ml. 100  $\mu$ L of the diluted antibody were added to a flat bottomed, high protein binding 96-well plate per well, then sealed and incubated at +4°C over night. The coating solution was aspirated and the plate washed three times with 250  $\mu$ L washing buffer (1x PBS, 0.05% Tween-20) per well. The residual buffer was removed by placing an absorbent paper on the blot plate. The blocking buffer (200 $\mu$ L; of 1 x Assay Diluents) was added to each well and incubated for 1 hour at room temperature. The plate was then washed once with wash buffer. To prepare standard concentrations, using 1 x Assay Diluent 2 fold serial dilutions of 1.7 ng/ml of MCP-1 of the top standard was added to make the standard curve for a total of 8 points. 100  $\mu$ L of the samples were added to the appropriate wells, the plates were then sealed and incubated at room temperature for 2 hours. Subsequently the plates were washed four times using washing buffer. 100  $\mu$ L of detection antibody (biotin-conjugated antibody) diluted in 1

x Assay Diluent was added in the plate per well, sealed and incubated for 1 hour at room temperature. The detection antibody was then aspirated and washed four times. Afterwards 100  $\mu$ L of Avidin-Horse radish peroxidase (HRP) were added per well and incubated at room temperature for 30 minutes. The plates were then soaked with wash buffer for 1 to 2 minutes, repeated for 5 times. 100  $\mu$ L of substrate solution (tetramethylbenzidine) was added to each well and incubated for 15 minutes at room temperature followed by 50  $\mu$ L of stop solution (1M  $\text{H}_3\text{PO}_4$ ). The absorbance at 450 nm using a microtiterplate spectrophotometer was measured. A standard curve was obtained by plotting the absorbance values against the concentration of the standards. The concentration of MCP-1 in the sample was determined by using the standard curve.

#### **2.2.15. SDF-1 $\alpha$ ELISA**

To quantify the amount of SDF-1 $\alpha$  (i.e. a potent chemoattractant molecule, which recruits mast cells and monocytes), we performed SDF-1 $\alpha$  ELISA from the serum of diproton A treated mice, or the control without ligation or control with ligation. 50  $\mu$ L of the Assay Diluent was added to each well followed by 50  $\mu$ L of standard, control or samples per well. The mixture were incubated for 2 hours at room temperature on a orbital microplate shaker set at 500 rpm. Afterwards, the wells were aspirated and washed four times using wash buffer (400  $\mu$ L). Subsequently, 100  $\mu$ L of mouse SDF-1 $\alpha$  conjugate was added to each well and incubated at room temperature for 2 hours on the shaking plate. The wells were then aspirated and washed four times using wash buffer. The substrate solution (200  $\mu$ L) was then added to the wells and incubated at room temperature in the dark for 30 minutes. Afterwards, 50  $\mu$ L of stop solution was added to each well and the optical density of each well were determined

within 30 minutes using microplate reader set to 450 nm.

For quantification of SDF-1 $\alpha$  in the collaterals, we performed SDF-1 $\alpha$  ELISA from the supernatants of isolated collaterals of diproton A treated mice and controls with ligation. The collaterals were placed in 100 $\mu$ L of cell lyses buffer and then treated 5 times for 2 seconds with ultrasound to dissolve. The samples were then centrifuged for 3 minutes at 7000 rpm and the supernatants were collected.

100  $\mu$ L of the standard and of the samples were added into appropriate wells. The wells were covered and incubated for 2.5 hours at room temperature on an orbital microplate shaker set at 500 rpm. Afterwards, the wells were aspirated and washed four times using wash solution (300  $\mu$ L). Subsequently, 100  $\mu$ L of 1x biotinylated antibody was added to each well and incubated at room temperature for 1 hours on the shaking plate. The wells were then aspirated and washed four times using wash solution. Afterwards, 100  $\mu$ L of streptavidin solution was added to each well followed by 45 minutes incubation at room temperature with gentle shaking. The solution was then discarded and washed three times using wash solution. One-step substrate reagent (200  $\mu$ L) was then added to each well and incubated at room temperature in the dark for 30 minutes with gentle shaking. Afterwards, 50  $\mu$ L of stop solution was added to each well and the optical density of each well were determined within 30 minutes using microplate reader set to 450 nm. For analysis, from both serum and collaterals the standard curve was created by plotting the mean absorbance of each standard on the y-axis (optical density) against the concentration on the x-axis (mouse SDF-1 $\alpha$  concentration) and drawing the curve through the points on the graph. Therefore, the results were obtained by averaging the duplicate reading for each standard, control and sample and the results were subtracted with the average

zero standard optical density.

#### **2.2.16. RNA extraction and real-time polymerase chain reaction (RT-PCR)**

For a quantitative analysis of gene expression of the chemoattractant molecule (MCP-1) in collateral arteries of the hind limb, we performed both RNA extraction followed by qRT-PCR. Total RNA was isolated according to the procedure of Chomczynsky and Sacchi (Chomczynski and Sacchi, 1987). 20 mg of collateral tissue was homogenised with 300 µl of TRIzol in homogenisation tubes for 3 minutes and left at room temperature for another 3 minutes. The samples were centrifuged for 10 min at 12,000 g at 4°C. Afterwards the supernatant was mixed with 60µl of chloroform in fresh tubes and shaken vigorously for 15 seconds followed by incubation at room temperature for 3 minutes. The mixture was centrifuged for 15 minutes at 12,000 g at 4°C. The aqueous phase was transferred into a fresh tube and 150µl of isopropanol were added. Then the solution was incubated for 10 minutes at room temperature followed by centrifugation at 12,000 g and at 4 °C. This time the supernatant liquid was discarded. The remaining pellets were washed with 75% ethanol and then again centrifuged at 8,000 g for 5 minutes at 4°C. Then the pellets were left to dry for 2 minutes.

For DNase I digestion, the pellets were resuspended in 48 µl of water and the DNase I master mix was added (96µl H<sub>2</sub>O, 12µl 10xBuffer and 12µl DNase I) and the mixture incubated at 37°C for 30 minutes. Afterwards the mixture was cleaned using RNeasy MinElute Cleanup kit (Qiagen) as instructed. For RNA purification and concentration measurements, 3 µl of RNA solution were diluted to 57 µl of 10mM Tris HCL buffer in an eppendorf cuvette. Optical density and concentration of RNA were measured with a bio photometer at 260, 280 and 230 nm.

The RNA purity of the sample was calculated using the ratio of 260nm/280nm (Protein contamination) and 260nm/230nm (buffer contaminations)

$$260/280 > 2$$

$$260/230 > 1,8$$

Values above 2 for protein contamination and 1.8 for buffer contamination were regarded as pure RNA samples.

For DNA synthesis we used 1st Strand cDNA synthesis kit (Roche). Firstly, RNA samples, reaction buffer, MgCl<sub>2</sub>, dNTPs, random and oligo dT primers and gelatin were put on ice. 250ng of RNA were mixed with distilled water to 7,8 µl and denatured at 65°C for 10 minutes using a thermal cycler, then placed on ice for 5 minutes. The master mix was then prepared as follows:

Volume	Component	End concentration
2µl	10x reaction buffer	1X
4µl	25mM MgCl <sub>2</sub>	5mM
2µl	deoxynucleotide mix	1mM
1µl	random primers	
1µl	oligo dT primers	
Finally and immediately before adding to the samples:		
1µl	RNase inhibitor	50 units
0,8µl	AMV-reverse transcriptase	20 units
0,4µl	Gelatin	0,01mg/ml

Afterwards the master mix was added to the RNA samples to a final volume of 20 µl. The RNA solution mixture was placed in a thermal cycler and programmed as follows:

10min to 25°C (primer annealing)

60min to 40°C (cDNA synthesis)  
 5min 99°C (reverse transcriptase inhibition)  
 4°C, and finally stored at -20°C

The following day, quantitative PCR was performed using Power Sybr Green master mix (Life technologies) as tabulated below.

<b>cDNA dilution</b>		
Volume	Component	End
80µl	H <sub>2</sub> O	
20µl	cDNA (250ng)	2,5ng/µl
= 100µl		
<b>Primer master mix preparation</b>		
180µl	H <sub>2</sub> O	
10µl	Forward primer (100µM)	5µM
10µl	Reverse primer (100µM)	5µM
<b>qPCR master mix</b>		
5µl	Sybr green Master mix	1x
1µl	Primer mix (forward+ reverse) 5µM	500nM
2µl	H <sub>2</sub> O	
= 8µl /sample		
<b>After pipetting 8µl of qPCR master mix to the wells:</b>		
2µl	cDNA (1:5 diluted)	5ng
= 10µl end volume /well		

The samples were then pipetted in a 96 well plate on ice. Before the run, the plates were centrifuged shortly at 4°C to avoid air bubbles.

The following program was employed:

Step	Polymerase activation	PCR		Melt curve		
	Hold	CYCLE (40x)		Step and hold		
		Denature	Anneal/Extend			
Temp.	95°C	95°C	64°C (18s and MCP-1)	95°C	64°C	+ 0,7°C/min until 95°C
Time	10min	15 sec	1 min	15 sec	1 min	

The data obtained on 18S rRNA expression was used for normalisation.

### 2.2.17. Statistical analysis

Statistical analyses were carried out using SigmaPlot® 12.0 (Systat Software, SPSS, Chicago, IL, USA). For statistical analyses, we performed unpaired Student's *t*-test when comparing two groups of the same experimental subject. Friedman Repeated Measures Analysis of Variance on Rank was used when each group of data from experimental mice is to be tested against a control group. Differences were accepted to be significant if  $P < 0.05$ . Data were presented as standard error of the mean (S.E.M).



### 3. RESULTS

#### 3.1. Collateral arteries change their shape after femoral artery occlusion

Femoral artery ligation resulted in the growth of pre-existing arteriolar connections. 21 days after femoral occlusion, two prominent superficial collateral arteries displayed a characteristic corkscrew appearance on adductor muscles on the occluded side (arrowheads; figure 9 A). On the non-occluded hind limb (sham side) pre-existing quiescent collaterals were present (figure 9 B). Apart from these superficial collaterals, deep muscular interconnecting arteries were made visible by an infusion of red cast material followed by muscle tissue maceration (figure 9 C).

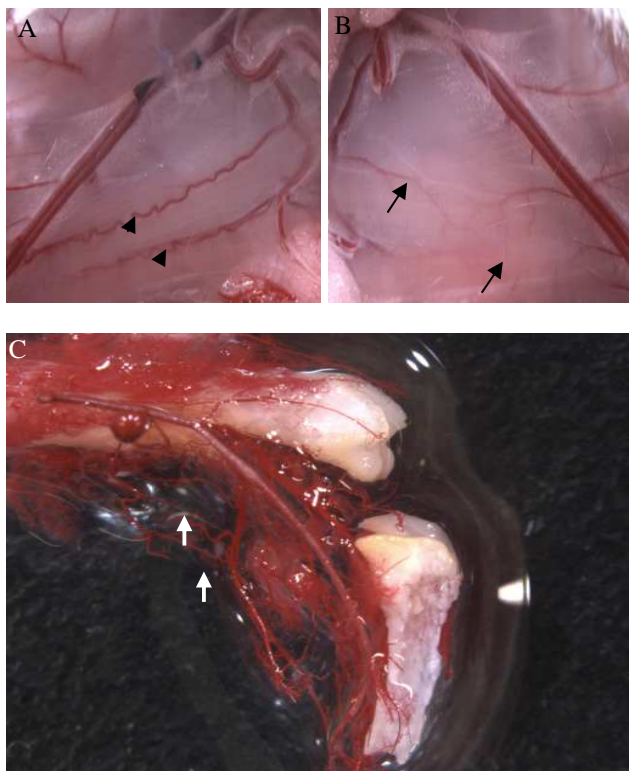


*Fig.9: Superficial collateral arteries 21 days after ligation.*

- A. Collateral vessels (arrow heads) consistently developed on the occluded side showing the characteristic tortuous phenotype.
- B. Sham operated limb showing pre-existing quiescent collateral arteries (arrows).
- C. A cast model showing the presence of deep collateral vessels after muscle tissue maceration (white arrows) on the sham operated limb.

### 3.2. Mast cells respond to femoral artery ligation with degranulation in the vicinity of growing collateral vessels

Quiescent undegranulated mast cells are present along the collateral arteries already before the process of arteriogenesis is initiated (figure 10 A). In the course of arteriogenesis, perivascular mast cells degranulate (figure 10B). Mast cells were not seen to degranulate within the first two hours after femoral artery ligation. However, mast cell degranulation around collateral arteries was progressively increasing with time, from no degranulation at 2 hours to 42.5% ( $\pm 2.5\%$ ) at 12 hours, to 54.25% ( $\pm 3\%$ ) at 24 hours and to 59% ( $\pm 6\%$ ) at 3 days after femoral ligation (figure 10 C). Three days after femoral ligation, an average of one degranulated mast cell per collateral was observed in histological sections of adductor muscles in the occluded limb. However, no degranulation of mast cells was seen in the sham-operated limb (figure 10 D).

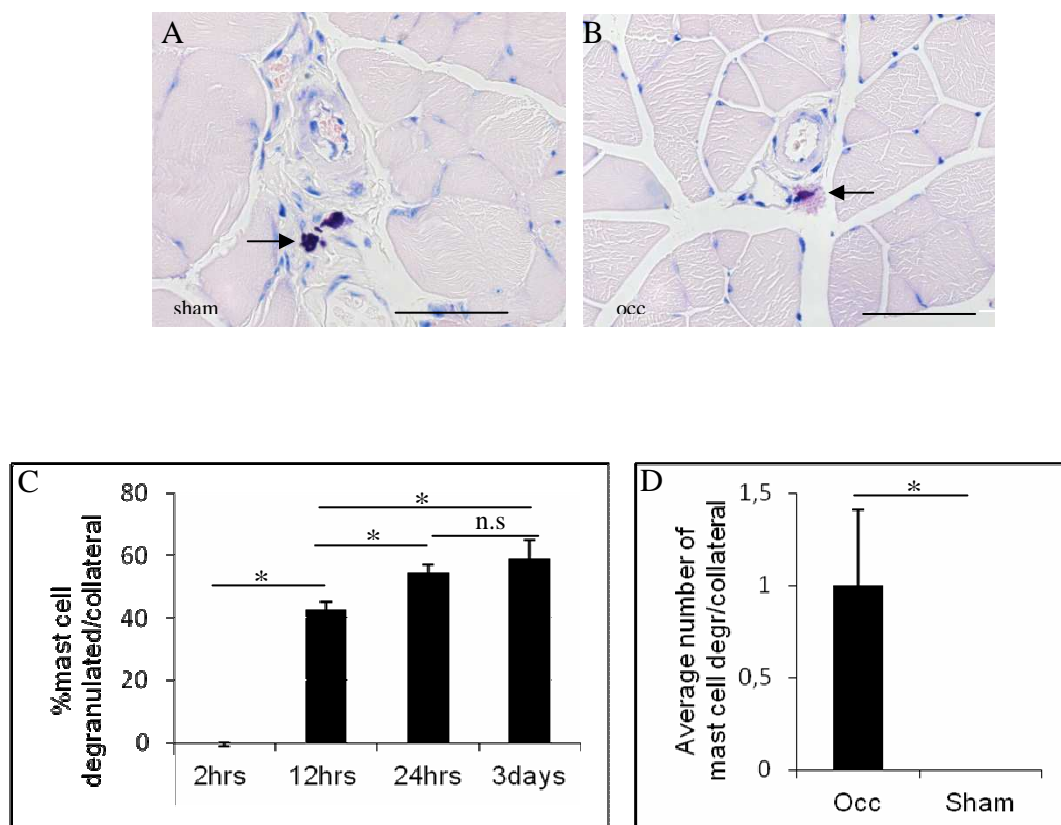


*Figure 10; Detection of mast cell degranulation during arteriogenesis*

A and B: Three days after femoral artery ligation mast cells detected in the perivascular space of pre-existing collaterals in the non-occluded (sham) side, showed no degranulation (arrow; A), while mast cells at the same location in the occluded side showed active degranulation (arrow; B). Scale bar; 100µm.

C: A Bar graph presents the number of degranulated mast cells per collateral in percent, 12 hours, 24 hours and 3 days after femoral artery ligation. (\*P<0.05, n.s = non significant)

D: Bar graph present the average number of mast cells degranulated per collateral from tissue sections of occluded or sham operated m. adductor 3 days after femoral artery ligation. (\*P<0.05).

### **3.3. Prevention of perivascular mast cell degranulation impairs arteriogenesis**

Cromolyn is a substance known to block the release of granula by mast cells (figure 11 A). In this experiment, we compared the time course of recovery of blood flow perfusion in the distal hindlimb of controls and of cromolyn treated mice after femoral artery ligation with the help of laser Doppler perfusion imaging (LDI). In both saline (control) and cromolyn treated groups, the perfusion ratio (right/left) before surgical occlusion was approximately one. Immediately after surgery, there was a similar decline in the distal hind limb blood flow on the occluded side of both groups (figure 11 B). However, cromolyn treated mice demonstrated a significantly slower recovery of blood flow at day 7, 14 and 21 when compared with control mice (Table I, figure 11 B).

Table I Perfusion ratio (right versus left) of cromolyn treated mice versus controls

Day 7	R/L: $0.29 \pm 0.03$ vs. $0.59 \pm 0.02$ ,	*** $P < 0.001$ treated v.s. saline
Day 14	R/L: $0.55 \pm 0.05$ vs. $0.66 \pm 0.04$ ,	* $P < 0.05$ treated v.s. saline
Day 21	R/L: $0.56 \pm 0.05$ vs. $0.76 \pm 0.05$	* $P < 0.05$ treated v.s. saline.

Next we investigated whether the effect of this reduced perfusion recovery was due to a blockage of mast cells around the growing collateral arteries in the cromolyn treated mice. We analyzed Giemsa stained histological sections from the adductor muscles from the occluded side (figure 11 C) of control and cromolyn treated mice and found that the percentage of degranulated mast cells was significantly lower 3 days after femoral artery occlusion when compared to the control group (figure 11 D).

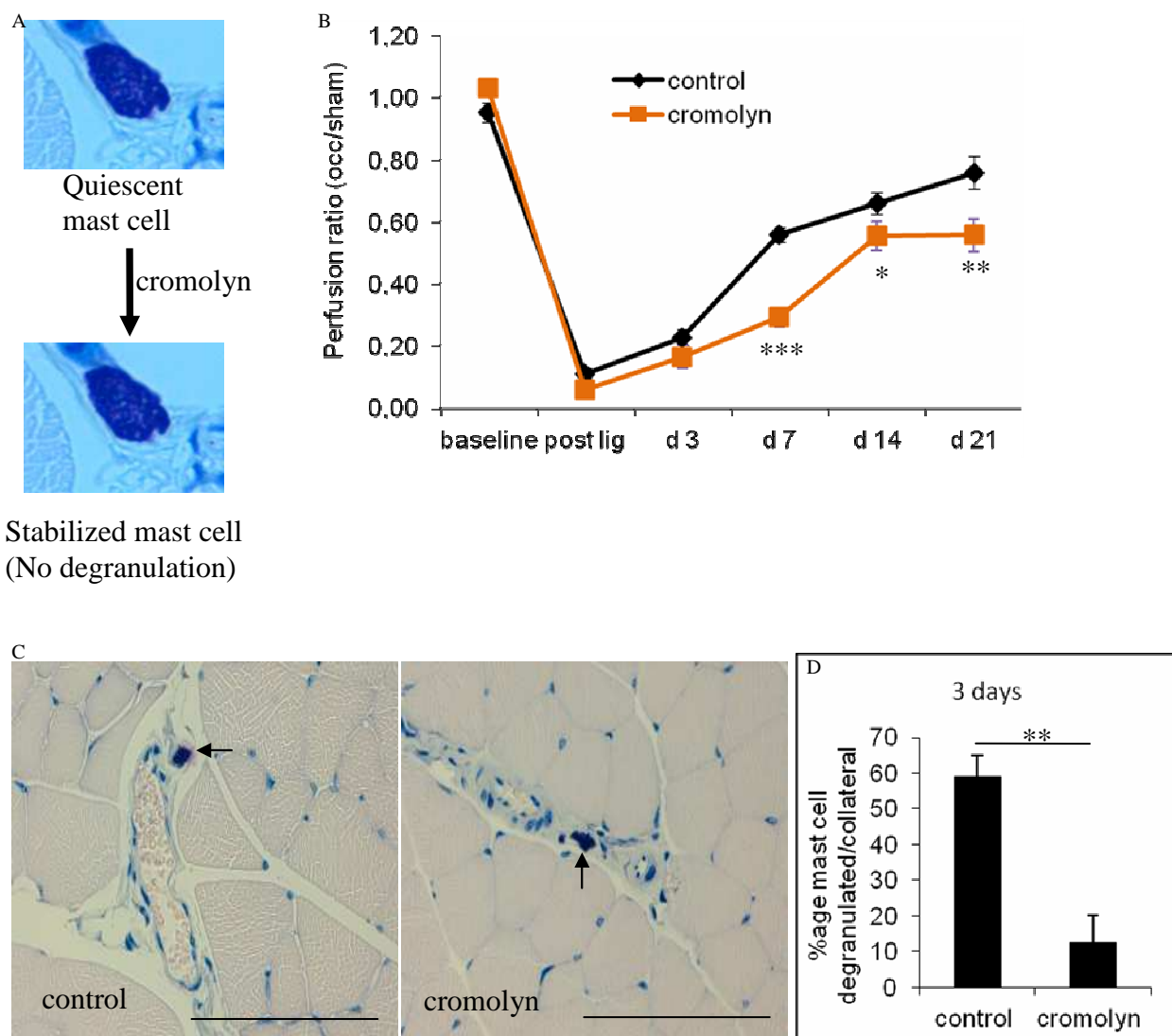


*Figure 11; Effect of cromolyn on hindlimb perfusion recovery and mast cell degranulation.*

A: A sketch diagram showing the function of cromolyn in blocking mast cell degranulation.

B: Line chart showing changes in the rate of hindlimb blood perfusion recovery of saline (control) or cromolyn treated mice after femoral artery ligation. The data are shown as mean  $\pm$  SEM,  $n=6$  per group. \* $P<0.05$ , \*\* $P<0.01$ , \*\*\* $P<0.001$ .

C: Giemsa stained pictures representing adductor sections of occluded saline (control) or cromolyn treated mice 3 days after femoral ligation. In the control, mast cells were seen to degranulate, while mainly non-degranulating mast cells were seen in sections of cromolyn treated mice (arrows). Scale bar = 100 $\mu$ m.

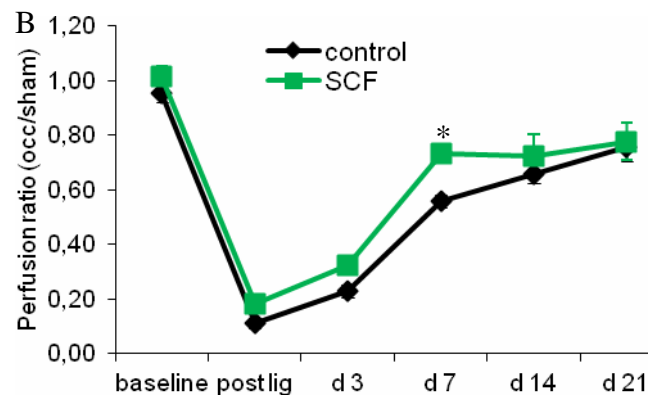
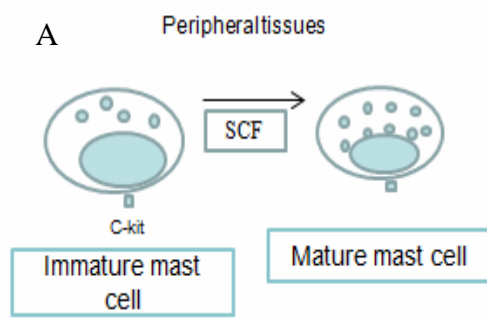
D: Bar graph representing the number of degranulated mast cells in percent per collateral in saline (control) or cromolyn treated animals at 3 days post femoral artery ligation. Data are shown as mean  $\pm$  SEM, n=3-4 per group. \*\*P<0.01.

### 3.4. Effect of stem cell factor and diprotin A on hind limb reperfusion recovery following femoral artery ligation.

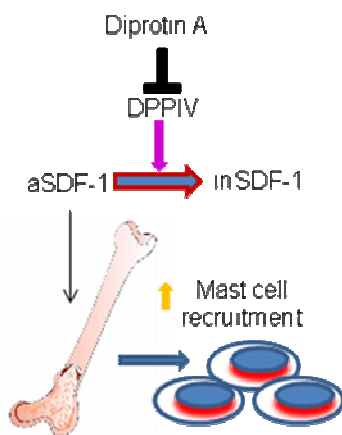
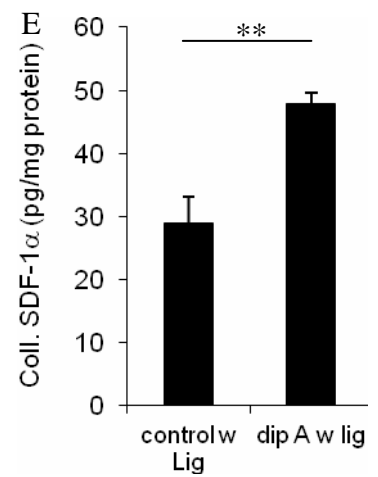
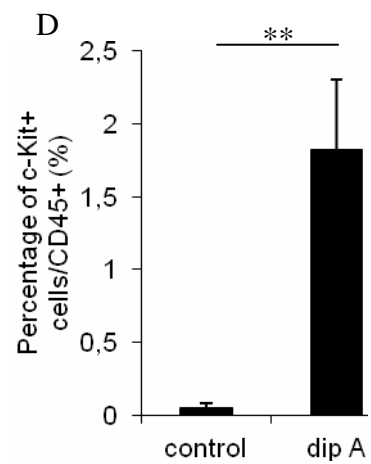
A group of mice was treated with stem cell factor (SCF), a cytokine which enhances mast cell maturation and differentiation, after femoral artery ligation (figure 12 A). With laser Doppler measurements I found a significantly increased rate of perfusion recovery of the hind limb on the occluded side at day 7 when compared to saline (control) treated mice (R/L ratio,  $0.73 \pm 0.02$  vs.  $0.56 \pm 0.02$ , \*P<0.05 SCF vs. control). However, 14 and 21 days after femoral ligation the perfusion had recovered virtually to the same extent in each of the two groups (figure 12 B). In a similar experiment, mice were treated with diprotin A, which increase the serum level of SDF-1 $\alpha$  through inhibition of DPPIV enzyme (figure 12 C), thereby enhance mast cell recruitment (c-Kit+; figure 12 D). The increase of SDF-1 $\alpha$  was significant in the collaterals of diprotin A compared to control (figure 12 E). However, the level of SDF-1 $\alpha$  in the serum was slightly higher in diprotin A treated mice, albeit not significant (figure 12 F). As a result, the rate of perfusion recovery had accelerated at days 7 and 14 in diprotin A treated mice with respect to controls (table II; figure 12 G).

Table II Diprotin A treated versus control mice

Day 7	R/L: $0.76 \pm 0.04$ vs. $0.56 \pm 0.02$	**P<0.01 diprotin A v.s. control
Day 14	R/L: $0.85 \pm 0.05$ vs. $0.66 \pm 0.04$	*P<0.05 diprotin A v.s. control
Day 21	R/L: $0.84 \pm 0.04$ vs. $0.76 \pm 0.05$	Not significant



**C**



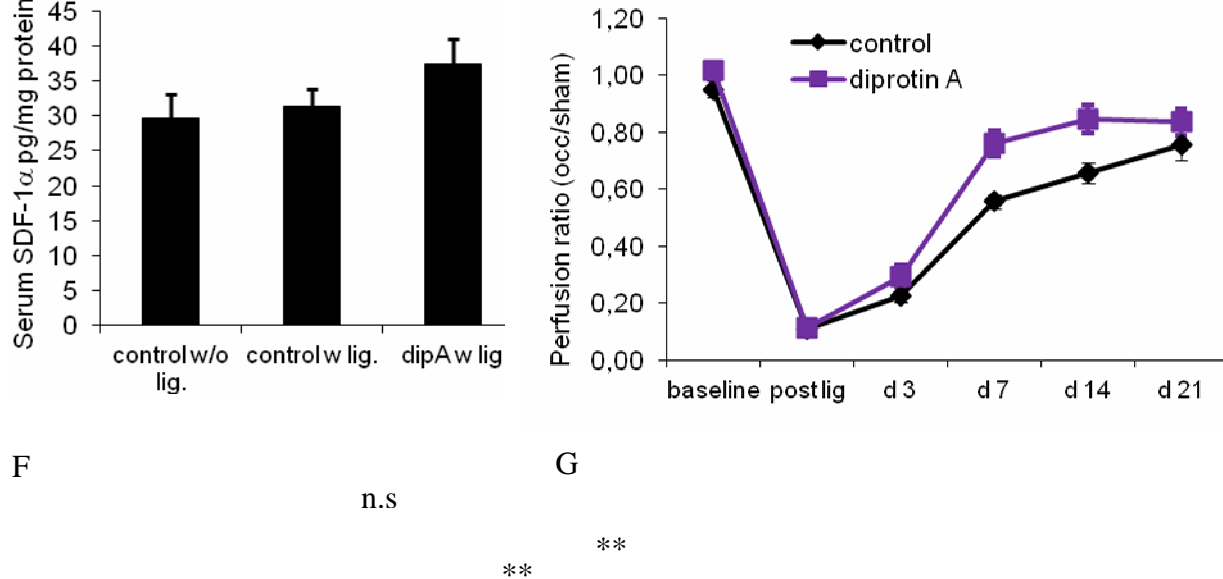


*Figure 12; Improved arteriogenic response in hindlimbs of SCF and diprotin A treated mice.*

A: Sketch diagram showing SCF mode of action toward mast cells.

B: Line charts showing laser Doppler quantitative analyses of perfusion measurement (occluded/sham) in saline (control) or SCF treated mice. \*P<0.05.

C: Sketch diagram showing diprotin A mode of action toward mast cells. inSDF-1 $\alpha$  (inactive stroma-cell-derived factor 1- $\alpha$ ), aSDF-1 $\alpha$  (active stroma-cell-derived factor 1- $\alpha$ ).

D. Bar graph displaying the results of mast cell (c-Kit<sup>+</sup>) counts by flow cytometry in the adductors of saline (control) or diprotin A treated mice 24 hours after femoral artery ligation

E. Quantification of collateral SDF-1 $\alpha$  levels (pg/mg) by means of ELISA of control with ligation (control w lig) or ligation and diprotin A treatment (dipA w lig) 24 hours after femoral artery ligation.

F. Bar graph showing ELISA results on quantification of serum SDF-1 $\alpha$  levels (pg/mg) of control (saline treated) mice without ligation (control w/o lig), control with ligation (w lig) or ligation and diprotin A treatment (dipA w lig) 24 hours after the surgery

G: Laser Doppler quantitative analyses of perfusion measurement (occlude/sham) in saline (control) or diprotin A treated mice. \*\*P<0.01.



### 3.5. Mast cell degranulation with the help of compound 48/80 accelerates hind limb perfusion recovery

The recovery of hind limb blood perfusion after femoral artery ligation was further studied in mice treated with compound (C) 48/80 and compared with saline treated control mice. To determine the progress of collateral artery growth, blood flow was measured before, directly after surgery and then 3 days, 7 days, 14 days and 21 days after surgery with laser Doppler imaging (LDI). With respect to control values the perfusion ratio of C 48/80 treated mice recovered significantly faster at day 7 and 14 (Table III; figure 13 A).

Table III C 48/80 treated versus control mice

Day 7	R/L: $0.79 \pm 0.03$ vs. $0.56 \pm 0.02$ ,	**P<0.01 treated v.s. saline
Day 14	R/L: $0.85 \pm 0.04$ vs. $0.66 \pm 0.04$ ,	*P<0.05 treated v.s. saline
Day 21	R/L: $0.84 \pm 0.06$ vs. $0.76 \pm 0.05$	Non-significant.

In order to examine whether the three substances which accelerate perfusion recovery (C 48/80, diprotin A and SCF), have additive effects, we treated one group of mice with C 48/80 + diprotin A and another group with C 48/80 + diprotin A + SCF. In the group of mice treated with C 48/80 + diprotin A we found a significantly faster blood flow recovery with respect to controls already at 3 day after surgery. The perfusion remained consistently better until day 21 (table IV; figure 13 A). Even though the group with a double treatment (C 48/80 + diprotin A) and the group with a triple treatment (C 48/80 + diprotin A + SCF) exhibited additive effects, the results

between these double and triple treated groups were not significantly different from each other (figure 13 A). Interestingly, a statistically significant recovery in blood flow was already detected at day 3 in mice treated with C 48/80 + diprotin A in contrast to mice treated exclusively with C 48/80 or with diprotin A.

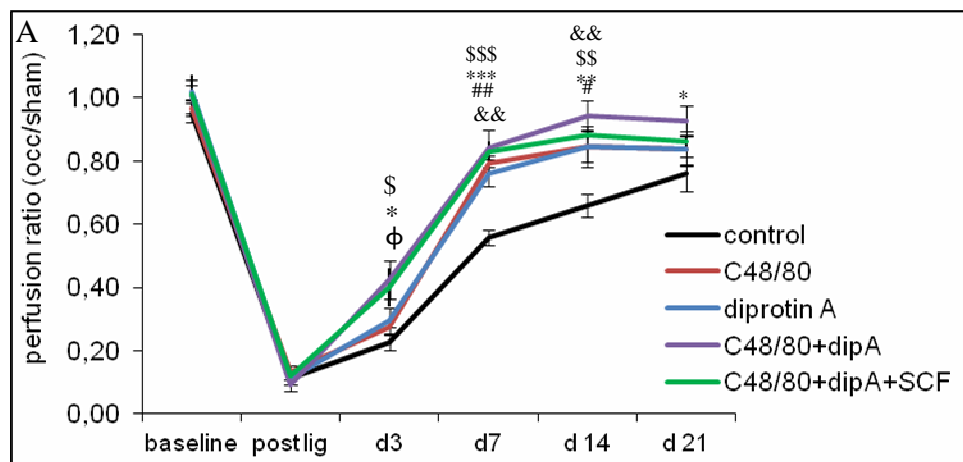
Table IV C 48/80 + diprotin A treated versus control mice

Day 3	R/L: $0.42 \pm 0.06$ vs. $0.23 \pm 0.02$ ,	*P<0.05 treated v.s. saline
Day 7	R/L: $0.84 \pm 0.06$ vs. $0.56 \pm 0.02$ ,	***P<0.001 treated v.s. saline
Day 14	R/L: $0.94 \pm 0.06$ vs. $0.66 \pm 0.04$ ,	**P<0.01 treated v.s. saline
Day 21	R/L: $0.92 \pm 0.05$ vs. $0.76 \pm 0.05$	*P<0.05 treated v.s. saline.

This accelerated recovery rate due to diprotin A treatment could have resulted exclusively from a contribution of mast cells or from a contribution of monocytes (which expresses the receptor for SDF-1 $\alpha$  i.e. CXCR-4). Alternatively, it could have resulted from a contribution of both cell types. In order to find out, we blocked the degranulation of mast cells by the application of cromolyn either in the presence or in the absence of diprotin A. The results of this experiment (figure 13 B) demonstrated that blocking mast cell degranulation significantly reduced perfusion recovery after femoral artery ligation with respect to controls. In the presence of cromolyn the rate of perfusion recovery was reduced with respect to controls, regardless of a single cromolyn treatment or a combined cromolyn plus Diprotin A treatment (figure 13 B).

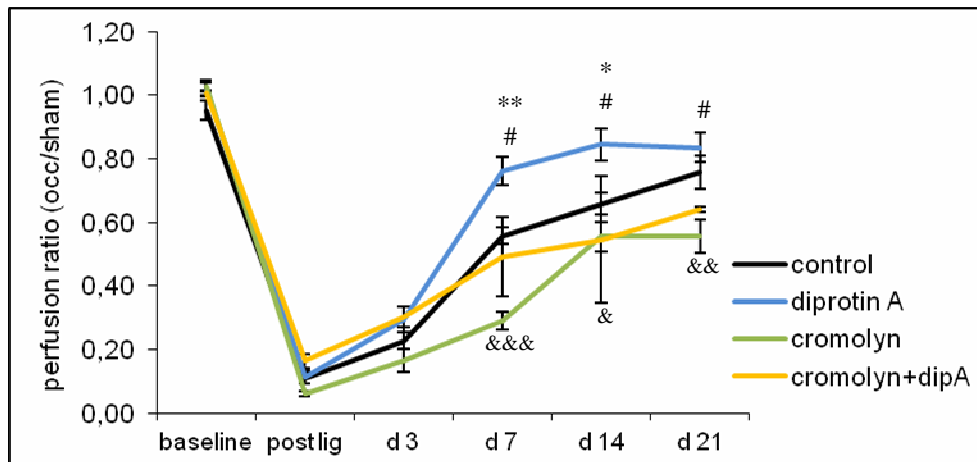
As shown above, mice treated with a combination of C 48/80 + diprotin A, exhibited a significant increase in perfusion recovery of their hind limb perfusion already 3 days after femoral artery ligation. To find out at what time the increase in blood flow had started we investigate the blood flow within the first 48 hours after femoral artery

ligation. In fact, we found a significantly increased perfusion already 6 hours after surgery (figure 13 C). This increase was persistent up to 48 hours post surgery, albeit it was not significant at 12 and at 24 hours post surgery (figure 13 C).

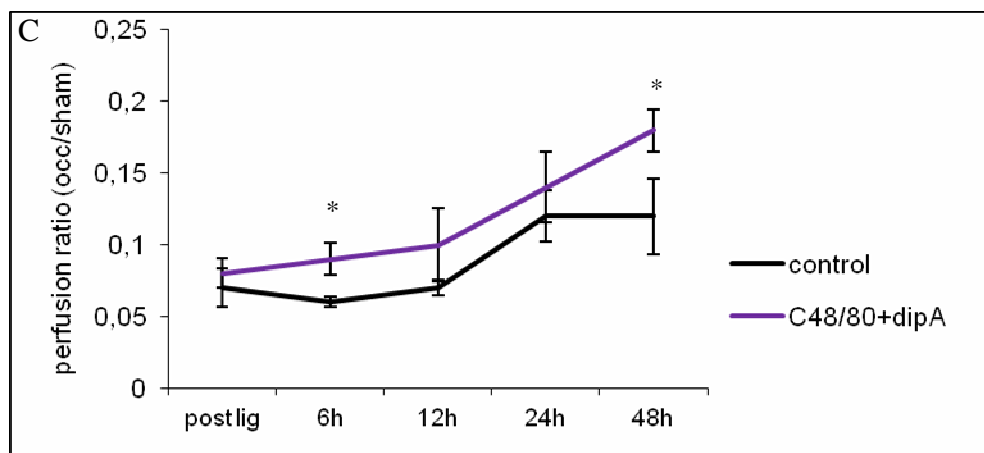


# - Diprotin A vs control  
 & - C48/80 vs control  
 \* - C48/80+dipA vs control  
 \$ - C48/80+dipA+SCF vs control  
 φ - C48/80+dipA or C48/80+dipA+SCF vs dipA or C48/80

B



\* - Diprotin A vs control  
 & - Cromolyn vs control  
 # - Cromolyn+dipA vs. cromolyn



\*C48/80 + dip A vs. control

*Fig. 13. LDI perfusion measurements after influencing mast cell function.*

A: Line charts of laser Doppler results showing the perfusion ratio (occluded/sham) in mice treated with compound 48/80, diprotin A (dipA), a combination of C 48/80 + diprotin A, and C 48/80 + diprotin A + SCF versus control. \* $P < 0.05$ , \*\* $P < 0.01$ , \*\*\* $P < 0.001$ . \$ $P < 0.05$ , \$\$ $P < 0.01$ , \$\$\$ $P < 0.001$ . # $P < 0.05$ , ## $P < 0.01$ . & $P < 0.05$ , && $P < 0.01$ .  $\phi P < 0.05$ .

B: Laser Doppler results displaying the perfusion ratio (occluded/sham) of mice treated with diprotin A, cromolyn, or a combination of diprotin A + cromolyn versus control mice. \* $P < 0.05$ , \*\* $P < 0.01$ . & $P < 0.05$ , && $P < 0.01$ , &&& $P < 0.001$ .

C: Quantification of perfusion ratio (occluded/sham) at 6, 12, 24 and 48 hours post ligation of combined C 48/80 + diprotin A treated mice versus control. (\* $P < 0.05$ ).

### 3.6. Mast cell degranulation promotes vascular remodeling through increased MMP enzymatic activity in collaterals

Given that an increased activity of matrix metalloproteinase (MMP) is known to promote arteriogenesis (Ota et al., 2009), we investigated the activity of MMP in collateral arteries 24 hours after femoral artery ligation of animals treated with stem cell factor (SCF) or with C48/80 + diprotin A and compared the results with saline treated animals (control). MMP activity had increased significantly in C48/80 + diprotin A treated mice by a factor of 2.2 with respect to controls (figure 14). We also observed a non-significant increased MMP activity in SCF treated mice versus control.

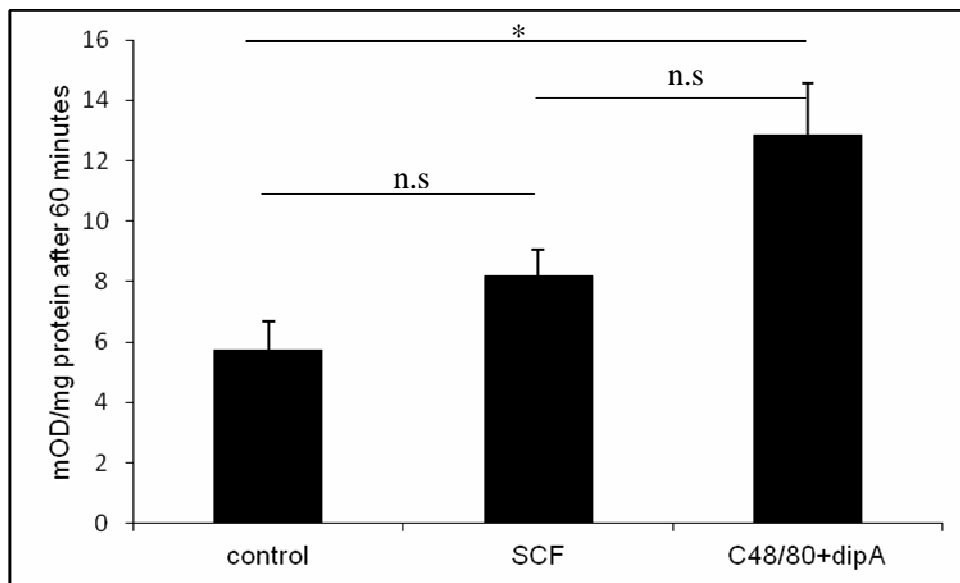


Fig. 14; Characterisation of MMPs activity in mouse collateral arteries 24 hours after femoral artery ligation.

Bar graph showing quantification of the enzymatic activity of MMPs expressed as mean optical density (mOD) measured by the intensity of the emitted fluorescence after 1 hour of incubation of homogenised occluded collaterals from saline (control),

SCF or C48/80 + diprotin A treated mice with MMP substrate solution. (Mean  $\pm$  SEM, \*P<0.05).

### **3.7. Protein array analysis showed elevated serum levels of PDGF-BB, angiopoietin-1 and MMP-3 and 9**

It had been proposed that degranulating mast cells release a number of cytokines/chemokines and growth factors; in addition they indirectly activate MMP (Gruber et al., 1989). Therefore, we performed in a cytokine assay approach a quantitative measurement of cytokines/chemokines in mice serum to identify specific proteins that are associated with collateral artery growth. In order to analyse the expression profile of arteriogenesis-related proteins in our experimental animals, blood was isolated from the three groups of mice (i.e. saline treated, controls without ligation; saline treated controls with ligation and of mice treated with a combination of C48/80 + Diprotin A). The data demonstrate a strong increase in angiopoietin 1 (by a factor of 9) and in the growth factor (PDGF-BB; by a factor of 5) in mice treated with a combination of C48/80 + diprotin A (table V; figure 15).

Table V. Mean pixel density in C48/80 + diprotin A vs. control

Serum protein	C48/80 + diprotin A versus control without ligation	C48/80 + diprotin A versus control with ligation
Angiopoietin 1	32418.5 vs. 3800.5	32418.5 vs. 3535
PDGF-BB	13031 vs. 2720	13031 vs. 3064.5

In addition, we observed a small increase in mean pixel density of MMP-3 and of MMP-9 proteins (figure 15).

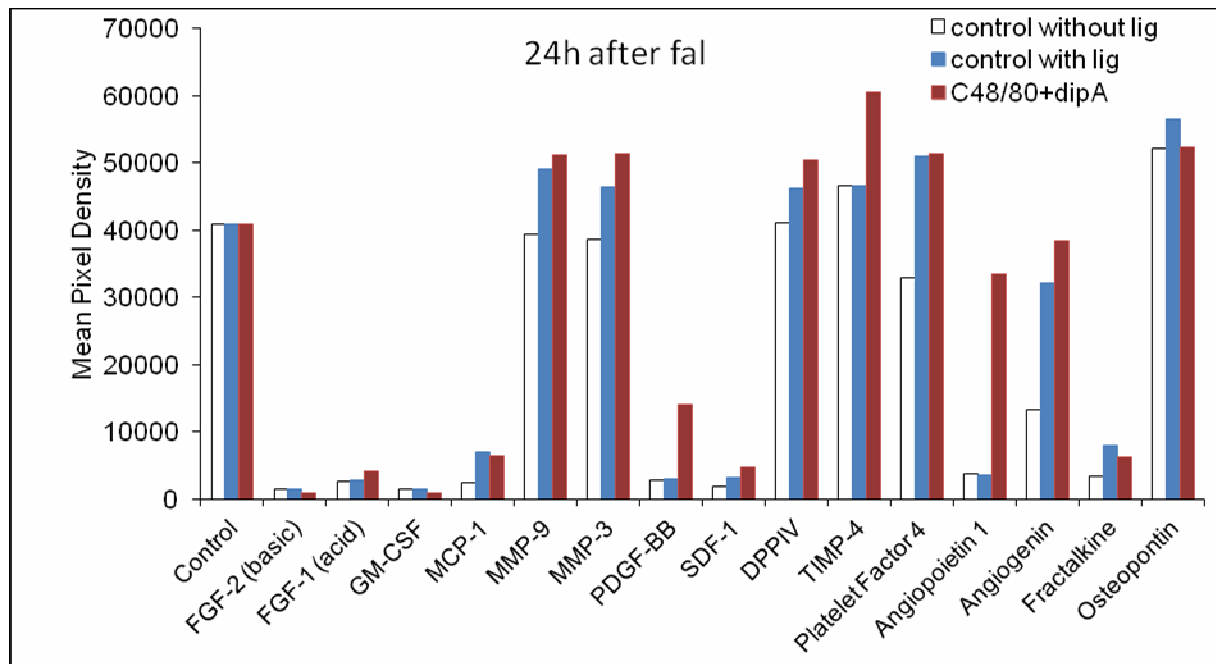


*Fig.15. Serum protein array*

Quantification of proteomic analysis of mouse serum of control without ligation, control with ligation or combination of C48/80 + diprotin A 24 hours after femoral artery ligation (fal).

### **3.8. The extent of mast cell degranulation covaries with the progress of vascular cell proliferation**

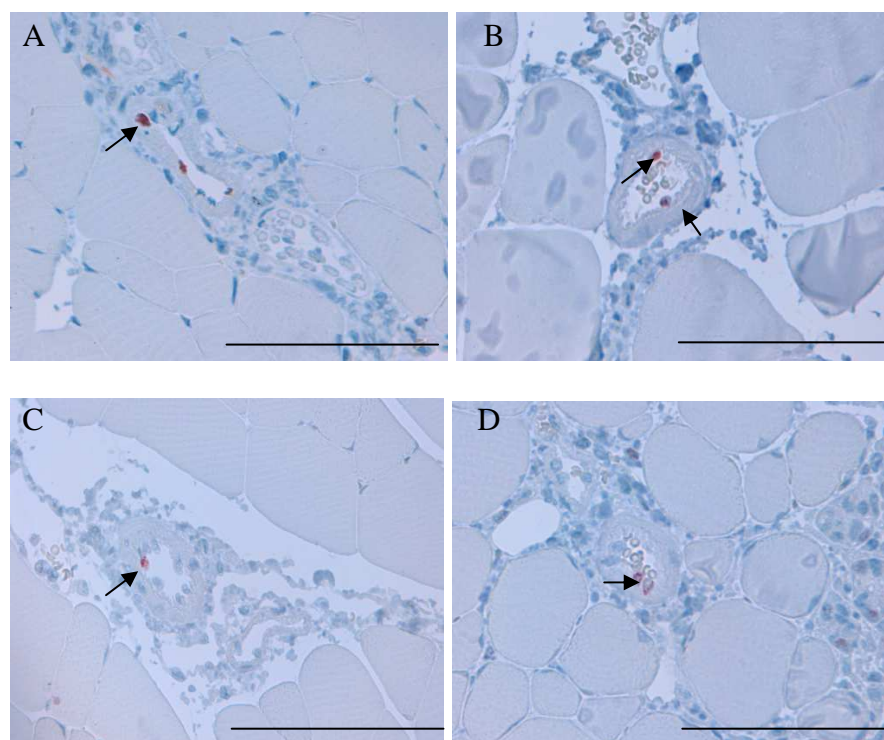
In order to identify proliferating cells in growing collateral arteries, we used the proliferation marker ki67 (figure 16). Three days after femoral artery ligation, nuclei of proliferating collateral vascular cells were stained with ki67.

With respect to controls, cells showing the Ki67 marker were more numerous in mice treated with C48/80 + diprotin A (figure 16 E). However, this difference was statistically not significant. In cromolyn treated and in cromolyn + diprotin A treated mice the number of Ki67 positive cells was smaller than in controls or in C48/80+diprotinA treated mice (figure 16 E). The differences between mice treated with cromolyn or with cromolyn + diprotin A and mice treated with C48/80 + diprotin A

were statistically significant (figure 16 E), whereas no significant differences were seen with respect to controls (table VI; figure 16 E).

Table VI. The number of Ki67<sup>+</sup> cell/collateral in experimental and control mice.

C48/80 + dip A vs. cromolyn	2.1 ± 0.4 vs. 1.16 ± 0.3	*P<0.05
C48/80 + dip A vs. cromolyn + dip A	2.1 ± 0.4 v.s. 1.08 ± 0.3	*P<0.05
C48/80 + dip A vs. control	2.1 ± 0.4 v.s. 1.6 ± 0.4	Non-significant



E



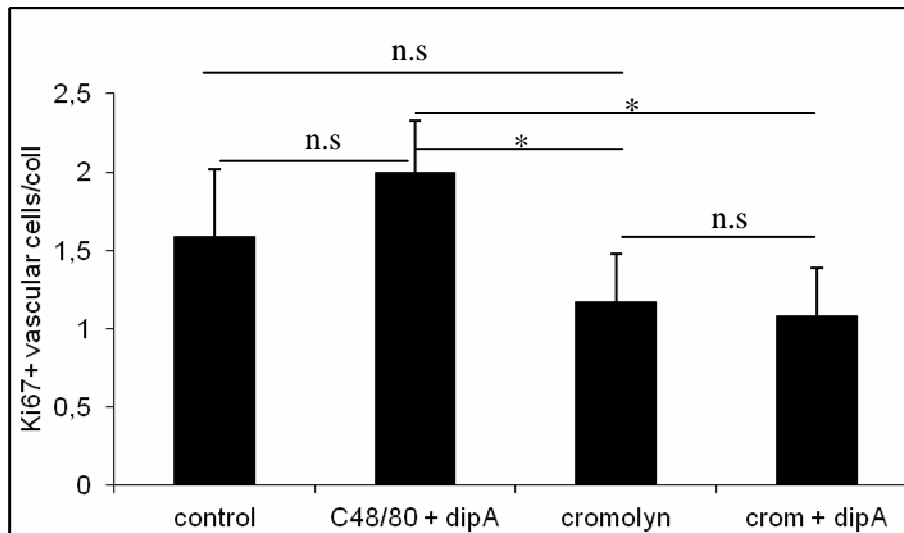


*Fig. 16.* Quantification of Ki67 staining in mice collateral arteries.

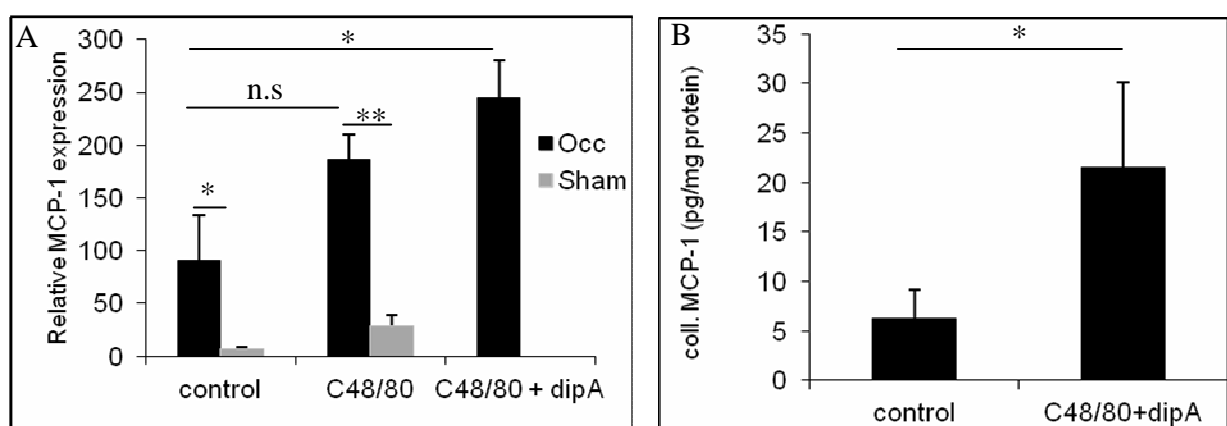
Immunohistochemical detection of Ki67 (red-brown cell nuclei) was performed on mice adductor sections from saline (control) (A), C48/80 + diprotin A (B), cromolyn (C), or cromolyn + diprotin A (D) treated animals. Black arrows point to Ki67+ nuclei in endothelial cells (arrows) and smooth muscle cells (arrow head). Scale bar = 100µm. E: Ki67<sup>+</sup> nuclei were quantified per collateral in animal treated with C48/80 + diprotin A, cromolyn + diprotin A or cromolyn versus control mice (\*P<0.05).

### **3.9. Degranulation of mast cells increases the expression of MCP-1 in collaterals**

An increased expression of monocyte chemoattractant protein (MCP)-1 during arteriogenesis is well described (Ito et al., 1997). It is so far unknown however, whether mast cells can influence the expression of MCP-1. To find out, we isolated collaterals 12 hours after femoral artery ligation from the occluded side and from the sham side of control mice (saline treated), of mice treated with C 48/80 and of mice treated with a combination of C 48/80 + diprotin A treated mice. We analyzed these collaterals with quantitative real time-polymerase chain reaction (qRT-PCR) to investigate mRNA levels. With respect to control mice was the expression of MCP-1 in collaterals of mice that were treated with a combination of C 48/80 + diprotin A

significantly increased (by a factor of 2.7). In mice that were treated with C 48/80 the expression of MCP-1 was not significantly increased (by a factor of 2.0; figure 17 A). Interestingly, the expression of MCP-1 on the sham-operated side was very small when compared to the occluded side of controls or of C 48/80 treated mice. Since mast cells degranulate mainly on the occluded side (see figure 10), the large difference in the expression of MCP-1 in collaterals on the sham operated and on the occluded side demonstrates the importance of mast cell degranulation for the expression of MCP-1.

This increase in the MCP-1 expression in collaterals could have materialized in a corresponding increase in the level of MCP-1 protein in mice treated with C 48/80 + diprotin A. Therefore, we evaluated the MCP-1 protein level of the collaterals 24 hours after femoral artery ligation. As a result, the MCP-1 protein in the collaterals of the occluded had increased significantly (a factor of 3.4; figure 17 B). However, at the same time the plasma concentrations of MCP-1 in C 48/80 + diprotin A treated mice and in controls were similar (figure 17 C).



C

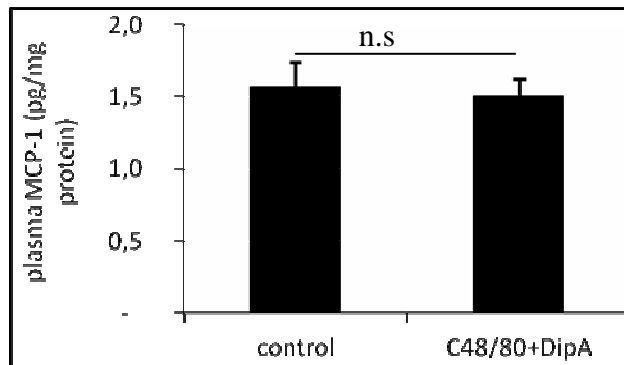


*Figure 17. Bar graphs showing relative collateral MCP-1 mRNA expression and m. adductor and plasma MCP-1 protein levels:*

- A. Bar graph representing the mRNA level of MCP1 in collaterals of saline (control), C 48/80 or C 48/80 + diprotin A treated animals as analyzed by qRT-PCR 12 hours after femoral artery occlusion (black bars) or sham (grey bars). \*P<0.05, \*\*P<0.01
- B. Quantitative analysis of collaterals MCP-1 protein levels by means of ELISA in saline (control) or combined C 48/80 + diprotin A treated mice 24 hours after femoral artery ligation. \*P<0.05.
- C. A histogram showing plasma MCP-1 protein level 24 hours after femoral artery ligation in saline (control) or C 48/80 + diprotin A treated animals.

### **3.10. Inhibition of mast cell degranulation reduces the release of TNF- $\alpha$ and lowers its plasma level.**

Tumor necrosis factor (TNF)- $\alpha$ , is a cytokine involved in inflammation (Bradley, 2008). With the help of ELISA, we could not detect any measurable amount of TNF- $\alpha$  in the plasma of control mice without femoral ligation. In control mice with femoral artery ligation, we found 1.47 pg/mg protein of plasma TNF- $\alpha$ . However, after mast cell degranulation had been inhibited by a treatment with cromolyn, mice with a ligation of the femoral artery exhibited a significant reduction in their plasma TNF- $\alpha$  protein levels with respect to controls with ligation ( $1.47 \pm 0.2$  v.s.

0.36  $\pm$  0.24 control with ligation versus cromolyn with ligation treated mice, \*P<0.05) (figure 18).

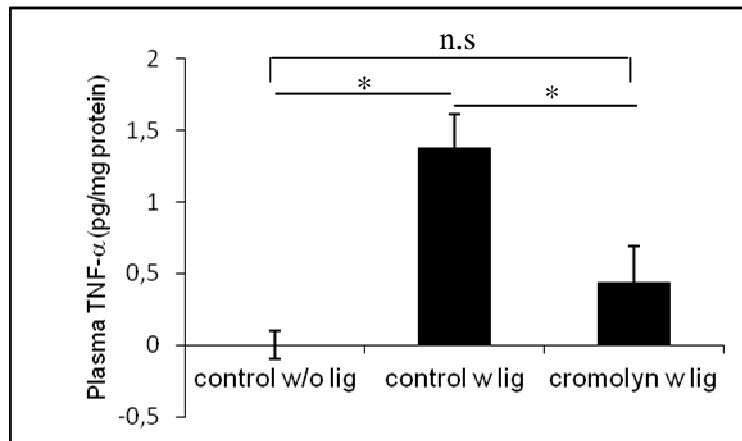


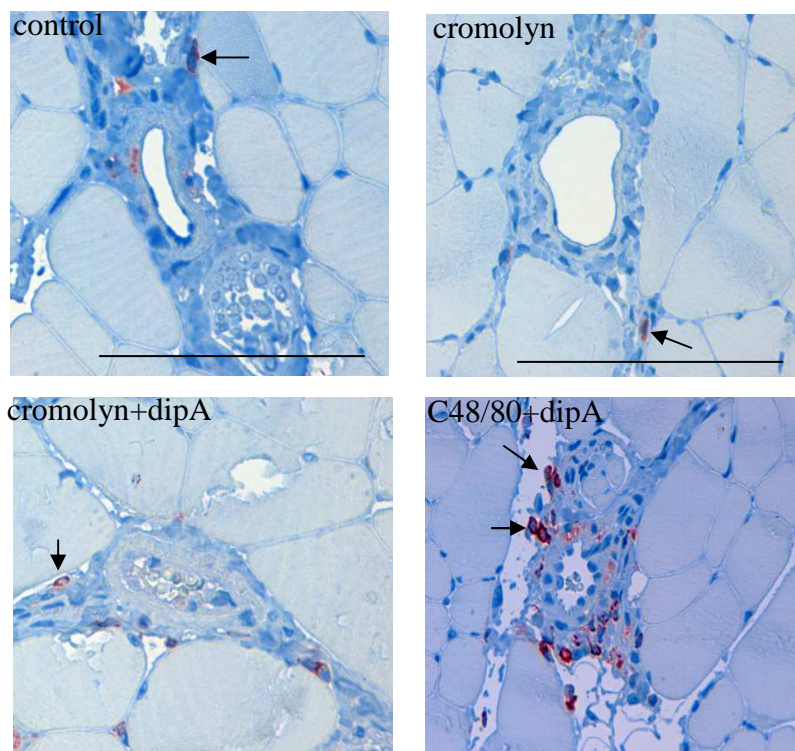
*Figure 18: Plasma TNF- $\alpha$  levels*

Bar graph showing ELISA results on quantification of plasma TNF- $\alpha$  levels (pg/mg) of control (saline treated) mice without ligation (control w/o lig), control with ligation (w lig) or ligation and cromolyn treatment (cromolyn w lig) 24 hours after the surgery (\*P<0.05)

### **3.11. Mast cell degranulation recruits leukocytes**

Leukocytes, especially monocytes are known to be recruited and to play a central role in the development of collateral arteries during the early phase of arteriogenesis from 24 hours to 3 days (Arras et al., 1998). As a first step, we assessed the number of leukocytes in the vicinity of growing collaterals three days after femoral artery ligation. Leukocytes were stained with CD45 antibodies (figure 19 A). In mice treated with C 48/80 + diprotin A we found significantly more perivascular leukocytes (on an average 8 CD45+ cells, i.e. leukocytes, per collateral) than in saline treated control animals (on average 2 leukocytes). On the other hand, the induction of leukocyte

recruitment was abrogated by the application of the mast cell stabilizer cromolyn (figure 19 B). We then assessed whether the recruitment of leukocytes provoked by the application of diprotin A can be suppressed by a concomitant application of the mast cell stabilizer cromolyn. As a result, the number of perivascular leukocytes in cromolyn + diprotin A treated mice was significantly smaller than in mice treated with C 48/80 + diprotin A, but with respect to cromolyn mice treated mice the number of leukocytes in cromolyn + diprotin A treated mice was slightly increased (figure 19 B).



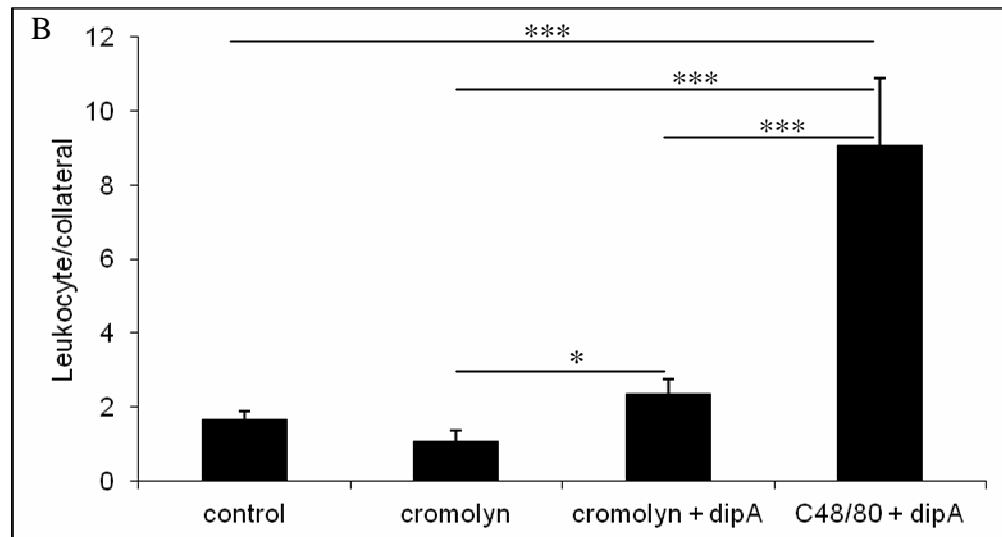


*Figure. 19. Histological quantification of perivascular leukocytes*

A: Representative images of immunohistochemical staining of leukocytes (CD45<sup>+</sup>, brown cells) in a combined C 48/80 + diprotin A treated group in comparison to saline (control), cromolyn, or combination of cromolyn + diprotin A (dipA) treated mice. Scale bar = 100μm.

B; Bar graph showing the average number of leukocytes per collateral 3 days after femoral artery ligation in control, cromolyn, combination of cromolyn + diprotin A, or combination of C 48/80 + diprotin A treated animals. (\*P<0.05, \*\*\*P<0.001).

To define the subpopulation of the perivascular leukocytes we investigated the differential cell population in the adductor muscles and in the blood by flow cytometry. The flow cytometric analysis of freshly isolated adductor muscle tissue from the occluded hindlimb 24 hours after femoral ligation revealed a significant

increase in the number of neutrophils and of macrophages (Table VII; figure 20 A-C). In addition, I analyzed the blood of the same two groups of mice 24 hours post femoral ligation. Flow cytometry analysis revealed an increased number of neutrophils (Gr-1<sup>+</sup> CD115<sup>-</sup>), Macrophages and monocytes (CD 115<sup>+</sup>), and T cell (CD4<sup>+</sup> and CD8<sup>+</sup>) (table VIII; figure 20 D-F).

Table VII. Leukocyte subpopulation in adductor muscles 24 hours after ligation.

cell marker	C 48/80 + dipA vs. control	Statistical significance
Gr-1 <sup>+</sup> CD115 <sup>-</sup>	8.4% ± 4.0% vs. 0.36% ± 0.37%	*P<0.05
F4/80 <sup>+</sup>	12.2% ± 2.1% vs. 1.65% ± 0.81%	**P<0.01

Table VIII. Leukocyte subpopulation in the blood 24 hours after ligation.

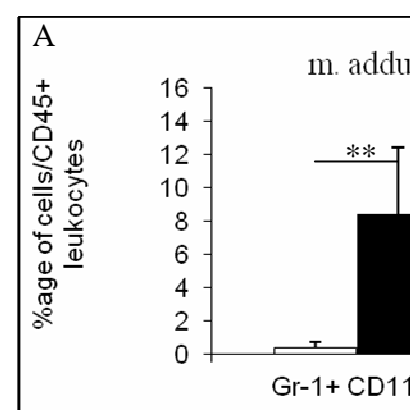
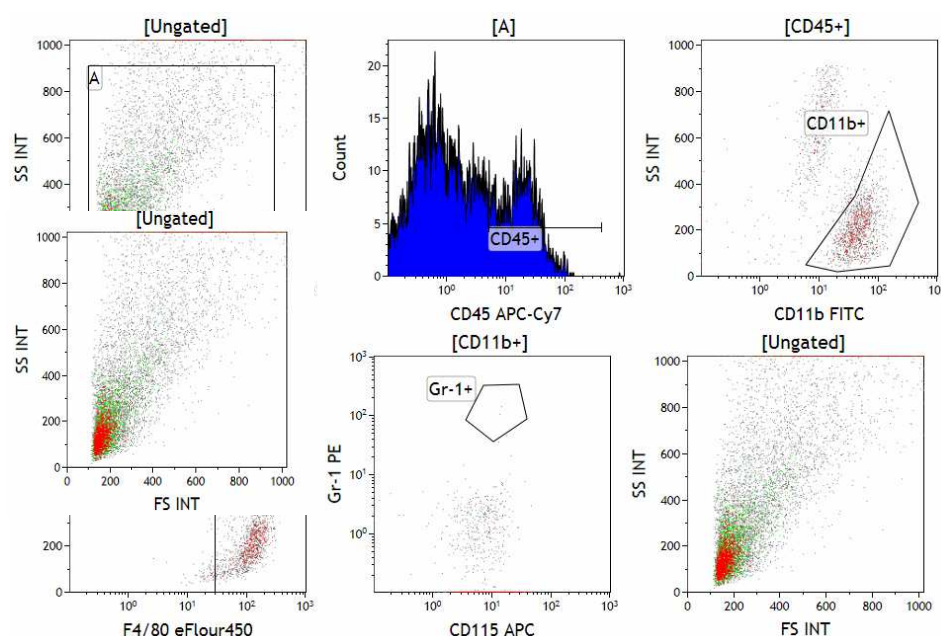
cell marker	C 48/80 + dipA vs. control	Statistical significance
Gr-1 <sup>+</sup> CD115 <sup>-</sup>	22.5% ± 2.6% vs. 0.91% ± 1.0%	**p<0.01
CD115 <sup>+</sup>	4.6% ± 0.95% vs. 3.3% ± 3.2%	Non-significant
CD4 <sup>+</sup>	3.5% ± 0.9% vs. 0.4% ± 0.4%	*P<0.05
CD8 <sup>+</sup>	2.4% ± 0.6% vs. 0.22% ± 0.18%	*P<0.05

In addition, we identified the subpopulations of leukocytes and compared their numbers three days after femoral artery ligation in freshly isolated adductor muscles from the occluded limbs of C 48/80 + diprotin A treated and of control mice. In the group of mice that received a combined C 48/80 + diprotin A treatment the numbers

of macrophages were significantly increased (table IX; figure 20 G-I). In the same two groups of mice, we assessed the pattern of leukocyte subpopulations in the blood 3 days post femoral ligation. Flow cytometric analysis showed no differences in the numbers of these cell subpopulations between mice treated with C 48/80 + diprotin A and control mice (figure 20 J-L).

Table IX. Leukocyte subpopulation in adductor muscles 3 days after femoral artery ligation.

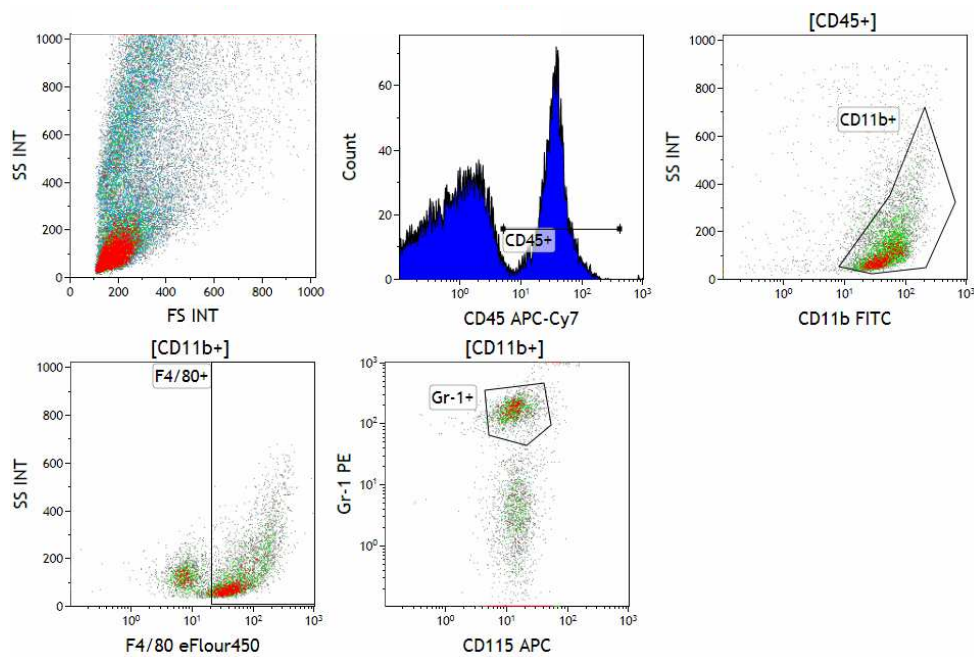
cell marker	C 48/80 + dipA vs. control	Statistical significance
Gr-1 <sup>+</sup> CD115 <sup>-</sup>	3.6% $\pm$ 1.9% vs. 0.06% $\pm$ 0.01%	Non-significant
F4/80 <sup>+</sup>	5.36% $\pm$ 1.0% vs. 0.26% $\pm$ 0.01%	**P<0.05



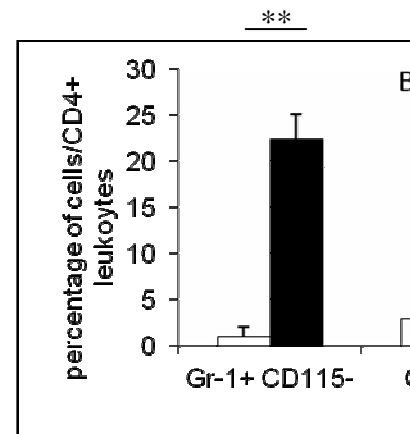
(B) Control adductor 24 h post



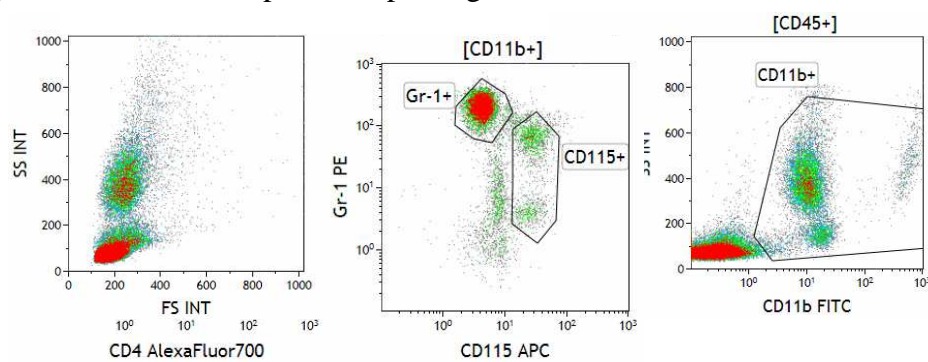
(C) C48/80+dipA adductor 24 h post lig



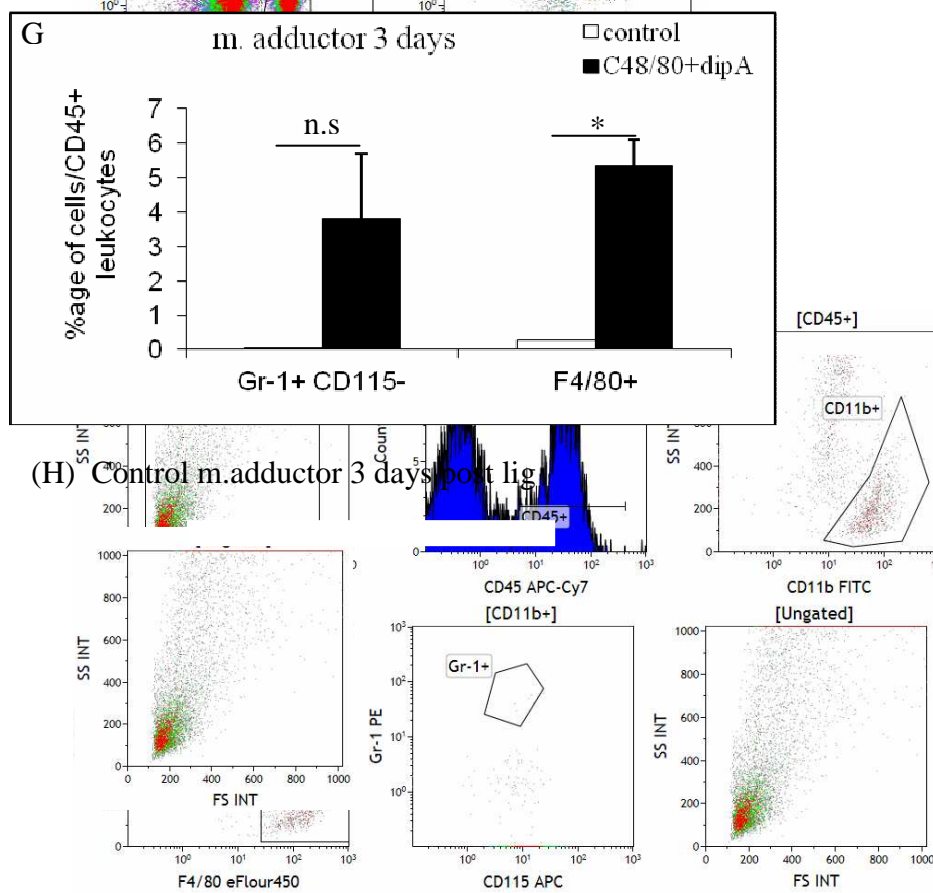
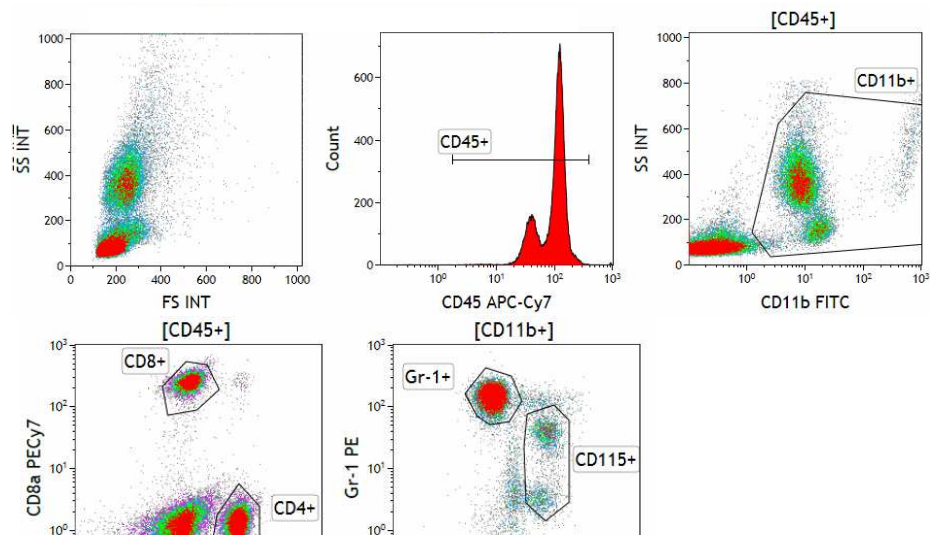
D



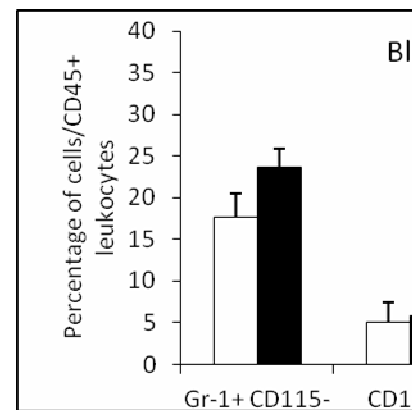
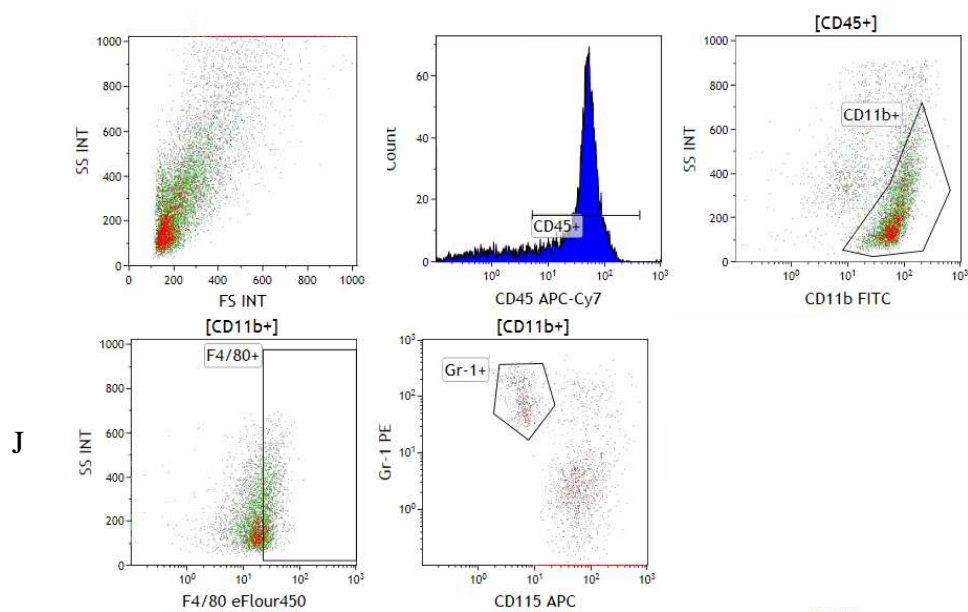
(E) Control blood samples 24 h post lig



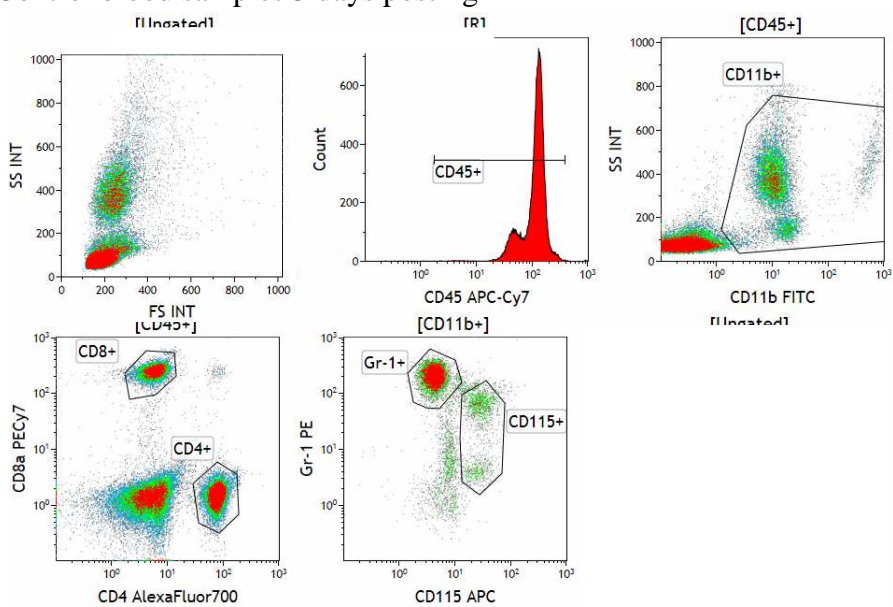
(F) C48/80+dipA blood samples 24 h post lig



(I) C48/80+dipA m.adductor 3 days post ligation



(K) Control blood samples 3 days post lig



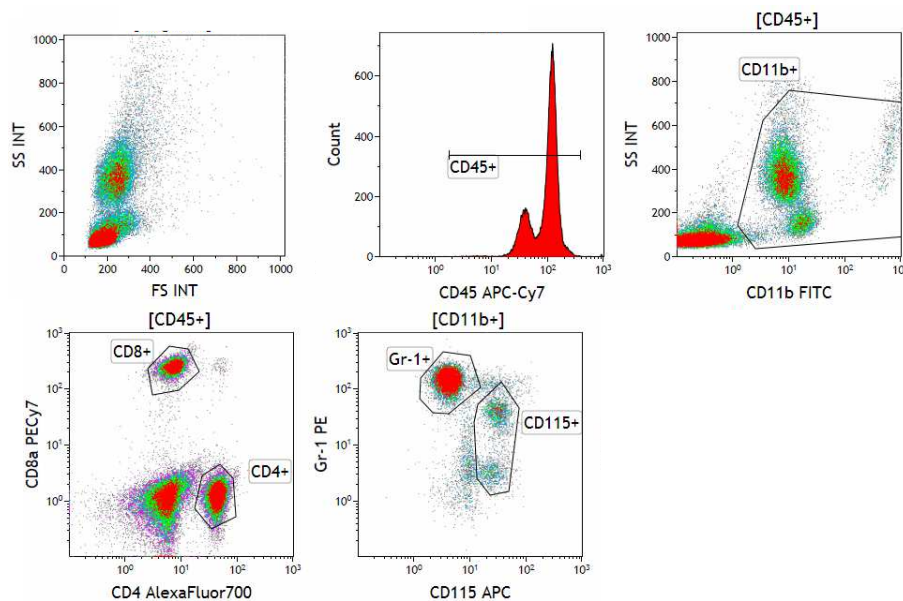


Figure 20:

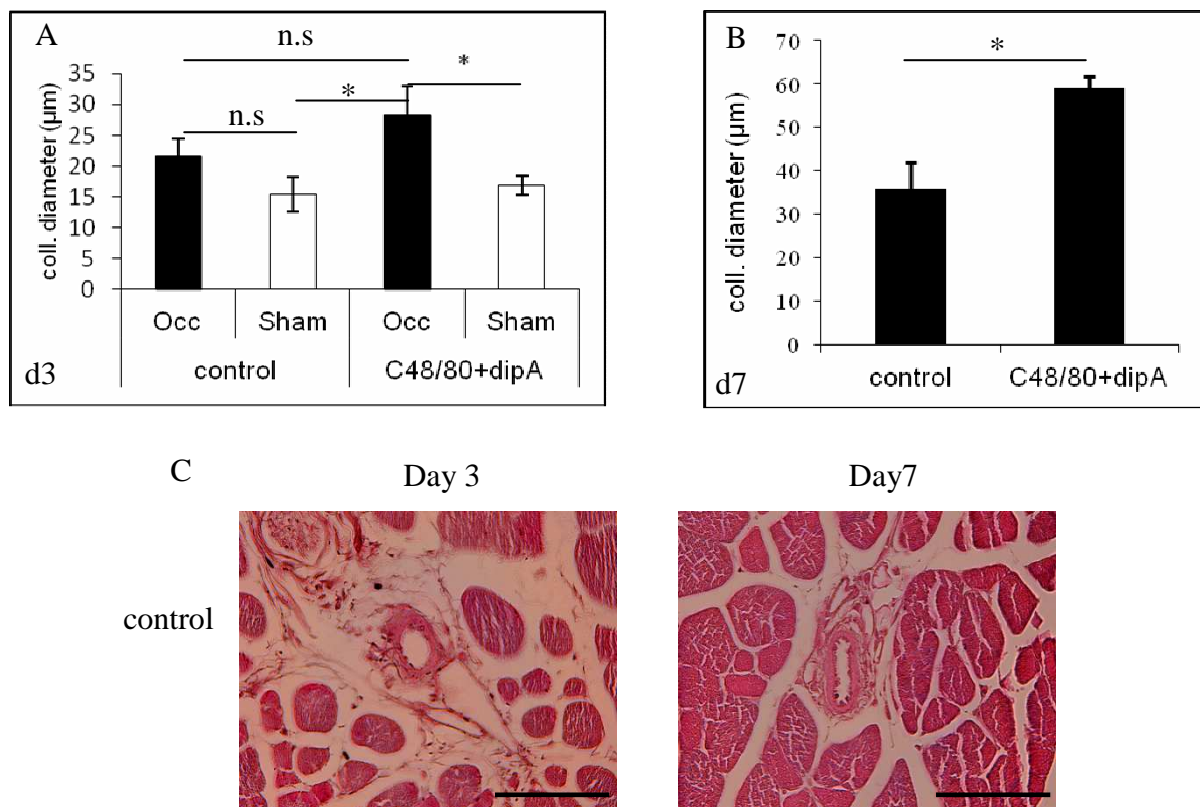
*Vertical bar charts and FACS images of m.adductor and blood samples 24 hours and 3 days post ligation.*

Vertical bar chart showing the results of cell counts by flow cytometry in the adductors (A) and blood (D) of saline (control) and combined C 48/80 + Dip A treated mice 24 hours after femoral artery ligation (fal). Representative images of flow cytometry analyses showing different cell population in the adductors of saline (control) (B) and combined C 48/80 + diprotin A (C) treated mice, and in the blood of control (E) and combined C 48/80 + diprotin A (F) 24 hours post ligation.

Bar graph displaying the results of cell counts by flow cytometry in the adductors (G) and blood (J) of saline (control) and combined C 48/80 + Dip A treated mice 3 days after femoral artery ligation (fal). Representative images of flow cytometry showing different cell population in the adductors of control (H) and combined C 48/80 + diprotin A (I) treated mice, and in the blood of control (K) and combined C 48/80 + diprotin A (L) 24 hours post ligation. (\*P<0.05).

### 3.12. Treatment of mice with C 48/80 + diproton A results in an increased collateral vessel diameter

To investigate whether the increased blood flow in the distal hind limb results from outward vascular remodeling, we measured the inner diameter of collateral arteries in the adductor muscle 3 and 7 days after femoral artery ligation. 3 days after femoral artery ligation we found an increase in the luminal diameter by a factor of 1.3 in C48/80 + Dip A treated mice with respect to control mice (figure 21 A). Seven days after femoral artery ligation, the collateral diameter in C 48/80 + diproton A treated mice was significantly increased by a factor of 1.7 with respect to control mice (figure 21 B). This increase in the diameter of collateral arteries explains the increase in the blood flow in the distal hind limb and can be expected to have a beneficial effect on the preservation of muscular tissue, e.g. the gastrocnemius muscle.





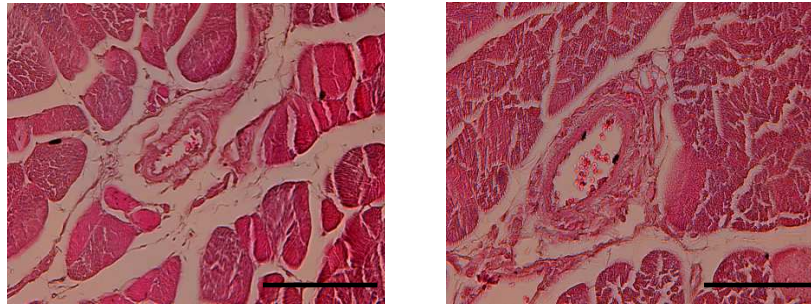


*Fig.21. Quantification of collateral artery enlargement*

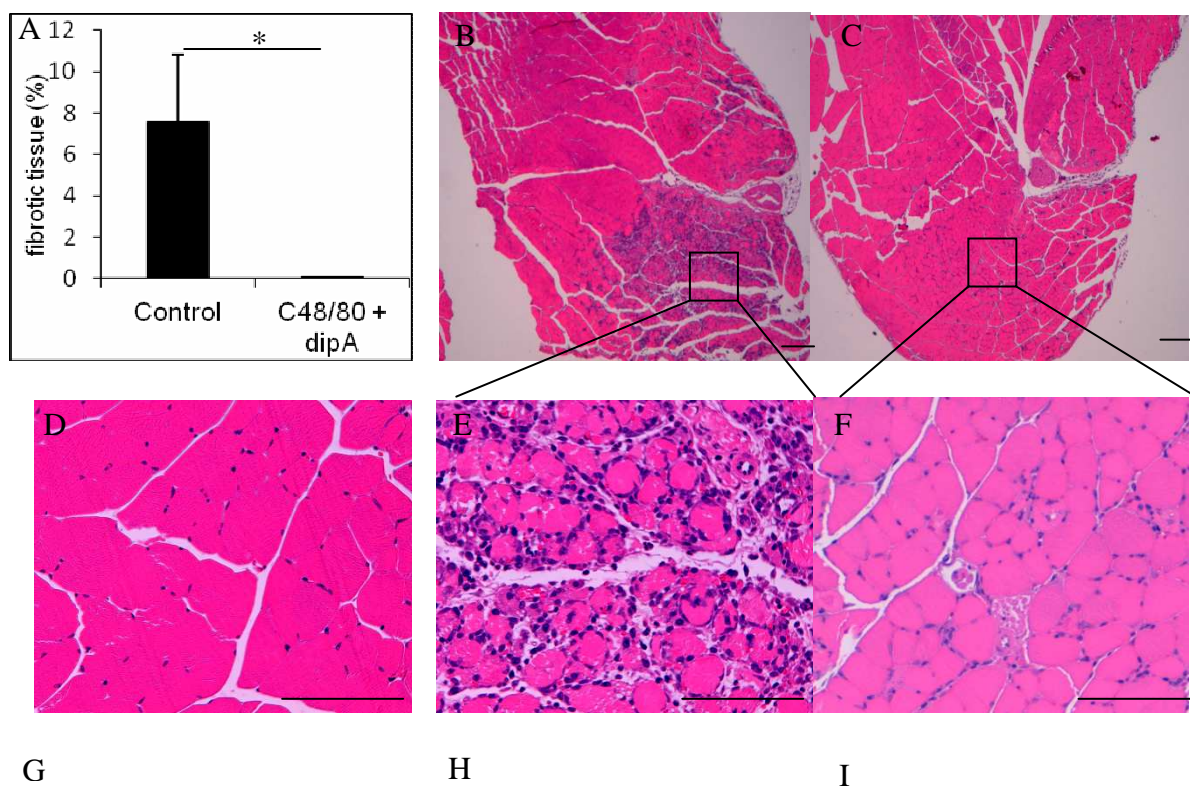
Bar graphs showing the quantification of luminal diameter ( $\mu\text{m}$ ) at day 3 (A), and day 7 (B) after femoral artery ligation in saline (control) or C 48/80 + diprotin A treated mice. (\* $P < 0.05$ ).

C: Representative pictures of hematoxylin-and-eosin (H&E) staining from adductor tissue sections of mice in ligated hind limbs at day 3 and 7 post femoral ligation in control or C 48/80 + Diprotin A treated mice. Scale bars =  $100\mu\text{m}$ .

#### **4.13. Improved perfusion reduces distal tissue ischemic damage**

Paraffin fixed tissue sections taken 3 days after femoral artery ligation were stained with haematoxylin and eosin. Histological analyses of the m. gastrocnemius three days after surgery revealed more pronounced fibrosis in saline treated control mice than in mice treated with a combination of C 48/80 + diprotin A. In the latter group of animals, almost no fibrosis was detected in the calf muscles (figure 22 A-F). Sections of the calf muscles were in addition assessed and quantified for leukocyte infiltration ( $\text{CD45}^+$  cells). Consistent with the large extent of tissue fibrosis seen in control mice, there was also an increase in the number of leukocytes in the tissues from control mice when compared to C 48/80 + diprotin A treated mice ( $\text{CD45}^+$  cells/ $\text{mm}^2$ :  $208 \pm 33$  in control mice vs.  $18 \pm 16$  in C 48/80 + diprotin A treated mice; \*\*\* $P < 0.001$ ; figure 22 G-I). Furthermore, the capillary endothelial cells in the gastrocnemius muscle were investigated by CD31 antibody staining. Our results revealed a significant increased ratio of capillaries per muscle fibre in the ligated hind limb of control group

when compared to C 48/80 + diprotin A treated mice (CD31<sup>+</sup> cells/muscle fibre:  $2.48 \pm 0.2$  in C 48/80 + diprotin A treated mice vs.  $1.1 \pm 0.1$  in control mice; \*\*\*P<0.001; figure 22 J). Interestingly, the ratio of capillaries per fibre in the gastrocnemius muscle of a ligated hind limb treated with C 48/80 + diprotin A mice were equivalent with the unligated (sham) side as well as that of unligated control (figure 22 J-L). Furthermore, we investigated whether the absence of tissue fibrosis seen in C 48/80 + diprotin A treated mice was related to mast cell degranulation in the gastrocnemius muscle. As a result, neither femoral artery ligation nor local application of C 48/80 in the upper leg resulted in mast cell degranulation in the gastrocnemius muscle (figure. 22 M). This implies that tissue preservation in the gastrocnemius muscle did not result from a local mast cell degranulation in this muscle but was rather the result of arteriogenesis in femoral collaterals.



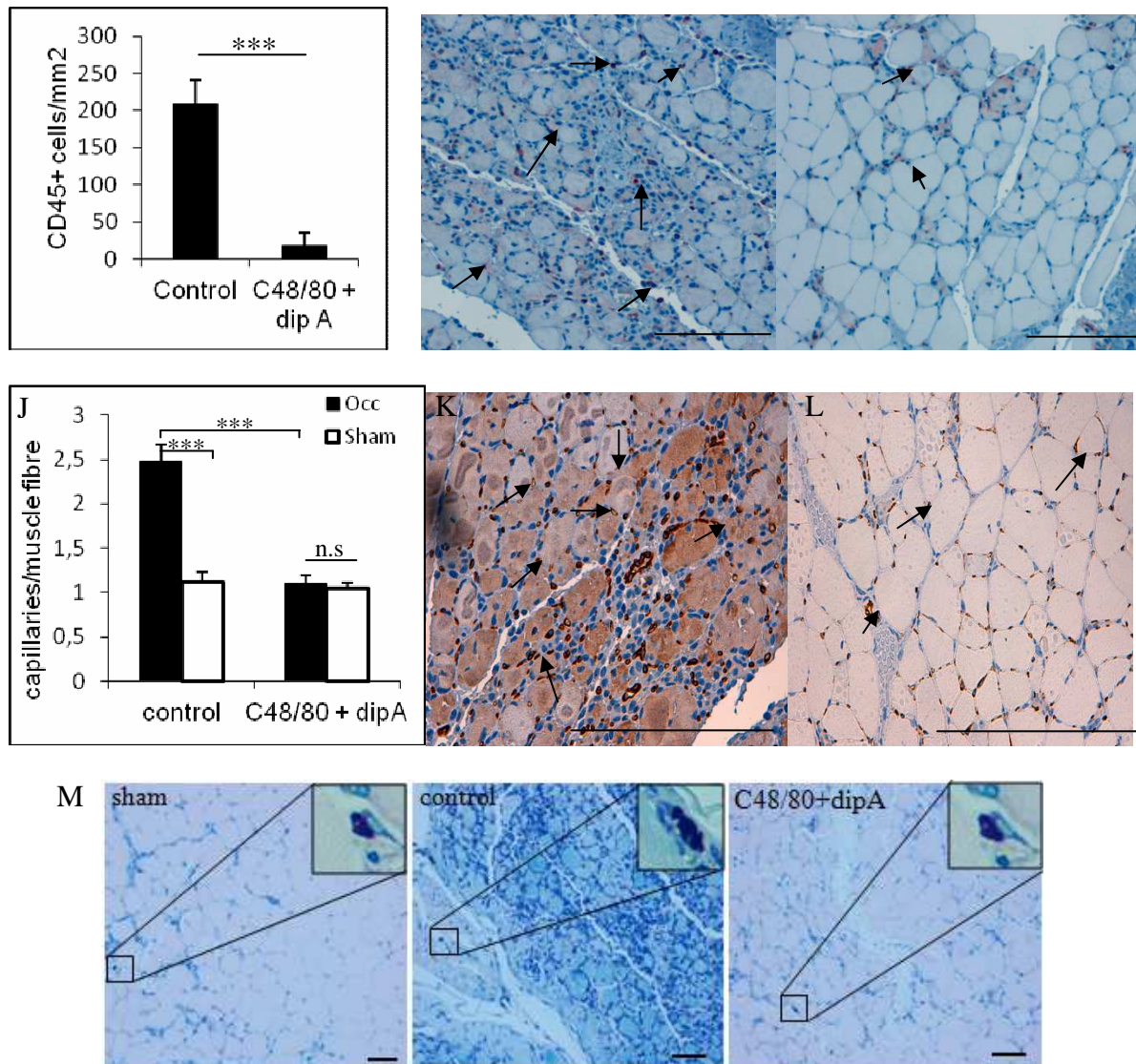


Fig. 22: Histological analysis of the m. gastrocnemius.

Quantification of fibrosis in the tissue sections of the gastrocnemius of saline (control) or combined C 48/80 + diprotin A treated mice (A) (\*P ≤ 0.05). Representative pictures of H&E stained m. gastrocnemius of control (B) or C 48/80 + diprotin A (C) treated mice (scale bar = 100µm). (D) Shows the m. gastrocnemius of a sham operated mouse and (E) and (F) present magnification of (B) and (C), respectively. (scale bar = 100µm).

Quantification of leukocyte (CD45<sup>+</sup> cells; stained brown, arrows) in m. gastrocnemius of control mice or C48/80 + diprotin A treated mice (G) (\*\*P ≤ 0.001). Representative pictures of CD45 positive cells in control (H) or C 48/80 + diprotin A treated mice (I) (scale bar = 100µm).



Bar chart showing the quantification of capillaries (CD31<sup>+</sup> cells) per muscle fibre, (J) in the m. gastrocnemius of saline (control) or C 48/80 + diprotin A treated mice (\*\*P ≤ 0.01). Representative pictures of CD31 antibody staining (stained brown, arrows) in saline (control) (K) or C 48/80 + diprotin A treated mice (L) (scale bar = 100µm). Representative Giemsa staining showing (M) mast cells and their magnification (top right) in the m. gastrocnemius of mice in the saline treated (control) sham, control with occlusion and in the occluded C 48/80+ diprotin A treated mice three days after femoral artery ligation. (Scale bar 100µm).

### **3.14. Mechanism of mast cell degranulation during untreated arteriogenesis**

As shown above, mast cells respond to femoral artery ligation with a degranulation (figure 10 E). This reaction is independent of the presence or the absence of a treatment. It is therefore of interest to understand the mechanisms that underlie this response. A number of candidates could be of importance in the induction of mast cell degranulation, such as the neuropeptide substance P or neutrophils.

In order to prevent substance P from an induction of mast cell degranulation, we administered RP-67580, which inhibits the release of substance P (Malcangio and Bowery, 1994). Laser Doppler imaging showed that inhibition of substance P had no effect in hind limb perfusion recovery rate (figure 23 A). Next we investigated whether neutrophils mediate the degranulation of mast cells. To that end we applied Ly6G (1A8) antibodies, which depleted circulating neutrophils (Daley et al., 2008) by 70% within 2 days after their application (figure 23 B). Treatment of wild type mice with 1A8 resulted in a significantly slower perfusion recovery 7 days after femoral artery occlusion ( $0.49 \pm 0.03$ ) than in controls ( $0.71 \pm 0.07$ ; \*p<0.05; figure 23 C). This slower recovery rate could have resulted from a reduced number of degranulated mast cells. A histological analysis of Giemsa stained adductor muscle sections from mice treated

with 1A8 antibodies revealed in fact a significantly decreased mast cell degranulation 24 hours after femoral artery ligation (figure 23 D).

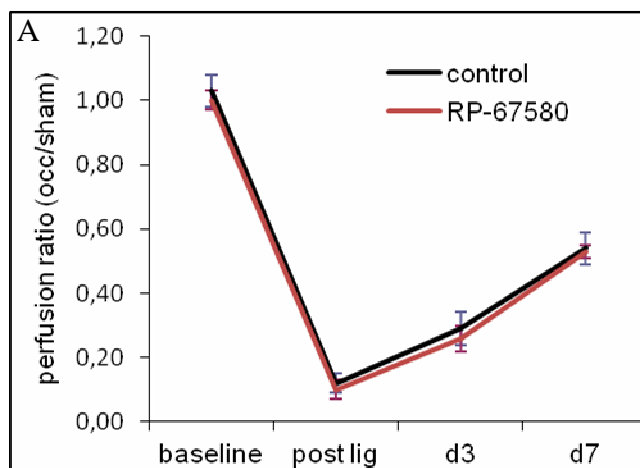
Since neutrophils are suggested to be the first cells recruited in the process of arteriogenesis (Behm et al., 2008) we investigated our working hypothesis, according to which neutrophils are involved in the degranulation of mast cells. More precisely, Nox 2 (NADPH oxidase) a major source of reactive oxygen species (ROS) in neutrophils is released by neutrophils upon platelets/neutrophils interaction (Vanichakarn et al., 2008). The release of ROS in turn degranulates mast cells.

To investigate this hypothesis we used Nox-2 null ( $\text{Nox2}^{-/-}$ ) mice. In  $\text{Nox2}^{-/-}$  mice femoral artery ligation was induced and the adductor muscle was analyzed histologically to quantify mast cell degranulation 24 hours and 3 days after surgery. We found that the extent of mast cell degranulation in  $\text{Nox2}^{-/-}$  deficient mice was significantly reduced 24 hours as well as 3 days after a ligation of the femoral artery with respect to control mice (figure 23 D and E).

Furthermore, I used the NADPH oxidase inhibitor (apocynine) or a ROS scavenger (N-acetylcystein) to block ROS. In both experiments histological analysis revealed a significant reduction in the number of degranulated mast cell upon femoral artery ligation (figure 23 D). These results indicate that a reduction in the production of ROS results in a smaller number of degranulated mast cells.

A similar reduction in the production of ROS was observed by (Evangelista et al., 2005) after the inhibition of the interaction between platelets and neutrophils. Therefore we investigated the degranulation of mast cells in histological sections of adductor muscles from  $\text{GPIb}\alpha^{-/-}$  mice (a platelet adhesion receptor) 3 days after femoral artery ligation. We found a significant reduction of mast cell degranulation in  $\text{GPIb}\alpha^{-/-}$  mice when compared to control mice (figure 23 E). Furthermore, we

investigated adductor muscle sections from urokinase plasminogen activator (uPA<sup>-/-</sup>) mice. These mice are deficient proteolytic activity of plasminogen to plasmin. In this experiment they revealed a significant reduction of mast cell degranulation when compared to control mice (figure 23 D). These results imply that mast cell degranulation during untreated arteriogenesis is mediated by neutrophil derived ROS production in the vicinity of collateral arteries. This process is dependent on platelet/neutrophil interaction mediated by the platelet receptor GP1b $\alpha$  as well as uPA dependent extravasation of neutrophils.



B

C

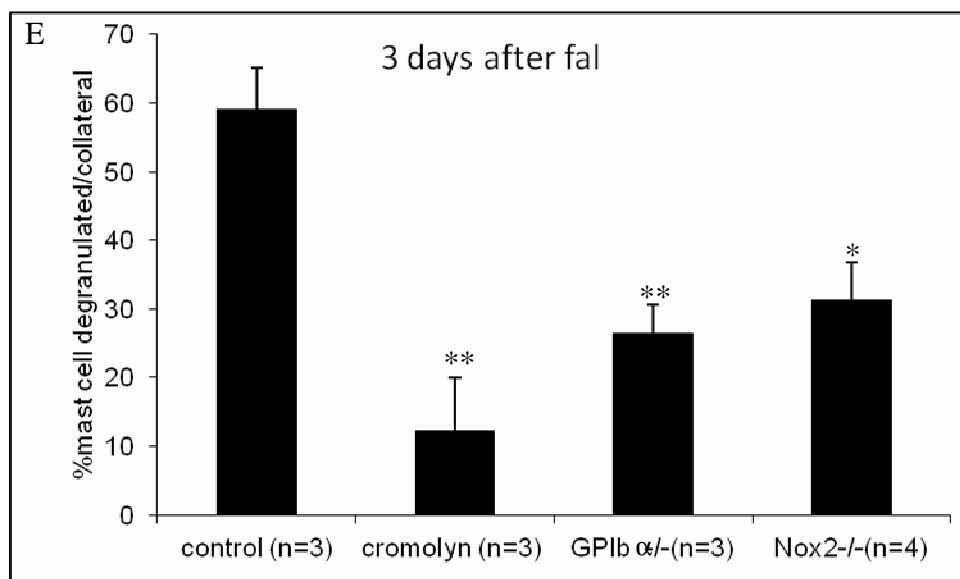
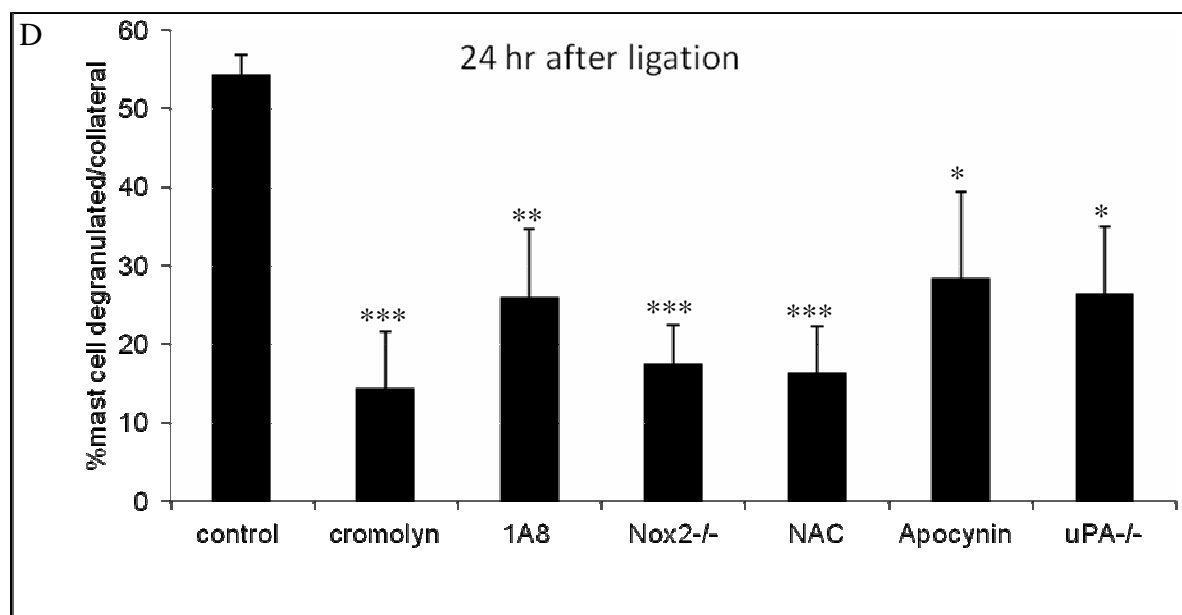
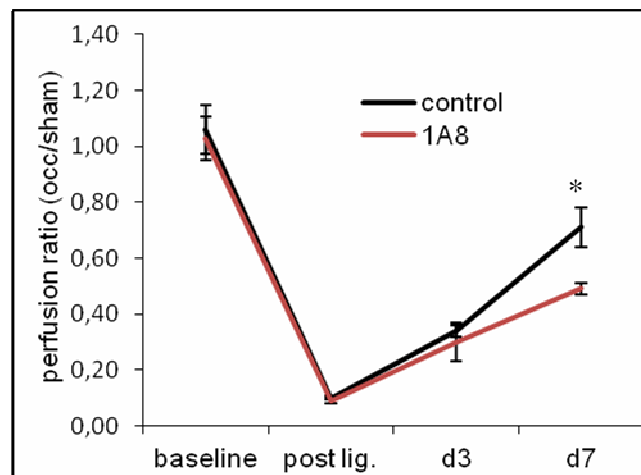
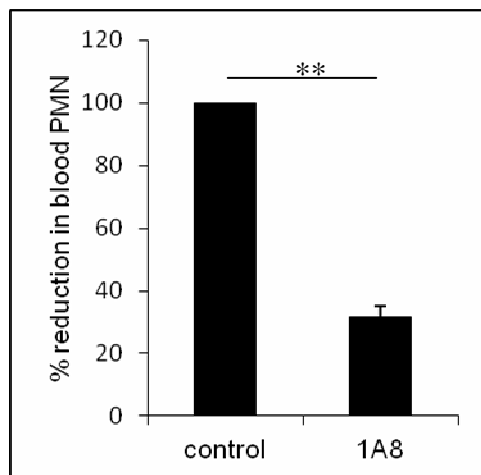


*Figure 23: Mast cell degranulation during un-influenced arteriogenesis.*

Quantification of perfusion recovery ratio (occluded/sham) of mice treated with substance P release inhibitor (RP-67580) versus saline treated (control) (A).

Bar graph displaying the effectiveness of a neutrophil depletion substance (1A8) in blood (B) (\*\*P<0.01). Laser Doppler measurements shows the perfusion ratio of 1A8 treated mice in comparison to saline treated (control) (C) (\*P<0.05).

D: A vertical bar chart of saline (control), cromolyn, 1A8, NAC (N-acetylcystein) and apocynin treated mice and uPA<sup>-/-</sup> and Nox2<sup>-/-</sup> mice showing the percentage of mast cell degranulated around growing collaterals 24 hours after femoral artery ligation (\*P<0.05, \*\*P<0.01, \*\*\*P<0.001).

E: Bar chart showing the percent of mast cell degranulated in saline (control) and cromolyn treated mice, as well as Nox2<sup>-/-</sup> and GPIIbα<sup>-/-</sup> mice 3 days after femoral artery ligation (fal) (E) (\*P<0.05, \*\*P<0.01, \*\*\*P<0.001).

## 4. DISCUSSIONS

The occlusion of an artery is followed by a redirection of the blood flow through pre-existing arterial collaterals. Due to outward remodelling, the diameter of these collaterals enlarges and their tortuous shape becomes more and more corkscrew-like. This process of arterial growth is assumed to be initiated by increased mechanical forces such as shear stress and circumferential wall stress (Yang et al., 2013). Thereby, the endothelium becomes activated, recruiting leukocytes and

endothelial and smooth muscle cells of pre-existing arterial collaterals proliferate. The enlargement of these pre-existing arterial collaterals is strongly dependent on the accumulation of perivascular leukocytes (especially monocytes), as a source of important growth factors and cytokines. In fact, Hoefer et al. (2005) showed that monocytes and macrophages locally supply growth factors and cytokines that promote collateral artery growth.

#### *4.1 Mast cells degranulate in response to arterial occlusion*

In addition to pericytes, mast cells are present in the vicinity of pre-existing arterial collaterals as well. Suggestive evidence indicated that mast cells may also be involved in tissue remodelling and in arteriogenesis. Mast cells accumulate in the adventitia of growing collaterals (Schaper and Scholz, 2003) and they are important immune effector and modulatory cells that are involved in tissue remodelling (Saito, 2005). In normal physiological state mast cells remain essentially quiescent. But activation of mast cells results in the release of a variety of mediators including important growth factors and enzymes, a process known as degranulation. Therefore, a prerequisite for a possible functional contribution of mast cells in arteriogenesis is degranulation in response to arterial occlusion. However, so far no reports were available concerning degranulation of mast cells in response to arterial occlusion. Therefore, we analysed the reaction of mast cells in our mouse model and observed in our histological investigation a progressively increased mast cell degranulation within the first 3 days after femoral artery ligation (figure 10 E). This activation of mast cells was restricted to the perivascular vicinity of pre-existing collaterals in the region of the occluded artery. Mast cells along corresponding collaterals in the non-operated limb were essentially stable and non-degranulating

(figure 10 D). Interestingly, no degranulation of mast cells was observed on the operated side in the lower limb (*m.gastrocnemius*), even when ischemia and tissue necrosis were severe (figure 23 E). This observation implies that ischemia and its consequences are not relevant signals for the activation of mast cells.

#### *4.2. Reduced mast cell degranulation slows down the speed of arteriogenesis*

Given that mast cells degranulate in response to the occlusion of an artery, we investigated a possible functional contribution of mast cells by the application of cromolyn, a substance which is known to stabilize mast cells by inhibiting their degranulation (Brogden et al., 1974). Our histological analysis revealed a significantly decreased percentage of degranulated mast cells around the growing collaterals in mice treated with cromolyn (figure 11 C and D). We analysed the functional consequences of a stabilization of mast cells with cromolyn for the blood flow reperfusion after femoral artery ligation with a laser Doppler imaging technique. As a result, the rate of recovery of the blood flow distal to the femoral artery ligation was slowed down for 21 days after the administration of cromolyn (figure 11 A). This result implies that mast cell degranulation in response to femoral artery occlusion is not just an event that parallels arteriogenesis. Rather, a reduced rate of release of granula by mast cells has a negative effect upon the speed of arteriogenesis and upon the rate of blood flow recovery.

#### *4.3. Enhanced mast cell degranulation accelerates the rate of blood flow recovery*

Compound 48/80, a mixture of polymers formed after the condensation of p-methoxyphenethylamine with formaldehyde, activates the secretory process of mast cells (Nakamura and Ui, 1985) through a direct activation of G-membrane proteins

(Mousli et al., 1990). With the application of C 48/80 we could further test our working hypothesis, according to which mast cell degranulation is an important factor for the progress of arteriogenesis in general and an enhanced rate of mast cell degranulation should improve the speed of arteriogenesis and the rate of blood flow recovery in particular. In fact, the application of C 48/80 increased the rate of hind limb blood flow reperfusion significantly at days 7 and 14 with respect to saline treated control animals (figure 13 C).

#### *4.4 Enhanced recruitment of mast cells and of other leukocytes accelerates the rate of blood flow recovery*

Diprotin A (Ile-Pro-Ile tripeptide) is a dipeptidyl aminopeptidase IV (DPP IV / CD26) inhibitor, an ectoenzyme protease, which cleaves the potent chemoattractant molecule SDF-1 $\alpha$  in the serum (Christopherson et al., 2004, Zaruba et al., 2009). Mice treated with diprotin A showed a significantly faster blood flow recovery than controls. The pattern of blood flow recovery was similar to that of mice treated with C48/80 (figure 12 B). Given that diprotin A increases the recruitment of stem cells from the bone marrow including immature mast cells and monocytes through an enhanced SDF-1 $\alpha$  level (Christopherson et al., 2004, Vagima et al., 2011). In our experiments we found that this reaction is also present in the context of growing collateral arteries (figure 12 D). Therefore, more bone marrow stem cells of leukocyte lineage differentiate and mature around the growing vessel and release more chemokines and growth factors, which are necessary for arteriogenesis.

It has previously been shown that those subtypes of stem cells which differentiate into endothelial cells and smooth muscle cells do not play a role in arteriogenesis



(Heil et al., 2004). However, those perivascular mast cells, which possess c-kit receptor for stem cell factor (SCF;(Costa et al., 1996) could be important for arteriogenesis. Therefore, we investigated the effect of SCF for arteriogenesis. SCF is a dimeric molecule, which binds and activates receptor tyrosine kinase c-kit. SCF has been associated with mast cell survival, migration, differentiation and proliferation (Galli et al., 1993). Application of SCF increased the rate of blood flow reperfusion only at day 7 and thereafter blood flow returned to normal control values (figure 12 A). The observed increased rate of recovery at day 7 could be explained by an increase in the total number of mast cells in the perivascular region of collateral vessels during the process of arteriogenesis.

#### *4.5. A combined increase in degranulation and recruitment has additive effects*

A combined treatment of mice with C 48/80 plus diprotin A was expected to exhibit a particularly strong effect on growing collateral arteries, given that C 48/80 enhances the degranulation of mast cells and that diprotin A enhances the recruitment of mast cells as well as of leukocytes. In fact, the recovery of blood flow in mice treated simultaneously with C 48/80 and diprotin A was significantly accelerated with respect to control mice already on day 3 after ligation of the femoral artery. This positive effect persisted until day 21. The increased rate of reperfusion at day 3 was not only significant with respect to the rate of reperfusion in controls, but also with respect to the rate of reperfusion in mice that had been treated either with C 48/80 or with Diprotin A alone (figure 13 D). The incremental effect of C 48/80 treatment when combined with diprotin A may have resulted on the one hand from the induction of mast cell degranulation with C 48/80 and the release of several mediators of

inflammation including chemoattractant molecules (MCP-1, GM-CSF) and proteases. On the other hand, application of diprotin A enhanced the SDF-1 $\alpha$  levels, which accelerated the recruitment of leukocytes including mast cells, which in turn provide growth factors and proteases for arteriogenesis.

#### *4.6. What is the relative contribution of mast cells and of leukocytes in arterial growth?*

The rate of blood flow recovery was significantly accelerated after the degranulation of mast cells was enhanced by the application of C 48/80 as well as after an enhancement of the recruitment of mast cells and of other leukocytes. Therefore, each of these mechanisms could have contributed in parallel to some extent to the final result, i.e. to the accelerated recirculation. Alternatively, the activation of one of these mechanisms (e.g. degranulation of mast cells) was a precondition for the activation of another mechanism (e.g. recruitment of leukocytes). To find out, a group of wild type mice was treated with a combination of diprotin A plus cromolyn. Thereby mast cells were stabilized (by applying cromolyn) and their recruitment remained ineffective whereas the recruitment of leukocytes was accelerated (by applying diprotin A). Interestingly, the significantly faster rate of blood flow recovery observed in diprotin A treated mice was absent in mice treated with a combination of diprotin A plus cromolyn (figure 13 E and F). We conclude that degranulation of mast cells and their release of growth factors and chemokines/cytokines provides a necessary environment for the recruitment of leukocytes. The small, non-significant increase in the rate of hindlimb reperfusion in cromolyn plus diprotin A treated versus cromolyn treated mice (figure 14D) might be explained by the relatively small number of

leukocytes that were recruited by diprotin A under the condition that mast cells were stabilized (see figure 20B). This result implies that diprotin A recruits leukocytes mainly indirectly via mast cells.

#### *4.7 Mast cell granula store a number of growth factors, cytokines and proteases*

Both, mast cells as well as leukocytes accelerate the rate of blood flow recovery. However, since mast cells are activated at an earlier stage to respond after the occlusion of an artery than leukocytes, our focus of interest had turned towards the content of mast cell granules. They contain growth factors (e.g. FGF-2 and PDGF-BB), chemoattractant cytokines, chemokines (e.g. MCP-1, TNF- $\alpha$ , GM-CSF and interleukines) and essential proteases (i.e. tryptase and chymase, which are essential for MMP activation) (Qu et al., 1998, Nakayama et al., 2006). Each of these compounds has been assumed in different studies to promote arteriogenesis (Wolf et al., 1998, Deindl et al., 2003, Hoefer et al., 2004). Of particular interest are MCP-1 and TNF- $\alpha$ , because upon up-regulation they exert a strong effect on arteriogenesis. Both MCP-1 and its receptor CCR-2 have been demonstrated to be induced in arteriogenesis (Hoefer et al., 2004) and MCP-1 was associated with increased perivascular leukocyte recruitment in growing collateral arteries (Ito et al., 1997). When mast cell granules were cultured with endothelial cells, significant levels of MCP-1 were released and gene expression of MCP-1 mRNA levels were also increased in comparison to control values (Kinoshita et al., 2005).

#### *4.8. Mast cells up-regulate MCP-1*

The level of MCP-1 mRNA in collaterals was up-regulated 12 hours after femoral artery ligation. With respect to the control mice, quantitative real time – polymerase chain reaction (qRT-PCR) exhibited a significant increase in MCP-1 mRNA levels in collaterals of mice treated with C 48/80 + diprotin A (figure 14 A). This result corresponds to the increase in protein levels of MCP-1 in the collaterals of the hind limb on the occluded side. However, plasma levels of MCP-1 were not significantly increased in mice treated with a combination of C 48/80 + diprotin A (Fig. 14C). The absence of such an increase could have resulted from a strong dilution of MCP-1 in the blood. Our results clearly show that mast cells up-regulate MCP-1 in growing collateral vessels and increase MCP-1 protein levels during arteriogenesis. Similar studies have shown that mast cells release the stored cytoplasmic MCP-1 following its activation as well as induce endothelial cell up-regulation and production of MCP-1 (Kinoshita et al., 2005, Nakayama et al., 2006). These findings clearly demonstrate that the increased MCP-1 upregulation resulted from mast cell degranulation. As a consequence, MCP-1 recruits monocytes which leave the vessel, become macrophages with growth factors. The release of these growth factors promotes proliferation of endothelial and smooth muscle cells (Arras et al., 1998).

#### *4.9. Mast cells release TNF- $\alpha$*

Another chemokine, that is released by mast cell granula is the tumor necrosis factor-alpha (TNF- $\alpha$ ) which promotes leukocyte recruitment and represents an important mediator of inflammation (Bradley, 2008). Although, monocytes and macrophages contains TNF- $\alpha$ , several studies revealed that mast cells are the major constituent of cytokines including TNF- $\alpha$  (Marone et al., 1995, Ribatti et al., 2001). Vascular endothelial cells respond to TNF- $\alpha$  by undergoing a number of pro-inflammatory

changes, which increase leukocyte adhesion and transendothelial migration (Munro et al., 1989). During arteriogenesis, TNF- $\alpha$  modulates collateral artery growth by activating the p55 receptor of endothelial cells (Hoefer et al., 2002). It has been reported in the same study that the perfusion of the distal hindlimb on the occluded side was impaired in TNF $\alpha^{-/-}$  mice compared to the wild-type mice 7 days after femoral ligation.

To find out whether mast cells are responsible for the release of TNF- $\alpha$ , one group of mice with a femoral artery ligation was treated with cromolyn, in order to inhibit mast cell degranulation, another group of mice with a femoral artery ligation was treated with saline (control with ligation) and a third group of mice without ligation was treated with saline as well (control without ligation). As a result, mice treated with cromolyn exhibited a reduced plasma level of TNF- $\alpha$  when compared to control with ligation (figure 15). These findings correlate with the results of an earlier study (Bissonnette et al., 1995), in which it was shown that sodium cromoglycate (cromolyn) inhibited the release of TNF- $\alpha$  from rat peritoneal mast cells.

Upon stimulation with ionomycin mast cells release extracellular RNA (eRNA; Prof. P. Klaus, Giessen Germany, pers. communication) which in turn promotes the TNF- $\alpha$  converting enzyme (TACE) and TACE was found to induce a cleavage of membrane bound pro-TNF- $\alpha$  from monocytes (Fischer et al., 2013). In essence, the elevated plasma level of TNF- $\alpha$  during arteriogenesis is achieved by mast cells. Degranulation and release of cytoplasmatic TNF- $\alpha$  is one mechanism and induction of monocytes/macrophages to release TNF- $\alpha$  through the eRNA-TACE pathway is another mechanism.

#### 4.10 Mast cells recruit leukocytes in the region of arteriogenesis

MCP-1 and TNF- $\alpha$  are associated with increased perivascular leukocyte recruitment in growing collateral arteries (Randolph and Furie, 1995, Ito et al., 1997). In agreement with these results we detected significant leukocyte recruitment in the perivascular space of adductor muscle sections of the hindlimb on the occluded side of C 48/80 + diprotin A treated mice when we used CD45<sup>+</sup>, a leukocyte marker for staining. Conversely, significantly lower perivascular leukocyte recruitment than in C 48/80 + diprotin A treated mice was seen after a treatment either with cromolyn or with a combination of cromolyn and diprotin A (figure 16).

The increased leukocyte recruitment during arteriogenesis in the perivascular space of collaterals and hence adductor muscles were further investigated quantitatively using flow cytometry. 24 hours post ligation we found in the adductor muscles of mice treated with C 48/80 + diprotin A that different markers for subtypes of leukocytes revealed significantly increased numbers of macrophages (marker F4/80<sup>+</sup>) and neutrophils (marker Gr-1<sup>+</sup> CD115<sup>-</sup>) in C 48/80 + diprotin A treated mice when compared to controls (figure 21A).

In the blood of the same mice we found 24 hours after femoral ligation significantly increased levels of neutrophils (marker Gr-1<sup>+</sup> CD115<sup>-</sup>) and T-lymphocytes (both CD4<sup>+</sup> and CD8<sup>+</sup> cells) in mice treated with a combination C 48/80 + diprotin A (figure 21 D). Furthermore, when we investigated leukocyte subpopulations in the *m.adductors* 3 days after ligation, the numbers of macrophages (marker F4/80<sup>+</sup>) were significantly elevated in C 48/80 + diprotin A treated mice, whereas the increase in the numbers of neutrophils was not significant anymore in comparison to control values. When

blood was analysed 3 days after ligation, we found no differences in the leukocyte subpopulations in C 48/80 + diprotin A treated mice versus control mice (figure 21 J).

As described previously, an increase in the number of perivascular leukocytes is an essential prerequisite for vessel growth during arteriogenesis (Schaper et al., 1976). Our results obtained in C 48/80 + diprotin A treated mice clearly demonstrate an increased number of leukocytes in the perivascular space of growing collateral arteries as well as in the blood. From the presence of increased numbers of leukocytes in adductor muscles and in the blood of mice treated with a combination of C 48/80 plus diprotin A we conclude that the activation of mast cells and their release of MCP-1 and TNF- $\alpha$  recruit leukocytes in the region of arteriogenesis.

#### *4.11. Mast cells promote vascular remodelling*

The growth of pre-existing arterial collaterals involves a degradation of extracellular matrix by specialized enzymes, called matrix metalloproteinases (MMP). This process of tissue reshaping has become the centre of attention in relation to physiological and pathological vascular remodelling. MMP are a family of enzymes that proteolytically degrade various components of the extracellular matrix proteins. They play a central role in morphogenesis, wound healing, and tissue repair and remodelling (Newby, 2005). Brower et al. (2002) reported that after the formation of an atrio-ventricular fistula there was a marked elevation in cardiac MMP activity, which corresponded with significant collagen degradation and a rapid increase in the number of cardiac mast cells.

Baram et al (2001) showed that MMP-9 is released by mast cells and when cultured mast cells were treated with phorbol 12-myristate 13-acetate they expressed MMP-9 mRNA (Kanbe et al., 1999). In our experiments, a significant increase in the MMP

activity with respect to control mice was present in mice which received a combined treatment with substances that recruit mast cells (diprotin A) and that in addition degranulate them (C 48/80). Conversely, the number of degranulated mast cells and the level of MMP activity decreased after the application of cromolyn.

The observed significant increase in the MMP activity after a treatment with C48/80 + diprotin A (figure 15) might have resulted from a release of MMP from activated mast cells or from the activation of pro-MMP to active MMP by proteases such as tryptase and chymase which are known to be released from activated mast cells (Baram et al., 2001). The importance of MMP in angiogenesis is mostly seen in the degradation of the vascular basement membrane and in the remodelling of the extracellular matrix which allows leukocytes to migrate and to invade the surrounding tissue (Rundhaug, 2005). Furthermore, mast cells are associated with the increased activation of MMP in up-regulating angiogenesis in squamous epithelial carcinogenesis (Coussens et al., 1999). In addition, the relevance of MMP-2 and 9 has also been described in arteriogenesis (Wolf et al., 1998, Cai et al., 2004). Although mast cell enzymes have been implicated in being involved in the MMP activation cascade by several in vitro and in vivo studies (Brower et al., 2002) our study is the first one to demonstrate that mast cells are capable of triggering significant MMP activation in growing collateral arteries. This result is novel in so far as mast cells are identified as potential regulators for the mechanism of vessel remodelling and luminal growth as shown by the increased size of collateral arteries 7 days after femoral ligation in the group of mice that received a combination of C 48/80 + diprotin A (figure 22 A).



#### *4.12 . Mast cells promote the proliferation of endothelial and smooth muscle cells*

The hallmark of vessel growth is vascular cell proliferation (Pasyk et al., 1982) which follows vascular remodelling. After a treatment of mice with C 48/80 + diprotin A we observed an increased MMP activity, which is an important factor for remodelling, but this treatment resulted in an increased proliferation of vascular cells as well. In the blood of C 48/80 + diprotin A treated mice we found an elevation in the level of the growth factor PDGF-BB. This growth factor as well as FGF-2 was shown to be present in mast cells in the perivascular space of collaterals (Max-Planck-Institute for Heart and Lung Research, Bad Nauheim, Germany; pers. communication). In addition, it has been shown previously in rats and rabbits that combined treatment with FGF-2 and PDGF-BB strongly promotes arteriogenesis (Cao et al., 2003). In order to inhibit the effect of diprotin A, we treated another group of mice with cromolyn + diprotin A, which resulted in fewer proliferating vascular cells than in C 48/80 + diprotin A treated mice (figure 17 A-D). Furthermore, a research group in Giessen has shown that in vitro degranulation of mast cells with ionomycin induces a proliferation of cultured endothelial cells (pers. communication). These in vitro result support our conclusion that mast cell derived factors promote vascular cell proliferation. Our results demonstrate for the first time a direct involvement of mast cells in the remodelling and in the proliferation of endothelial and smooth muscle cells during arteriogenesis. These two findings have the power to open a new concept in the chapter of arteriogenesis.

#### *4.13. Accelerated perfusion after femoral artery ligation reduces muscle damage*

The extent of tissue damage in distal hindlimb muscles on the occluded side is expected to be dependent on the time course of the recovery of an efficient perfusion and hence on the progress of arteriogenesis. The degree of skeletal muscle damage will directly correlate with the severity and duration of ischemia and inversely with the extent of collateral vascular growth and the resulting reperfusion (Scholz et al., 2002). The same study compared the cell damage in the gastrocnemius muscle tissue of two different strains of mice (Balb/Cs and C57BL/6). Balb/Cs mice had a 50% poorer perfusion recovery in comparison to C57BL/6 mice and their poorer perfusion recovery was associated with an increased angiogenesis and muscle tissue damage.

An efficient reperfusion requires an enlargement of the diameters of growing collateral arteries. Therefore, we analysed histological sections of distal adductor muscle from the occluded side of C 48/80 + diprotin A treated mice and compared them with sections from the controls. Already 3 days post ligation an increase in the luminal diameter of collateral vessels by a factor of 1.3 was observed. A further increase by a factor of 1.7 was seen 7 days after ligation with respect to control values (figure 21). This collateral luminal expansion correlates to our laser Doppler perfusion imaging data, which showed a faster recovery of the blood flow in the distal hindlimb after femoral artery ligation in combined C 48/80 + diprotin A treated mice in comparison to controls.

In the distal lower limb a significantly smaller area of damaged calf muscle tissue was revealed by histological analysis in mice treated with a combination of C 48/80 + diprotin A with respect to control mice. The preserved calf muscles tissue seen in the histological sections might have resulted from an earlier increase in blood flow recirculation in mice with a combined C 48/80 + diprotin A treatment as shown by

laser Doppler imaging (LDI; figure 13D and figure 22 M). In this group of mice with a combined C 48/80 + diprotin A treatment the muscle tissue looked very similar to that on the sham operated side. Correspondingly, the ratio of capillary per muscle fibre in mice with a combined C 48/80 + diprotin A treatment was significantly reduced with respect to control mice (figure 22). This implies that angiogenesis was also reduced in mice with a combined C 48/80 + diprotin A treatment.

In reaction to ischemic injury, leukocyte infiltration is increased (Ysebaert et al., 2000). Given that the calf muscle on the occluded side of treated mice was so well preserved, we expected that fewer leukocytes had infiltrated the gastrocnemius muscle of treated mice. Therefore, we assessed the number of leukocytes in this muscle with the help of CD45 antibody staining. Consistent with our expectation we found significantly fewer numbers of leukocytes in mice treated with a combination of C 48/80 + diprotin A than in control mice.

#### *4.14. Reactive oxygen species activate mast cell degranulation in response to arterial occlusion*

In this study we have clearly shown that mast cells are located in the perivascular space of quiescent collateral arteries (figure 10 A). Following femoral artery ligation, mast cell releases their granular content by a process known as degranulation (figure 10 B). However, so far the mechanism of mast cell degranulation is not understood. In a series of experiments, we attempted to find the likely cause for mast cell degranulation during untreated arteriogenesis. Given the close proximity between mast cells, nerve fibres and accompanying blood vessels, the release of substance P from nerve endings could be responsible for the degranulation. Substance P has been reported in several studies as a potent mast cell degranulator

(Suzuki et al., 1995, Saban et al., 2002). However, after we had blocked the release of substance P in a group of mice the time course of blood flow recovery in this group was not different from the time course of recovery in control mice.

Reactive oxygen species (ROS) are produced in cells as normal product of cellular metabolism. The cellular level of these products is regulated by specific enzymes e.g. dismutase and catalase to prevent deleterious effects (Stadtman, 1992). Reactive oxygen species (ROS) have been implicated in inducing mast cell activation (McCauley et al., 2005, Swindle and Metcalfe, 2007). Since neutrophils are the first cells to promote inflammation and since they release oxygen free radicals (Tidball, 1995), we propose that neutrophils might be involved in mast cell degranulation through the production of ROS. When we applied a substance which depletes neutrophils (Ly6G/1A8) we found a significant reduction in the rate of recovery of blood flow at day 7. A histological analysis documented a decreased percentage of mast cell degranulation 24 hours after femoral artery ligation. To further investigate a possible role of reactive oxygen species in mast cell degranulation during arteriogenesis, we stained sections of adductor muscles from *Nox-2<sup>-/-</sup>* mice and found a reduced percentage of degranulated mast cells around the collaterals 24 hour after femoral artery ligation. Next, we treated mice with N-acetylcysteine or apocynin to reduce the level of ROS. In this experiment, we investigated the degranulation of mast cells 24 hour after femoral artery ligation. In both groups of mice, the percentages of degranulated mast cells were significantly decreased when compared to control values. This suggests that ROS derived from extravasated neutrophils plays a role in mast cell degranulation during arteriogenesis. A crucial role of platelets in arteriogenesis is further emphasized by

the fact that the percentage of mast cell degranulation in  $\text{GPIb}\alpha^{-/-}$  mice was decreased 3 days after femoral artery occlusion when compared with wild type mice. In essence we suggest, neutrophils interact with platelets through the platelets receptor  $\text{GPIb}\alpha$  (Zarbock et al., 2007, von Bruhl et al., 2012) with the result that urokinase-type plasminogen activator (UPA) promote more neutrophils to accumulate in the perivascular space (Reichel et al., 2011) and finally ROS release (figure 24).

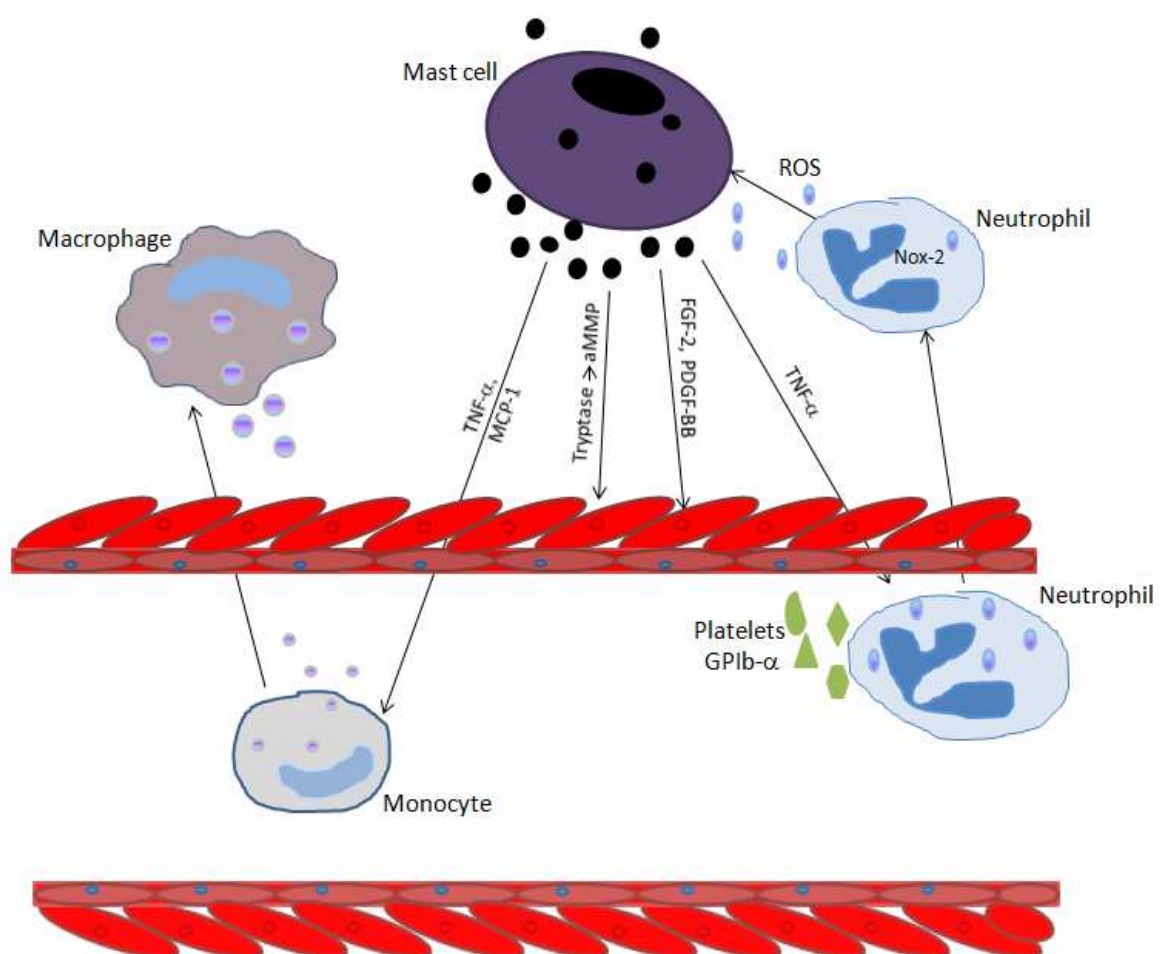


*Figure 24. A proposed model showing mechanism of mast cell degranulation and action*

After femoral artery ligation neutrophils and platelets interact in collateral arteries. This interaction results in uPA dependent extravasation of neutrophils and in a release of neutrophil derived ROS from Nox 2. Next, ROS degranulate mast cells. Mast cells release factors which promote vascular remodelling (MMP), vascular cell proliferation (FGF-2 and PDGF-BB) and leukocyte recruitment (TNF- $\alpha$ , MCP-1). Finally resulting in enhanced collateral artery growth.

#### *4.15. Mast cell activation – a therapeutic target for patients?*

This study has demonstrated that the recovery of perfusion after arterial occlusion can be accelerated by enhanced mast cell recruitment and degranulation. The pharmacological treatment of mice with diproton A and with the compound 48/80 encouraged the enlargement of collateral arteries, improved the blood supply of distal muscles and reduced the ischemia related damage of distal muscle tissue after the occlusion of a major artery. These beneficial consequences of mast cell recruitment and degranulation could also be exploited clinically by an application of diproton A and C 48/80 in patients with vascular occlusive diseases. In fact, drugs like sitagliptin (The dipeptidylpeptidase–IV inhibitor) are used in the clinic to treat patients with type-2 diabetes mellitus (Eurich et al., 2013), this drug also can be employed to mobilize leukocytes to the region of collateral artery growth. Since there is no known clinical means of inducing mast cell degranulation, this is left as an important area to research.

## **5. SUMMARY**

In a mouse model, we investigated the functional role of mast cells for the growth of pre-existing arterial collaterals into functional bypasses after the ligation of the femoral artery on one side. A major finding consisted in the discovery of a regionally restricted mast cell degranulation in the vicinity of growing collaterals. Such a mast cell response was neither present in ischemic muscles of the lower limb nor on the sham-operated side. The observed degranulation stimulated our search for functional contributions of mast cells in arteriogenesis.

The functional consequence of mast cell degranulation for the recovery of the blood flow distal to the ligation was quantified with the help of laser Doppler imaging. The recovery of blood flow in the distal hindlimb was accelerated both by an enhanced degranulation of mast cells (after the application of C 48/80) as well as by an enhanced recruitment of mast cells (after the application of diprotin A). A combined

application of C 48/80 plus diprotin A synergistically accelerated the recovery of distal blood flow. Stabilization of mast cells (after the application of cromolyn) reduced the number of degranulated mast cells and slowed down the speed of recovery of distal blood flow.

Mast cell degranulation up regulated the monocyte chemotactic protein (MCP)-1 and increased the release of TNF- $\alpha$ . Both cytokines are essential for leukocyte recruitment as shown by CD45<sup>+</sup> antibody staining. Hence, degranulation of mast cells mediates the activation of leukocytes, which play an important role in arteriogenesis.

In addition, activated mast cells supply FGF-2 and PDGF-BB, which are important for endothelial and smooth muscle cell proliferation. Mice treated with a combination of C 48/80 + diprotin A exhibited an increased vascular cell proliferation. Hence, we conclude from these results that C 48/80 + diprotin A degranulate mast cells, which release growth factors like FGF-2 and PDGF-BB and thereby enhance vascular cell proliferation. As a consequence, the diameters of collateral arteries increase and vascular blood flow improves.

The growth of collateral arteries is known to be accompanied by an activation of matrix metalloproteinases (MMP). These enzymes are responsible for vascular remodelling and the degradation of the extracellular matrix. In our experiments, the MMP activity was significantly increased with respect to control mice whenever mast cell recruitment and mast cell degranulation were both enhanced by the combined application of C 48/80 plus diprotin A.

The accelerated rate of arteriogenesis in the upper hind limb due to an enhanced degranulation of mast cells resulted in a reduced amount of tissue damage in the



gastrocnemius muscle. This reduced tissue damage was accompanied by less capillary proliferation and by fewer leukocytes infiltrating the gastrocnemius muscle. Given the important role of mast cells in arteriogenesis, we finally investigated how mast cell degranulation is accomplished during the untreated growth of collateral arteries. As a result, our study showed an involvement of platelets and neutrophils. The latter release reactive oxygen species and thereby activate mast cells. Taken together these data demonstrate that mast cells are major players in arteriogenesis. Their degranulation accelerates the enlargement of collateral arteries and as a consequence reduces ischemic damage of the distal tissues.

## 7. REFERENCES

- Arras, M., Ito, W. D., Scholz, D., Winkler, B., Schaper, J. & Schaper, W. 1998. Monocyte activation in angiogenesis and collateral growth in the rabbit hindlimb. *J Clin Invest*, **101**, 40-50.
- Baram, D., Vaday, G. G., Salamon, P., Drucker, I., HersHKoviz, R. & Mekori, Y. A. 2001. Human mast cells release metalloproteinase-9 on contact with activated T cells: juxtacrine regulation by TNF- $\alpha$ . *J Immunol*, **167**, 4008-16.
- Behm, C. Z., Kaufmann, B. A., Carr, C., Lankford, M., Sanders, J. M., Rose, C. E., Kaul, S. & Lindner, J. R. 2008. Molecular imaging of endothelial vascular cell adhesion molecule-1 expression and inflammatory cell recruitment during vasculogenesis and ischemia-mediated arteriogenesis. *Circulation*, **117**, 2902-11.
- Bissonnette, E. Y., Enciso, J. A. & Befus, A. D. 1995. Inhibition of tumour necrosis factor- $\alpha$  (TNF- $\alpha$ ) release from mast cells by the anti-inflammatory

- drugs, sodium cromoglycate and nedocromil sodium. *Clin Exp Immunol*, **102**, 78-84.
- Blank, U., Ra, C., Miller, L., White, K., Metzger, H. & Kinet, J. P. 1989. Complete structure and expression in transfected cells of high affinity IgE receptor. *Nature*, **337**, 187-9.
- Boyce, J. A. 2007. Mast cells and eicosanoid mediators: a system of reciprocal paracrine and autocrine regulation. *Immunol Rev*, **217**, 168-85.
- Bradley, J. R. 2008. TNF-mediated inflammatory disease. *J Pathol*, **214**, 149-60.
- Brogden, R. N., Speight, T. M. & Avery, G. S. 1974. Sodium cromoglycate (cromolyn sodium): a review of its mode of action, pharmacology, therapeutic efficacy and use. *Drugs*, **7**, 164-282.
- Brooks, A. C., Whelan, C. J. & Purcell, W. M. 1999. Reactive oxygen species generation and histamine release by activated mast cells: modulation by nitric oxide synthase inhibition. *Br J Pharmacol*, **128**, 585-90.
- Brower, G. L., Chancey, A. L., Thanigaraj, S., Matsubara, B. B. & Janicki, J. S. 2002. Cause and effect relationship between myocardial mast cell number and matrix metalloproteinase activity. *Am J Physiol Heart Circ Physiol*, **283**, H518-25.
- Buschmann, I. R., Hoefer, I. E., van Royen, N., Katzer, E., Braun-Dulleaus, R., Heil, M., Kostin, S., Bode, C. & Schaper, W. 2001. GM-CSF: a strong arteriogenic factor acting by amplification of monocyte function. *Atherosclerosis*, **159**, 343-56.
- Cai, W., Vosschulte, R., Afsah-Hedjri, A., Koltai, S., Kocsis, E., Scholz, D., Kostin, S., Schaper, W. & Schaper, J. 2000. Altered balance between extracellular proteolysis and antiproteolysis is associated with adaptive coronary arteriogenesis. *J Mol Cell Cardiol*, **32**, 997-1011.
- Cai, W. J., Kocsis, E., Wu, X., Rodriguez, M., Luo, X., Schaper, W. & Schaper, J. 2004. Remodeling of the vascular tunica media is essential for development of collateral vessels in the canine heart. *Mol Cell Biochem*, **264**, 201-10.
- Cao, R., Brakenhielm, E., Pawliuk, R., Wariaro, D., Post, M. J., Wahlberg, E., Leboulch, P. & Cao, Y. 2003. Angiogenic synergism, vascular stability and improvement of hind-limb ischemia by a combination of PDGF-BB and FGF-2. *Nat Med*, **9**, 604-13.

- Carmeliet, P. 2000. Mechanisms of angiogenesis and arteriogenesis. *Nat Med*, **6**, 389-95.
- Chalothorn, D. & Faber, J. E. 2010. Formation and maturation of the native cerebral collateral circulation. *J Mol Cell Cardiol*, **49**, 251-9.
- Chomczynski, P. & Sacchi, N. 1987. Single-step method of RNA isolation by acid guanidinium thiocyanate-phenol-chloroform extraction. *Anal Biochem*, **162**, 156-9.
- Christopherson, K. W., 2nd, Hangoc, G., Mantel, C. R. & Broxmeyer, H. E. 2004. Modulation of hematopoietic stem cell homing and engraftment by CD26. *Science*, **305**, 1000-3.
- Costa, J. J., Demetri, G. D., Harrist, T. J., Dvorak, A. M., Hayes, D. F., Merica, E. A., Menchaca, D. M., Gringeri, A. J., Schwartz, L. B. & Galli, S. J. 1996. Recombinant human stem cell factor (kit ligand) promotes human mast cell and melanocyte hyperplasia and functional activation in vivo. *J Exp Med*, **183**, 2681-6.
- Coussens, L. M., Raymond, W. W., Bergers, G., Laig-Webster, M., Behrendtsen, O., Werb, Z., Caughey, G. H. & Hanahan, D. 1999. Inflammatory mast cells up-regulate angiogenesis during squamous epithelial carcinogenesis. *Genes Dev*, **13**, 1382-97.
- Cox, G. S., Hertzner, N. R., Young, J. R., O'Hara, P. J., Krajewski, L. P., Piedmonte, M. R. & Beven, E. G. 1993. Nonoperative treatment of superficial femoral artery disease: long-term follow-up. *J Vasc Surg*, **17**, 172-81.
- Daley, J. M., Thomay, A. A., Connolly, M. D., Reichner, J. S. & Albina, J. E. 2008. Use of Ly6G-specific monoclonal antibody to deplete neutrophils in mice. *J Leukoc Biol*, **83**, 64-70.
- de Paula, E. V., Flores-Nascimento, M. C., Arruda, V. R., Garcia, R. A., Ramos, C. D., Guillaumon, A. T. & Annichino-Bizzacchi, J. M. 2009. Dual gene transfer of fibroblast growth factor-2 and platelet derived growth factor-BB using plasmid deoxyribonucleic acid promotes effective angiogenesis and arteriogenesis in a rodent model of hindlimb ischemia. *Transl Res*, **153**, 232-9.
- Deindl, E., Buschmann, I., Hoefer, I. E., Podzuweit, T., Boengler, K., Vogel, S., van Royen, N., Fernandez, B. & Schaper, W. 2001. Role of ischemia and of hypoxia-inducible genes in arteriogenesis after femoral artery occlusion in the rabbit. *Circ Res*, **89**, 779-86.

- Deindl, E., Hoefer, I. E., Fernandez, B., Barancik, M., Heil, M., Strniskova, M. & Schaper, W. 2003. Involvement of the fibroblast growth factor system in adaptive and chemokine-induced arteriogenesis. *Circ Res*, **92**, 561-8.
- Dell'italia, L. J., Balcells, E., Meng, Q. C., Su, X., Schultz, D., Bishop, S. P., Machida, N., Straeter-Knowlen, I. M., Hankes, G. H., Dillon, R., Cartee, R. E. & Oparil, S. 1997. Volume-overload cardiac hypertrophy is unaffected by ACE inhibitor treatment in dogs. *Am J Physiol*, **273**, H961-70.
- Drechsler, M., Megens, R. T., van Zandvoort, M., Weber, C. & Soehnlein, O. 2010. Hyperlipidemia-triggered neutrophilia promotes early atherosclerosis. *Circulation*, **122**, 1837-45.
- Engels, W., Reuters, P. H., Daemen, M. J., Smits, J. F. & van der Vusse, G. J. 1995. Transmural changes in mast cell density in rat heart after infarct induction in vivo. *J Pathol*, **177**, 423-9.
- Eurich, D. T., Simpson, S., Senthilselvan, A., Asche, C. V., Sandhu-Minhas, J. K. & McAlister, F. A. 2013. Comparative safety and effectiveness of sitagliptin in patients with type 2 diabetes: retrospective population based cohort study. *Bmj*, **346**, f2267.
- Evangelista, V., Manarini, S., Dell'Elba, G., Martelli, N., Napoleone, E., Di Santo, A. & Lorenzet, P. S. 2005. Clopidogrel inhibits platelet-leukocyte adhesion and platelet-dependent leukocyte activation. *Thromb Haemost*, **94**, 568-77.
- Falus, A. & Meretey, K. 1992. Histamine: an early messenger in inflammatory and immune reactions. *Immunol Today*, **13**, 154-6.
- Fischer, S., Gesierich, S., Griemert, B., Schanzer, A., Acker, T., Augustin, H. G., Olsson, A. K. & Preissner, K. T. 2013. Extracellular RNA liberates tumor necrosis factor-alpha to promote tumor cell trafficking and progression. *Cancer Res*, **73**, 5080-9.
- Galli, S. J., Tsai, M. & Wershil, B. K. 1993. The c-kit receptor, stem cell factor, and mast cells. What each is teaching us about the others. *Am J Pathol*, **142**, 965-74.
- Gruber, B. L., Marchese, M. J., Suzuki, K., Schwartz, L. B., Okada, Y., Nagase, H. & Ramamurthy, N. S. 1989. Synovial procollagenase activation by human mast cell tryptase dependence upon matrix metalloproteinase 3 activation. *J Clin Invest*, **84**, 1657-62.

- Grundmann, S., Hoefer, I., Ulusans, S., van Royen, N., Schirmer, S. H., Ozaki, C. K., Bode, C., Piek, J. J. & Buschmann, I. 2005. Anti-tumor necrosis factor- $\alpha$  therapies attenuate adaptive arteriogenesis in the rabbit. *Am J Physiol Heart Circ Physiol*, **289**, H1497-505.
- Haas, T. L., Doyle, J. L., Distasi, M. R., Norton, L. E., Sheridan, K. M. & Unthank, J. L. 2007. Involvement of MMPs in the outward remodeling of collateral mesenteric arteries. *Am J Physiol Heart Circ Physiol*, **293**, H2429-37.
- Heil, M., Ziegelhoeffer, T., Mees, B. & Schaper, W. 2004. A different outlook on the role of bone marrow stem cells in vascular growth: bone marrow delivers software not hardware. *Circ Res*, **94**, 573-4.
- Heil, M., Ziegelhoeffer, T., Pipp, F., Kostin, S., Martin, S., Clauss, M. & Schaper, W. 2002. Blood monocyte concentration is critical for enhancement of collateral artery growth. *Am J Physiol Heart Circ Physiol*, **283**, H2411-9.
- Helisch, A. & Schaper, W. 2003. Arteriogenesis: the development and growth of collateral arteries. *Microcirculation*, **10**, 83-97.
- Helisch, A., Wagner, S., Khan, N., Drinane, M., Wolfram, S., Heil, M., Ziegelhoeffer, T., Brandt, U., Pearlman, J. D., Swartz, H. M. & Schaper, W. 2006. Impact of mouse strain differences in innate hindlimb collateral vasculature. *Arterioscler Thromb Vasc Biol*, **26**, 520-6.
- Hoefer, I. E., Grundmann, S., van Royen, N., Voskuil, M., Schirmer, S. H., Ulusans, S., Bode, C., Buschmann, I. R. & Piek, J. J. 2005. Leukocyte subpopulations and arteriogenesis: specific role of monocytes, lymphocytes and granulocytes. *Atherosclerosis*, **181**, 285-93.
- Hoefer, I. E., van Royen, N., Rectenwald, J. E., Bray, E. J., Abouhamze, Z., Moldawer, L. L., Voskuil, M., Piek, J. J., Buschmann, I. R. & Ozaki, C. K. 2002. Direct evidence for tumor necrosis factor- $\alpha$  signaling in arteriogenesis. *Circulation*, **105**, 1639-41.
- Hoefer, I. E., van Royen, N., Rectenwald, J. E., Deindl, E., Hua, J., Jost, M., Grundmann, S., Voskuil, M., Ozaki, C. K., Piek, J. J. & Buschmann, I. R. 2004. Arteriogenesis proceeds via ICAM-1/Mac-1- mediated mechanisms. *Circ Res*, **94**, 1179-85.
- Hunt, S. A. 2006. Taking heart--cardiac transplantation past, present, and future. *N Engl J Med*, **355**, 231-5.

- Ito, W. D., Arras, M., Winkler, B., Scholz, D., Schaper, J. & Schaper, W. 1997. Monocyte chemotactic protein-1 increases collateral and peripheral conductance after femoral artery occlusion. *Circ Res*, **80**, 829-37.
- Kanbe, N., Tanaka, A., Kanbe, M., Itakura, A., Kurosawa, M. & Matsuda, H. 1999. Human mast cells produce matrix metalloproteinase 9. *Eur J Immunol*, **29**, 2645-9.
- Kasapis, C. & Gurm, H. S. 2009. Current approach to the diagnosis and treatment of femoral-popliteal arterial disease. A systematic review. *Curr Cardiol Rev*, **5**, 296-311.
- Keller, M., Simbruner, G., Gorna, A., Urbanek, M., Tinhofer, I., Griesmaier, E., Sarkozy, G., Schwendimann, L. & Gressens, P. 2006. Systemic application of granulocyte-colony stimulating factor and stem cell factor exacerbates excitotoxic brain injury in newborn mice. *Pediatr Res*, **59**, 549-53.
- Kennedy, P. G., Rodgers, J., Jennings, F. W., Murray, M., Leeman, S. E. & Burke, J. M. 1997. A substance P antagonist, RP-67,580, ameliorates a mouse meningoencephalitic response to *Trypanosoma brucei brucei*. *Proc Natl Acad Sci U S A*, **94**, 4167-70.
- Kinoshita, M., Okada, M., Hara, M., Furukawa, Y. & Matsumori, A. 2005. Mast cell tryptase in mast cell granules enhances MCP-1 and interleukin-8 production in human endothelial cells. *Arterioscler Thromb Vasc Biol*, **25**, 1858-63.
- Kirshenbaum, A. S., Kessler, S. W., Goff, J. P. & Metcalfe, D. D. 1991. Demonstration of the origin of human mast cells from CD34+ bone marrow progenitor cells. *J Immunol*, **146**, 1410-5.
- Kitamura, Y. & Ito, A. 2005. Mast cell-committed progenitors. *Proc Natl Acad Sci U S A*, **102**, 11129-30.
- Kovanen, P. T. 2007. Mast cells: multipotent local effector cells in atherothrombosis. *Immunol Rev*, **217**, 105-22.
- Lagunoff, D., Martin, T. W. & Read, G. 1983. Agents that release histamine from mast cells. *Annu Rev Pharmacol Toxicol*, **23**, 331-51.
- Li, W. W., Guo, T. Z., Liang, D. Y., Sun, Y., Kingery, W. S. & Clark, J. D. 2012. Substance P signaling controls mast cell activation, degranulation, and nociceptive sensitization in a rat fracture model of complex regional pain syndrome. *Anesthesiology*, **116**, 882-95.

- Liao, C. H., Akazawa, H., Tamagawa, M., Ito, K., Yasuda, N., Kudo, Y., Yamamoto, R., Ozasa, Y., Fujimoto, M., Wang, P., Nakauchi, H., Nakaya, H. & Komuro, I. 2010. Cardiac mast cells cause atrial fibrillation through PDGF-A-mediated fibrosis in pressure-overloaded mouse hearts. *J Clin Invest*, **120**, 242-53.
- Lin, T. J., Issekutz, T. B. & Marshall, J. S. 2001. SDF-1 induces IL-8 production and transendothelial migration of human cord blood-derived mast cells. *Int Arch Allergy Immunol*, **124**, 142-5.
- Liu, Y., Davidson, B. P., Yue, Q., Belcik, T., Xie, A., Inaba, Y., McCarty, O. J., Tormoen, G. W., Zhao, Y., Ruggeri, Z. M., Kaufmann, B. A. & Lindner, J. R. 2013. Molecular imaging of inflammation and platelet adhesion in advanced atherosclerosis effects of antioxidant therapy with NADPH oxidase inhibition. *Circ Cardiovasc Imaging*, **6**, 74-82.
- Malcangio, M. & Bowery, N. G. 1994. Effect of the tachykinin NK1 receptor antagonists, RP 67580 and SR 140333, on electrically-evoked substance P release from rat spinal cord. *Br J Pharmacol*, **113**, 635-41.
- Marone, G., de Crescenzo, G., Adt, M., Patella, V., Arbustini, E. & Genovese, A. 1995. Immunological characterization and functional importance of human heart mast cells. *Immunopharmacology*, **31**, 1-18.
- Mazurek, N., Weskamp, G., Erne, P. & Otten, U. 1986. Nerve growth factor induces mast cell degranulation without changing intracellular calcium levels. *FEBS Lett*, **198**, 315-20.
- McCauley, S. D., Gilchrist, M. & Befus, A. D. 2005. Nitric oxide: a major determinant of mast cell phenotype and function. *Mem Inst Oswaldo Cruz*, **100 Suppl 1**, 11-4.
- Mierke, C. T., Ballmaier, M., Werner, U., Manns, M. P., Welte, K. & Bischoff, S. C. 2000. Human endothelial cells regulate survival and proliferation of human mast cells. *J Exp Med*, **192**, 801-11.
- Mousli, M., Bronner, C., Landry, Y., Bockaert, J. & Rouot, B. 1990. Direct activation of GTP-binding regulatory proteins (G-proteins) by substance P and compound 48/80. *FEBS Lett*, **259**, 260-2.
- Munro, J. M., Pober, J. S. & Cotran, R. S. 1989. Tumor necrosis factor and interferon-gamma induce distinct patterns of endothelial activation and associated leukocyte accumulation in skin of *Papio anubis*. *Am J Pathol*, **135**, 121-33.

- Nakamura, T. & Ui, M. 1985. Simultaneous inhibitions of inositol phospholipid breakdown, arachidonic acid release, and histamine secretion in mast cells by islet-activating protein, pertussis toxin. A possible involvement of the toxin-specific substrate in the Ca<sup>2+</sup>-mobilizing receptor-mediated biosignaling system. *J Biol Chem*, **260**, 3584-93.
- Nakayama, T., Mutsuga, N., Yao, L. & Tosato, G. 2006. Prostaglandin E2 promotes degranulation-independent release of MCP-1 from mast cells. *J Leukoc Biol*, **79**, 95-104.
- Newby, A. C. 2005. Dual role of matrix metalloproteinases (matrixins) in intimal thickening and atherosclerotic plaque rupture. *Physiol Rev*, **85**, 1-31.
- Oskeritzian, C. A., Zhao, W., Min, H. K., Xia, H. Z., Pozez, A., Kiev, J. & Schwartz, L. B. 2005. Surface CD88 functionally distinguishes the MCTC from the MCT type of human lung mast cell. *J Allergy Clin Immunol*, **115**, 1162-8.
- Ota, R., Kurihara, C., Tsou, T. L., Young, W. L., Yeghiazarians, Y., Chang, M., Mobashery, S., Sakamoto, A. & Hashimoto, T. 2009. Roles of matrix metalloproteinases in flow-induced outward vascular remodeling. *J Cereb Blood Flow Metab*, **29**, 1547-58.
- Pagel, J. I., Ziegelhoeffer, T., Heil, M., Fischer, S., Fernandez, B., Schaper, W., Preissner, K. T. & Deindl, E. 2012. Role of early growth response 1 in arteriogenesis: impact on vascular cell proliferation and leukocyte recruitment in vivo. *Thromb Haemost*, **107**, 562-74.
- Panizo, A., Mindan, F. J., Galindo, M. F., Cenarruzabeitia, E., Hernandez, M. & Diez, J. 1995. Are mast cells involved in hypertensive heart disease? *J Hypertens*, **13**, 1201-8.
- Pasyk, S., Schaper, W., Schaper, J., Pasyk, K., Miskiewicz, G. & Steinseifer, B. 1982. DNA synthesis in coronary collaterals after coronary artery occlusion in conscious dog. *Am J Physiol*, **242**, H1031-7.
- Patella, V., de Crescenzo, G., Lamparter-Schummert, B., De Rosa, G., Adt, M. & Marone, G. 1997. Increased cardiac mast cell density and mediator release in patients with dilated cardiomyopathy. *Inflamm Res*, **46 Suppl 1**, S31-2.
- Qu, Z., Kayton, R. J., Ahmadi, P., Liebler, J. M., Powers, M. R., Planck, S. R. & Rosenbaum, J. T. 1998. Ultrastructural immunolocalization of basic fibroblast growth factor in mast cell secretory granules. Morphological evidence for bfgf release through degranulation. *J Histochem Cytochem*, **46**, 1119-28.



- Qu, Z., Liebler, J. M., Powers, M. R., Galey, T., Ahmadi, P., Huang, X. N., Ansel, J. C., Butterfield, J. H., Planck, S. R. & Rosenbaum, J. T. 1995. Mast cells are a major source of basic fibroblast growth factor in chronic inflammation and cutaneous hemangioma. *Am J Pathol*, **147**, 564-73.
- Randolph, G. J. & Furie, M. B. 1995. A soluble gradient of endogenous monocyte chemoattractant protein-1 promotes the transendothelial migration of monocytes in vitro. *J Immunol*, **155**, 3610-8.
- Reichel, C. A., Uhl, B., Lerchenberger, M., Puhr-Westerheide, D., Rehberg, M., Liebl, J., Khandoga, A., Schmalix, W., Zahler, S., Deindl, E., Lorenzl, S., Declerck, P. J., Kanse, S. & Krombach, F. 2011. Urokinase-type plasminogen activator promotes paracellular transmigration of neutrophils via Mac-1, but independently of urokinase-type plasminogen activator receptor. *Circulation*, **124**, 1848-59.
- Reliene, R., Fischer, E. & Schiestl, R. H. 2004. Effect of N-acetyl cysteine on oxidative DNA damage and the frequency of DNA deletions in atm-deficient mice. *Cancer Res*, **64**, 5148-53.
- Resnick, N., Einav, S., Chen-Konak, L., Zilberman, M., Yahav, H. & Shay-Salit, A. 2003. Hemodynamic forces as a stimulus for arteriogenesis. *Endothelium*, **10**, 197-206.
- Ribatti, D., Vacca, A., Nico, B., Crivellato, E., Roncali, L. & Dammacco, F. 2001. The role of mast cells in tumour angiogenesis. *Br J Haematol*, **115**, 514-21.
- Rundhaug, J. E. 2005. Matrix metalloproteinases and angiogenesis. *J Cell Mol Med*, **9**, 267-85.
- Saban, R., Gerard, N. P., Saban, M. R., Nguyen, N. B., DeBoer, D. J. & Wershil, B. K. 2002. Mast cells mediate substance P-induced bladder inflammation through an NK(1) receptor-independent mechanism. *Am J Physiol Renal Physiol*, **283**, F616-29.
- Saito, H. 2005. Role of mast cell proteases in tissue remodeling. *Chem Immunol Allergy*, **87**, 80-4.
- Santos, F. X., Arroyo, C., Garcia, I., Blasco, R., Obispo, J. M., Hamann, C. & Espejo, L. 2000. Role of mast cells in the pathogenesis of postburn inflammatory response: reactive oxygen species as mast cell stimulators. *Burns*, **26**, 145-7.
- Schaper, J., Konig, R., Franz, D. & Schaper, W. 1976. The endothelial surface of growing coronary collateral arteries. Intimal margination and diapedesis of

- monocytes. A combined SEM and TEM study. *Virchows Arch A Pathol Anat Histol*, **370**, 193-205.
- Schaper, W., De Brabander, M. & Lewi, P. 1971. DNA synthesis and mitoses in coronary collateral vessels of the dog. *Circ Res*, **28**, 671-9.
- Schaper, W. & Scholz, D. 2003. Factors regulating arteriogenesis. *Arterioscler Thromb Vasc Biol*, **23**, 1143-51.
- Schirmer, S. H., van Nooijen, F. C., Piek, J. J. & van Royen, N. 2009. Stimulation of collateral artery growth: travelling further down the road to clinical application. *Heart*, **95**, 191-7.
- Scholz, D., Cai, W. J. & Schaper, W. 2001. Arteriogenesis, a new concept of vascular adaptation in occlusive disease. *Angiogenesis*, **4**, 247-57.
- Scholz, D., Ito, W., Fleming, I., Deindl, E., Sauer, A., Wiesnet, M., Busse, R., Schaper, J. & Schaper, W. 2000. Ultrastructure and molecular histology of rabbit hind-limb collateral artery growth (arteriogenesis). *Virchows Arch*, **436**, 257-70.
- Scholz, D., Ziegelhoeffer, T., Helisch, A., Wagner, S., Friedrich, C., Podzuweit, T. & Schaper, W. 2002. Contribution of arteriogenesis and angiogenesis to postocclusive hindlimb perfusion in mice. *J Mol Cell Cardiol*, **34**, 775-87.
- Schulz, R., Murzabekova, G., Egemnazarov, B., Kraut, S., Eisele, H. J., Dumitrascu, R., Heitmann, J., Seimetz, M., Witzenrath, M., Ghofrani, H. A., Schermuly, R. T., Grimminger, F., Seeger, W. & Weissmann, N. 2014. Arterial hypertension in a murine model of sleep apnea: role of NADPH oxidase 2. *J Hypertens*, **32**, 300-5.
- Schwartz, L. B., Irani, A. M., Roller, K., Castells, M. C. & Schechter, N. M. 1987. Quantitation of histamine, tryptase, and chymase in dispersed human T and TC mast cells. *J Immunol*, **138**, 2611-5.
- Seiler, C. 2003. The human coronary collateral circulation. *Heart*, **89**, 1352-7.
- Sovari, A. A., Morita, N. & Karagueuzian, H. S. 2008. Apocynin: a potent NADPH oxidase inhibitor for the management of atrial fibrillation. *Redox Rep*, **13**, 242-5.
- Stabile, E., Burnett, M. S., Watkins, C., Kinnaird, T., Bachis, A., la Sala, A., Miller, J. M., Shou, M., Epstein, S. E. & Fuchs, S. 2003. Impaired arteriogenic response to acute hindlimb ischemia in CD4-knockout mice. *Circulation*, **108**, 205-10.

- Stabile, E., Kinnaird, T., la Sala, A., Hanson, S. K., Watkins, C., Campia, U., Shou, M., Zbinden, S., Fuchs, S., Kornfeld, H., Epstein, S. E. & Burnett, M. S. 2006. CD8<sup>+</sup> T lymphocytes regulate the arteriogenic response to ischemia by infiltrating the site of collateral vessel development and recruiting CD4<sup>+</sup> mononuclear cells through the expression of interleukin-16. *Circulation*, **113**, 118-24.
- Stadtman, E. R. 1992. Protein oxidation and aging. *Science*, **257**, 1220-4.
- Suzuki, H., Miura, S., Liu, Y. Y., Tsuchiya, M. & Ishii, H. 1995. Substance P induces degranulation of mast cells and leukocyte adhesion to venular endothelium. *Peptides*, **16**, 1447-52.
- Swindle, E. J. & Metcalfe, D. D. 2007. The role of reactive oxygen species and nitric oxide in mast cell-dependent inflammatory processes. *Immunol Rev*, **217**, 186-205.
- Tang, Y. L., Yang, Y. Z., Wang, S., Huang, T., Tang, C. K., Xu, Z. X. & Sun, Y. H. 2009. Mast cell degranulator compound 48-80 promotes atherosclerotic plaque in apolipoprotein E knockout mice with perivascular common carotid collar placement. *Chin Med J (Engl)*, **122**, 319-25.
- Tidball, J. G. 1995. Inflammatory cell response to acute muscle injury. *Med Sci Sports Exerc*, **27**, 1022-32.
- Tyagi, S. C., Kumar, S., Cassatt, S. & Parker, J. L. 1996. Temporal expression of extracellular matrix metalloproteinases and tissue plasminogen activator in the development of collateral vessels in the canine model of coronary occlusion. *Can J Physiol Pharmacol*, **74**, 983-95.
- Vagima, Y., Lapid, K., Kollet, O., Goichberg, P., Alon, R. & Lapidot, T. 2011. Pathways implicated in stem cell migration: the SDF-1/CXCR4 axis. *Methods Mol Biol*, **750**, 277-89.
- van Weel, V., Toes, R. E., Seghers, L., Deckers, M. M., de Vries, M. R., Eilers, P. H., Sipkens, J., Schepers, A., Eefting, D., van Hinsbergh, V. W., van Bockel, J. H. & Quax, P. H. 2007. Natural killer cells and CD4<sup>+</sup> T-cells modulate collateral artery development. *Arterioscler Thromb Vasc Biol*, **27**, 2310-8.
- Vanichakarn, P., Blair, P., Wu, C., Freedman, J. E. & Chakrabarti, S. 2008. Neutrophil CD40 enhances platelet-mediated inflammation. *Thromb Res*, **122**, 346-58.

- von Bruhl, M. L., Stark, K., Steinhart, A., Chandraratne, S., Konrad, I., Lorenz, M., Khandoga, A., Tirniceriu, A., Coletti, R., Kollnberger, M., Byrne, R. A., Laitinen, I., Walch, A., Brill, A., Pfeiler, S., Manukyan, D., *et al.* 2012. Monocytes, neutrophils, and platelets cooperate to initiate and propagate venous thrombosis in mice in vivo. *J Exp Med*, **209**, 819-35.
- Wolf, C., Cai, W. J., Vosschulte, R., Koltai, S., Mousavipour, D., Scholz, D., Afsah-Hedjri, A., Schaper, W. & Schaper, J. 1998. Vascular remodeling and altered protein expression during growth of coronary collateral arteries. *J Mol Cell Cardiol*, **30**, 2291-305.
- Yang, B. L., Wu, S., Wu, X., Li, M. B., Zhu, W., Guan, Y., Liu, L. H., Luo, M. Y., Cai, W. J., Schaper, J. & Schaper, W. 2013. Effect of shunting of collateral flow into the venous system on arteriogenesis and angiogenesis in rabbit hind limb. *Acta Histochem Cytochem*, **46**, 1-10.
- Ysebaert, D. K., De Greef, K. E., Vercauteren, S. R., Ghielli, M., Verpooten, G. A., Eyskens, E. J. & De Broe, M. E. 2000. Identification and kinetics of leukocytes after severe ischaemia/reperfusion renal injury. *Nephrol Dial Transplant*, **15**, 1562-74.
- Zafarullah, M., Li, W. Q., Sylvester, J. & Ahmad, M. 2003. Molecular mechanisms of N-acetylcysteine actions. *Cell Mol Life Sci*, **60**, 6-20.
- Zarbock, A., Polanowska-Grabowska, R. K. & Ley, K. 2007. Platelet-neutrophil-interactions: linking hemostasis and inflammation. *Blood Rev*, **21**, 99-111.
- Zaruba, M. M., Theiss, H. D., Vallaster, M., Mehl, U., Brunner, S., David, R., Fischer, R., Krieg, L., Hirsch, E., Huber, B., Nathan, P., Israel, L., Imhof, A., Herbach, N., Assmann, G., Wanke, R., *et al.* 2009. Synergy between CD26/DPP-IV inhibition and G-CSF improves cardiac function after acute myocardial infarction. *Cell Stem Cell*, **4**, 313-23.
- Zhang, D., Huang, W., Dai, B., Zhao, T., Ashraf, A., Millard, R. W., Ashraf, M. & Wang, Y. 2010. Genetically manipulated progenitor cell sheet with diprotin A improves myocardial function and repair of infarcted hearts. *Am J Physiol Heart Circ Physiol*, **299**, H1339-47.

## **8. INDEXES**

### **i. Acknowledgement**

It would not have been possible to write this doctoral thesis without the help and support of the kind people around me, to only some of whom it is possible to give particular mention here.

I am deeply grateful to my principal supervisor, PD. Dr. rer. nat. Elisabeth Deindl for her advice and insightful comments and suggestions during the whole project. Without her guidance and persistent help, this thesis would not have been possible.

The good advice, support and friendship of my second supervisor, Prof. Norbert Dieringer, has been so valuable on both an academic and a personal level, for which I am extremely grateful. I am also particularly appreciated his constructive comments and warm encouragement given by him.

I would like to offer my special thanks to my colleagues, Eike Kleinert and Amelia Caballero who inspired my final effort and experimental work despite the enormous work pressures we were facing together.

I have greatly benefited from Dr. Judith Pagel for her general introduction to the topic of arteriogenesis and experimental procedures in our laboratory.

I want to thank Christine Csapo, Mei-Ping Wu, Alke Schropp, Frau Schaefer and Frau Sendlhofer for their technical assistance.

I would like to thank and acknowledge Prof. Ulrich Pohl for accepting to conduct research in his institute (Walter-Brendel-Centre of Experimental Medicine). I also appreciate the academic and technical support of the institute and the University (Ludwig-Maximilian-University-Munich) as well as its staffs.

I thank the financial support from Fritz-Bender-Stiftung, DAAD in collaboration with the Government of Tanzania and the Münchener Universitätsgesellschaft.

Above all, I would like to thank my wife Zenna and my sons Karim and Ayman for their personal support and great patience at all times, and for the several months they spent without me. I am deeply sorry for that. Also to my parents, brothers and sisters who have given me their moral support throughout the time I stayed in Germany.

## **ii. List of abbreviations**

1. BMCs ..... Bone marrow derived cells
2. BSA ..... Bovine serum albumin
3. CVDs ..... Cardiovascular diseases
4. DPPIV ..... Dipeptidylpeptidase IV
5. ELISA ..... Enzyme-linked immunosorbent assay
6. FACS ..... Fluorescence activated cell sorting
7. GFP ..... Green fluorescence protein
8. FGF-2 ..... Fibroblast growth factor -2
9. GM-CSF ..... Granulocyte monocyte-colony stimulating factor
10. ICAM-1 ..... Intracellular adhesion molecule -1
11. LDI ..... Laser Doppler Imaging
12. MCP-1 ..... Monocyte chemoattractant protein -1
13. MMP ..... Matrix metalloproteinase
14. NAC ..... N-acetylcystein

15. NADPH ..... Nicotinamide adenine dinucleotide phosphate
16. Nox ..... NADPH oxidase
17. PAD ..... Peripheral artery disease
18. PBS ..... Phosphate-buffered saline
19. PDGF-BB ..... Platelet-derived growth factor - BB
20. PTA ..... Percutaneous transluminal angioplasty
21. PTCA ..... Percutaneous transluminal coronary angioplasty
22. qR-PCR ..... Quantitative real time – polymerase chain reaction
23. ROI ..... Region of interest
24. ROS ..... Reactive oxygen species
25. SCF ..... Stem cell factor
26. SDF-1 $\alpha$  ..... Stem cell derived factor – 1 $\alpha$
27. TBS ..... Tris-buffered saline
28. TGF- $\beta$  ..... Transforming growth factor-  $\beta$
29. TNF- $\alpha$  ..... Tumor necrosis factor -  $\alpha$
30. RNA ..... Ribonucleic acid
31. uPA ..... urokinase plasminogen activator

### iii. Curriculum Vitae

<b>Personal information</b>	
First name(s) / Surname(s)	<b>Omary Chillo.</b>
Address(es)	
Fax	
E-mail	<a href="mailto:omary_chillo@yahoo.com">omary_chillo@yahoo.com</a>
Nationality	Tanzanian
Date of birth	20.04.1982
Languages	English, Swahili and German.
<b>Desired employment / Occupational field</b>	
<b>Work experience</b>	
Dates	September 2008 to September 2009
Occupation or position held	Intern doctor
Responsibilities	Attending patients and follow-up
Employer	Muhimbili National Hospital – Dar es Salaam, Tanzania.

Dates	November 2009 to date
Occupation or position held	Tutorial assistant
Responsibilities	Teaching and supervising medical students Conducting medical researches
Employer	Muhimbili University of Health and Allied Sciences – Dar es Salaam, Tanzania
<b>Education and training</b>	
Dates	October 2010 to November 2014
Title of qualification awarded	Dr. med (cardiovascular physiology)
Name and type of organisation providing education and training	Walter Brandel Centre of Experimental Medicine – LMU, Munich
Sponsorship	Deutscher Akademischer Austausch Dienst (DAAD) and The Government of Tanzania
Dates	2003 to 2008
Title of qualification awarded	Medical Doctor
Name and type of organisation providing education and training	Muhimbili University of Health and Allied Sciences – Dar es Salaam



## 1.

**Poster presentations**

- a. **Chillo O**, Pagel JI, Mauer A, Trenkwalder T, Reichel C, Deindl E.  
The functional role of mast cells in Arteriogenesis. Doktameday of the Ludwig-Maximilian-University Munich and the Technical University Munich. 2011, Munich, Germany.
- b. **Chillo O**, Pagel JI, Mauer A, Trenkwalder T, Reichel C, Deindl E.  
Mast cells in arteriogenesis. Joint meeting of European Society for Microcirculation and Germany Society of Microcirculation and Vascular Biology. 2011, Munich, Germany.
- c. Mauer A, **Chillo O**, Pagel JI, Reichel CA, Preissner KT, Fischer S, Deindl E.  
Mast cells contribute to arteriogenesis in a PI3 Kinase  $\gamma$ -dependent manner. Joint meeting European Society for Microcirculation and the Germany Society of Microcirculation and Vascular Biology. 2011, Munich, Germany.
- d. Starke RD, Paschalaki K, Pagel J, **Chillo O**, Mazi S, Sahutoglu T, Cutler J, Payne E, Millar C, Deindl E, Laffan M, Randi A.  
Von Willebrand factor regulates angiogenesis in Von Willebrand disease patient's blood outgrowth endothelial cells. International Vascular Biology Meeting. 2012, Wiesbaden, Germany.

2. **Oral presentations**

- a. **Chillo O**, Pagel JI, Mauer A, Trenkwalder T, Reichel C, Deindl E.  
Mast cells in arteriogenesis. Walter Brendel Centre doctoral student day. 2012, Munich, Germany.
- b. **Chillo O**, Pagel JI, Mauer A, Caballero-Martinez A, Kleinert EC, Trenkwalder T, Kurz A, Mueller-Hoecker J, Troidl K, Fischer S, Preissner KT, Reichel C, Deindl E.  
Mast cells: Key player in leukocyte recruitment during arteriogenesis. 7<sup>th</sup> International Leukocyte Signal Transduction Conference. 2013, Kos, Greece.
- c. Starke RD, **Chillo O**, Pagel J, Elder JM, Laffan MA, Deindl E and Randi AM.  
Von Willebrand factor regulates physiological and pathological angiogenesis through VEGF Receptor-2 signalling. International Society on Thrombosis and Haemostasis. 2013, Amsterdam, The Netherlands. Published in the Journal of Thrombosis and Haemostasis. Volume 11, Supplement 1.

3. **Original articles**

- a. Di Qin, Trenkwalder T., Lee S., **Chillo O**, Deindl E., Kupatt C. & Hinkel R.  
Early vessel destabilization mediated by Angiopoietin-2 and subsequent vessel maturation via Angiopoietin-1 induce functional neovasculature after ischemia. *PLoS One*, 2013; **8**, e61812.
- b. **Omar Chillo**, Judith Irina Pagel, Eike Christian Kleinert, Amelia Caballero, Silvia Fischer, Annika Mauer, Kerstin Troidl, Angela Kurz, Sue Chandraratne, Gerald Assmann, Josef Mueller-Hoecker, Steffen Massberg, Norbert Weissmann, Klaus T. Preissner, Christoph Reichel, Elisabeth Deindl. Mast cells are central in arteriogenesis and their degranulation saves tissue from severe damage (in preparation).